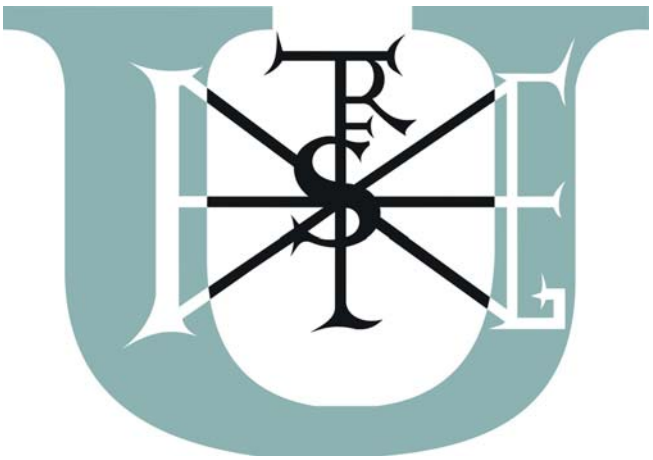

SZENT ISTVÁN UNIVERSITY

DEVELOPMENT OF NOVEL CRYOPRESERVATION METHOD FOR MAMMALIAN OOCYTE

Jun Liu

GÖDÖLLŐ

2009

The PhD program

Name: Animal Husbandry Science PhD School

Discipline: Animal Husbandry Science

Leader: **Prof. Dr. Miklós Mézes DSc**
Head of Department,
Szent István University, Faculty of Agricultural and Environmental Sciences,
Department of Nutrition

Supervisor: **Prof. Dr. András Dinnyés, DSc**
Head of Molecular Animal Biotechnology Laboratory,
Szent István University, Faculty of Agricultural and Environmental Sciences,
Institute for Basic Animal Sciences

…… …….

Approval of the PhD School Leader Approval of the Supervisor

TABLE OF CONTENTS

CHAPTER 1. INTRODUCTION 8

1.1 THE SIGNIFICANCE OF MAMMALIAN OOCYTE CRYOPRESERVATION 8

1.2 CRYOPRESERVATION METHODS 9

1.2.1 Interrupted Slow Freezing 9

1.2.2 Vitrification 11

1.2.3 Ultrarapid Vitrification 11

1.3 THE STATE OF THE ART OF OOCYTE CRYOPRESERVATION 12

1.4 COMPLICATIONS OF THE OOCYTE CRYOPRESERVATION 15

1.5 DEVELOPMENTS OF OPTIMIZED CRYOPRESERVATION METHODS VIA FUNDAMENTAL APPROACH AND THEORETICAL ANALYSIS 16

1.6 OUTLINE OF THE STUDY 18

CHAPTER 2. THEORY OF FUNDAMENATAL CRYOBIOLOGY AND EQUATION DERIVATION 20

2.1 BIOPHYSICAL EVENTS DURING CRYOPRESERVATION 20

2.2 MATHEMATICAL FORMULATION OF THE MEMBRANE PERMEABILITY COEFFICIENTS 22

2.3 ACTIVATION ENERGIES FOR PARAMETERS 24

2.4 CALCULATIONS OF INTRACELLULAR WATER VOLUME AND CPA CONCENTRATIONS DURING FREEZING AND THAWING. 24

CHAPTER 3. A THEORETICAL MODEL FOR THE DEVELOPMENT OF INTERRUPTED SLOW FREEZING PROCEDURES 27

3.1 INTRODUCTION 27

3.2 MATERIALS AND METHODS 29

3.2.1 Theoretical Prediction of Intracellular Water Volume and Solute Mole Number at Varying Temperatures 29

3.2.2 Assumptions Pertaining to Intracellular Ice Formation (IIF) 31

3.2.3 Source of Embryos for Ice Nucleation Experiments 32

3.2.4 Determination of Critical Concentration 32

3.2.5 Measurement of Cooling and Warming Rates Inside Straws 33

3.2.6 Prediction of the Theoretically Optimized Cryopreservation Protocol 33

3.3 RESULTS 35

3.3.1 Cooling/Warming Rates in 0.25 ml Plastic Straws 35

3.3.2 Estimation of Critical Concentration. 35

3.3.3 Experimental Determination of Intracellular Nucleation Temperature 36

3.3.4 Estimation of Optimal Plunging Temperature 37

3.4 DISCUSSION 38

CHAPTER 4. ACCUMULATIVE OSMOTIC DAMAGE MODEL FOR OOCYTE CRYOPRESERVATION 45

4.1 INTRODUCTION 45
4.2 MATERIALS AND METHOD 46
4.2.1 Oocyte collection 46
4.2.2 Determination of the permeability coefficients 48
4.2.3 Parthenogenetic activation and development 48
4.2.4 Theoretical simulations and accumulative osmotic damage model 49
4.2.5 Statistical analyses 49
4.3 RESULTS 50
4.3.1 Rabbit oocyte CPA permeabilities 50
4.3.2 Blastocyst Development and AOD 50
4.4 DISCUSSION 53
4.4.1 CPA permeabilities 54
4.4.2 AOD model 54

CHAPTER 5. DEVELOPMENT OF A NOVEL CRYOPRESERVATION THREE-STEP METHOD FOR MAMMALIAN OOCYTE 56

5.1 INTRODUCTION 56
5.2 METHOD 57
5.2.1 Physical events involved in "three-step" cryopreservation 57
5.2.2 Additional Equations 59
5.2.3 Calculation of the probability of intracellular ice formation (P_{IIF}) 59
5.2.4 Determination of P_{IIF} parameters 60
5.2.5 Presentation of calculation results 61
5.2.6 Experiments to validate the theoretical predictions. 61
5.3 RESULTS 63
5.3.1 IIF Observation and Determination of IIF Parameters 63
5.3.2 Determination of the P_{IIF} values for different combinations of T_p, C^0, and t_h 64
5.3.3 Experimental results versus the theoretical predictions 65
5.3.4 Optimization of an oocyte freezing protocol 66
5.4 DISCUSSION 67
5.4.1 General discussion of P_{IIF}-Plot 67
5.4.2 IIF Observations and Prediction 67

CHAPTER 6. NEW SCIENTIFIC RESULTS 69

CHAPTER 7. CONCLUSION 71

CHAPTER 8. SUMMARY 78

CHAPTER 9. LIST OF PUBLICATIONS 80

CHAPTER 10. REFERENCE 83

CHAPTER 11. ACKNOWLEDGEMENTS 90

Descriptions, units and values of the symbols and abbreviations

$[CPA]^0$	Initial DMSO concentration	molal	
$[CPA]_c$	Critical intracellular solute concentration	g/100g	40
$[S]^i$	Intracellular solute concentration	g/100g	variable
A	surface area of a cell	μm^2	parameter
AOD	accumulative osmotic damage		
Al	artificial insemination		
ART	Assisted reproductive technology		
B	cooling rate	$^oCx\ min^{-1}$	Parameter
B_1	slow cooling rate (in step 1 of ISF)	$^oCxmin^{-1}$	0-2.5
B_2	cooling rate inside a straw during plunging (step 2)	$^oCx\ min^{-1}$	Parameter
B_3	warming rate inside the cell container (during thaw)	$^oCx\ min^{-1}$	Parameter
C	total extracellular solute concentration	g/100g	variable
Cc	Critical intracellular solute concentration	molal	paramater
C_i	Initial DMSO concentration	molal	0- 4
CPA	cryoprotective agent		
DMSO	dimethyl sulfoxide		
e	Superscripts for extracellular		
E_a	activation energy	$Kcalxmole^{-1}$	parameter
EG	ethylene glycol		
GV	germinal vesicle		
i	Superscripts for intracellular		
i	Subscripts for the index of different conditions		
ICSI	Intracytoplasmic Sperm Injection		
IIF	intracellular ice formation		
ISF	interrupted slow freezing		
IVP	in vitro produced		
L_p	hydraulic conductivity	$\mu mxmin^{-1}xatm^{-1}$	parameter
Me_2SO	dimethyl sulfoxide		
MII	the metaphase II		
MW	molecular weight of substance	g/mole	variable

n	Subscripts for NaCl		
n^i_s	moles of solute inside a cell	moles	variable
NT	nuclear transfer		
o	Subscripts for a reference point		
P_{CPA}	solute permeability	$cmxmin^{-1}$	parameter
OPS	open-pulled straw		
PG	propylene glycol		
P_{IIF}	probability of intracellular ice formation		
R	the universal gas constant	$Kcalxmole^{-1}\square K^{-1}$	$1.987x10^{-3}$
R_t	ratio of CPA weight to NaCl weight		parameter
s	Subscripts for solute		
SCN	surface catalyzed nucleation		
SSV	solid-surface vitrification		
T	temperature	K	variable
t	time	seconds	variable
$\square$	Duration of slow cooling	seconds	variable
T_{end}	the end temperature point of calculation	K	parameter
T_m	melting point of a solution	K	variable
T_p	plunging temperature	K	parameter
T_h	Holding temperature	K	parameter
T_{seed}	the seeding temperature	K	parameter
V_{10}	molar volume of water	μm^3xmole^{-1}	$1.8x10^{12}$
VCN	volume catalyzed nucleation		
V_b	osmotically inactive volume	μm^3	parameter
V_{bp}	the percentage of osmotically inactive cell volume		parameter
V_c	volume of a cell	μm^3	variable
V_{iso}	isotonic cell volume	μm^3	parameter
V_w	volume of cell water	μm^3	variable
w	Subscripts for water		

CHAPTER 1. INTRODUCTION

1.1 THE SIGNIFICANCE OF MAMMALIAN OOCYTE CRYOPRESERVATION

Mammalian oocyte cryopreservation has applications in animal agriculture, biomedical research, human reproductive medicine and biodiversity preservation. Among species used for animal agriculture, cryopreserved oocytes would play an important role in developing improved breeding programs. By using in vitro produced (IVP) embryos from elite animals, significant improvements in reducing the generational interval can be attained (Presicce et al., 1997). This technology would also allow the rescue of gametes from otherwise infertile animals, as well as the use of abattoir-derived oocytes that are increasingly being used in research (Day, 2000). Additionally, those highly valuable transgenic animals make successful cryopreservation critical. For one thing it will allow international distribution of these genotypes. Secondly, it will facilitate the creation of repositories in the event of a catastrophe such as disease outbreak or natural disaster.

Production of transgenic lab animals (such as mice, rats, rabbit and hamster) provides a powerful model to explore the regulation of gene expression as well as the regulation of cellular and physiological processes (Glenister et al., 1990; Leibo et al., 1991). Recent years, genetically-modified animals have been created in large numbers. Given their value as models for biological systems, it is desirable to preserve these strains indefinitely for future studies. The high costs of producing and maintaining genetically altered animal needs reliable cryopreservation protocols in order to preserve specific strains for experimental purposes, without perpetuating these strains through continuous live breeding. Cryopreservation of germplasm offers a way to reduce these costs by allowing the maintenance of "frozen" colonies as a backup in the event of a disease outbreak or other emergency, or as a full replacement of breeding colonies that are not currently in use but whose maintenance is desired for future research (Critser and Russell, 2000). Additionally, a frozen colony derived from founder animals would help alleviate inbreeding depression and genetic drift, thus maintaining overall genetic vigor while minimizing the number of animals necessary for maintenance of a live colony (Whittingham, 1974). At the present time, nuclear transfer (NT) technology is relatively inefficient, and relies on the ready access to mature oocytes. Having an efficient means to cryopreserve oocytes would ensure a steady supply of these cells for NT procedures, and could alleviate inefficiencies associated with seasonal variability of oocyte quality (Rutledge et al., 1999).

The demand for human reproductive medical services continues to increase (Andersen et al., 2006). Cryopreservation of spermatozoa and preimplantation embryos has been an integral component of patient services for many years. It has been shown that the use of embryo cryopreservation can improve the chance of a successful pregnancy from each oocyte collection (Schnorr et al., 2000). Unfortunately, cryopreservation of supernumerary embryos presents ethical concerns for some individuals (Michelmann and Nayudu, 2006); in some countries embryo cryopreservation is not permitted (Benagiano and Gianaroli, 2004). In such cases, oocyte cryopreservation has been adopted as a replacement technique in an effort to

improve the chances of pregnancy per oocyte retrieval cycle, and lighten these ethical and legal concerns by allowing the creation of only the numbers of embryos deemed appropriate for transfer, by preserving the potential for future attempts at pregnancy should the initial one fail. Oocyte cryopreservation also provides an opportunity to preserve the fertility of women undergoing potentially deleterious iatrogenic procedures such as chemotherapy, which usually results in the loss of gonadal function and subsequent infertility. Oocyte cryopreservation is also important for family planning given that the average age of childbearing continues to increase and embryo cryopreservation is not desirable for many women without partners.

Additionally, having successful methods available to cryopreserve human oocytes would allow the establishment of oocyte banks to assist those female patients who cannot produce viable oocytes (Karow, 1997). Oocyte cryopreservation would not only obviate cycle synchronization between donor and recipient, a method that is not always successful, but it would allow sufficient time for seroconversion of the donor in the event of a recent infection with a transmittable disease (Critser et al., 1997). Such practices are routine in semen banks and are facilitated by the ability to cryopreserve human semen.

To some extent gamete storage can provide insurance for preserving the existing genetic diversity within endangered species. These species survive in nature but often in fragmented habitats, or live in geographically disparate zoos and they are also susceptible to inbreeding depression, environmental catastrophes, epidemics, and even to drastic shifts in social and political structures. Application of assisted reproduction technologies using frozen–thawed gametes of rare and endangered species will become increasingly important in conservation biology programs (Dinnyes et al., 2007; Wildt, 2000).

1.2 CRYOPRESERVATION METHODS

In general, the cryopreservation of cells involves an initial exposure to cryoprotective agents (CPAs), cooling to subzero temperatures, storage, thawing, and finally, dilution and removal of the CPA, with return to physiological environment. Currently, there are three main strategies: interrupted slow freezing (ISF), traditional vitrification (vitrification in straws) and ultrarapid vitrification.

1.2.1 Interrupted Slow Freezing

The most common cryopreservation method is the ISF procedure, consisting of an initial slow, controlled-rate cooling to subzero temperatures followed by rapid cooling as the sample is plunged into liquid nitrogen (LN2) for storage. During the controlled slow cooling extracellular ice formation is induced (seeding) at a temperature just below the solution's freezing point, and then the cooling continues at a given rate in the presence of a growing extracellular ice phase, which raises the extracellular solute concentration in the unfrozen fraction and results in water being removed from the cell via exosmosis. Permeating CPAs, such as glycerol (GLY), dimethyl sulfoxide (Me_2SO or DMSO), ethylene glycol (EG) or propylene glycol (PG) are typically included in the freezing medium, to protect the cells against injury from the high concentrations of electrolytes that develop as water is removed from the solution as ice. These CPAs become increasingly concentrated intracellularly as the cell dehydrates. The slow cooling step is terminated

at an intermediate temperature (T_p, in the range of -30 to -80 ^oC) then plunging, a rapid cooling step, is initiated in which the remaining intracellular water either vitrifies or form small non-damaging ice crystals.

Control of the cooling and warming rates is crucial. If cells are cooled too rapidly during the controlled slow cooling process, water does not exit the cells fast enough to maintain equilibrium and, therefore, the embryos freeze intracellularly, resulting in death in most cases. If cooling is too slow, the long duration can cause 'solution effects' injury resulting from the high concentration of extra-and intracellular solutes, probably due to the effects of the solutes on the cellular membrane or through osmotic dehydration. Oocyte cryopreservation protocols commonly use controlled cooling rates in the range of 0.3 - 0.6°C/ min. During warming the small intracellular ice crystals might subsequently undergo re-crystallization, forming bigger ice crystals that rupture the cell membrane, thus leading to fatal damage. Rapid thawing can prevent the re-crystallization (Van den Abbeel et al., 1994).

In general, we can expect coupled flows of water and CPAs when CPAs are added, during freezing, thawing and when CPAs are removed from the cells, resulting in a series of anisosmotic conditions. During freezing the cells dehydrate and shrink and remain shrunken during storage, but return to their isosmotic volume upon thawing. Finally, the cells are subjected to potentially lethal swelling upon CPA dilution and removal. The addition/dilution of permeating CPAs and non-permeating CPAs (e.g. sucrose, glucose, or trehalose) to/from the cells are usually conducted in a multiple-step manner to minimize the magnitude of volume excursion (Fig. 1.1).

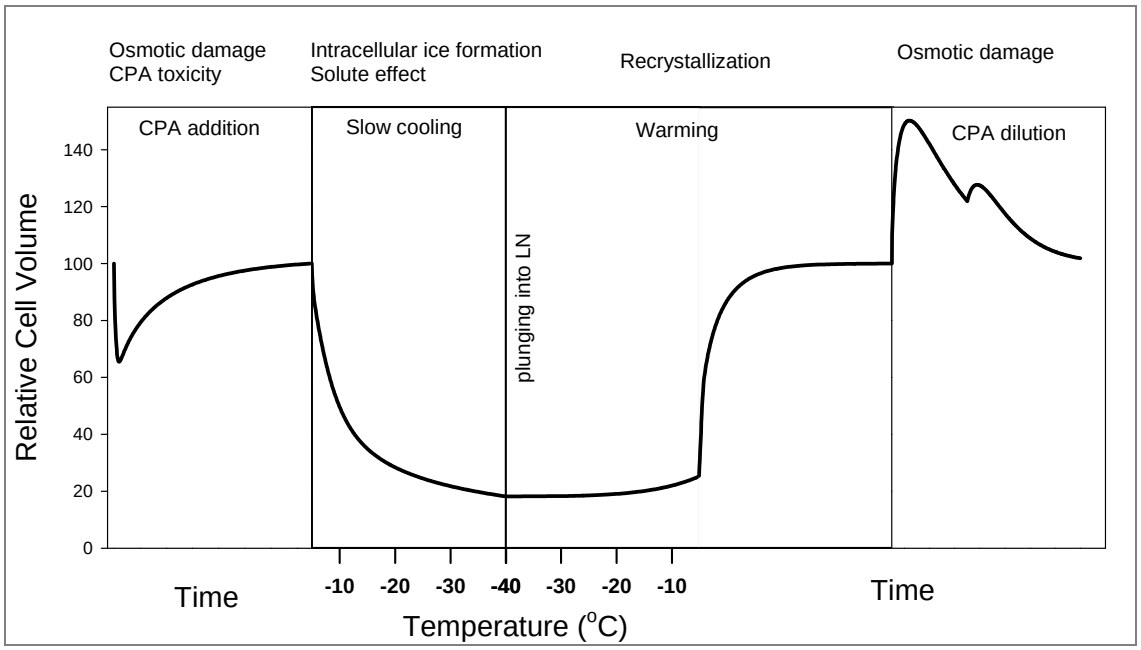

Figure 1.1. Cell volume changes during a typical ISF cryopreservation procedure, in this case ISF terminated at -40 ^oC and a two-step dilution without non-permeating CPA (such as sucrose) was used. Time and temperature scales were used for the x-axis.

1.2.2 Vitrification

Vitrification, cryopreservation without ice formation, is a process of converting a solution into a glass-like amorphous solid state that is free of any crystalline structures. This can be achieved by utilizing high cooling rates with high concentrations of CPAs (Fahy et al., 1984). A typical vitrification protocol requires a high concentration of CPAs in the medium (30-50% compared with 5-10% for ISF) at a cooling rate easily achievable for conventional laboratory conditions and set-ups. Such high CPA concentrations can be detrimental to oocytes, causing both biochemical alterations and lethal osmotic injury. Various strategies have been described to counter the potential toxicity of solutions including: (1) the use of a combination of CPA solutes, each of which is below a toxic concentration, yet in combination would allow vitrification; (2) addition of non-permeating CPAs such as disaccharides (e.g. sucrose or trehalose) or high molecular weight molecules (e.g. Ficoll, polyvinylalcohol or polyvinylpyrrolidone) can significantly reduce the amount of permeable CPA required, (3) the use of compounds which counteract the toxicity of other agents (e.g. acetamide with DMSO; and (4) reducing the time for which and/or the temperature at which the embryos are exposed to CPAs.

1.2.3 Ultrarapid Vitrification

Reducing the solute concentrations in combination with higher cooling rates is an efficient strategy employed to achieve vitrification of oocytes. To achieve very high cooling rates, the volume of the vitrification solution should be minimized by using specially designed containers, open-pulled straws (Vajta et al., 1998), electron microscope copper grids (Martino et al., 1996b), cryo-loops (Lane et al., 1999), cryotops (Kuwayama et al., 2005), and by solid-surface vitrification (Dinnyes et al., 2000). When solution concentrations are reduced, the likelihood of devitrification during warming increases. Hence, the high warming rate is important. Many of these novel technologies use direct exposure of samples to LN2, which often precludes effective biocontainment (Dinnyes et al., 2007).

Optimal cryopreservation methodology varies by species and breeds, mostly due to variations in membrane permeability and embryo sensitivity to CPAs. Cryo-sensitivity is altered by the developmental stage of the embryo, reflecting its changing membrane permeability towards water and CPAs, and effective cell repair and protective mechanisms (Table 1-1).

Table 1-1. Comparison of the three approaches for embryo cryopreservation

	Cryopreservation techniques		
Parameters	Interrupted Slow Freezing	In-straw vitrification	Ultra-rapid vitrification
Embryo storage container	Straw, Cryovial	Straw	Special devices (such as open-pulled straw, cryo-loops, cryo-top, solid surface)

CPA concentration (additional sucrose concentration)	1.3 to 1.5M (0 to 0.3 M)	5.5 to 7.5M (0 to 0.3 M)	3.5 to 5.5 (0 to 0.5 M)	M
Time in the equilibration CPA solution	N/A	2 to 5 min	2 to 5 min	
Time in final CPA concentration for cooling	15 to 20 min	> I min	> 10 s	
Time required for cooling to final storage temperature	90 to 120 min	2 to 3 min	< 0.1 s	
Ice crystal formation in embryo suspension	Yes	No	No	
Osmotic injury	Low risk	High risk	High risk	
Toxic injury	Low risk	High risk	High risk	
Chilling injury	High risk	Low risk	Low risk	
Warming rate	Low to moderate	Moderate to high	High	
Cost of cooling apparatus	High	Low	Low	
Commercial applications	Extensive	Limited	Limited	

1.3 THE STATE OF THE ART OF OOCYTE CRYOPRESERVATION

The majority of the investigations of oocyte cryopreservation summarized in this section has focused on empirical optimization of the several variables known to influence oocyte cryo-survival. First, the ‘‘best’’ CPAs are identified in terms of the type and concentration, alone or as a mixture that yields the highest post-thaw survival. Then, the effects of cooling rates are examined. Often, attempts are made to determine the approaches for CPA addition/dilution (such as CPA concentrations steps, step durations and conducting temperatures), the optimum intermediate subzero temperature that precedes the plunge of oocytes into liquid nitrogen.

The mouse II oocyte is the first mammalian oocyte that was successfully frozen and stored in liquid nitrogen, and subsequently developed into live offspring (Whittingham, 1977). Todorow and colleagues (Todorow et al., 1989) directly compared the effects of DMSO, PG or a combination of the two (all at a final concentration of 1.5 M with 0.1 M sucrose) in a slow-cooling procedure. These authors tested a stepwise addition (5 equal molar steps) and a 5-step removal as well as cooling to either -35 or -80 °C at a cooling rate of 0.3 °C /min. addition and removal. Surrey and Quinn also compared DMSO and PG in a slow-cooling method (Surrey and Quinn, 1990). The temperature at which the controlled cooling was terminated differed between the two compounds (-40 °C vs. -30 °C, respectively). In addition, 0.2 M sucrose was present with the PG, but no sucrose was present with DMSO.

Reports of vitrification of mouse oocytes appeared in the literature shortly after the successful vitrification of mouse embryos by Rall and Fahy (Rall and Fahy, 1985). In 1988, Kola and colleagues vitrified cumulus-intact oocytes using vitrification solution 1 (VS1), containing 2.5 M DMSO, 2.36 M acetamide, 1.19M PG, 5.4% polyethylene glycol (Kola et al., 1988). In 1989, Nakagata and colleagues (Nakagata, 1989) reported very high survival of oocytes vitrified using VS1 medium when the total time for exposure to the solution was 10 seconds or less and the dilution was conducted by immediate transferring to a l0X volume of 0.3M sucrose. Shaw and colleagues also reported on the effects of brief exposures of mouse oocytes to 90 % VS1 solutions and the subsequent viability (Shaw et al., 1992). They investigated exposing oocytes directly to the solution for 10, 15, 30, 60, or 300 seconds. These results suggest that the cells are able to tolerate high osmotic stress for brief periods of time. The time of exposure to a 6.0 M DMSO solution has also been shown to be important to mouse oocytes. These authors used a stepwise exposure to DMSO instead of a direct addition to the final solution. With the short exposure time, the percent of viable fetuses was shown to be similar between the untreated control, DMSO exposure, and vitrified groups. Results such as these have lead to the development of certain practices for vitrifying oocytes and embryos from mammals, incorporating very brief times of exposure to the CPA. In general vitrification procedures are becoming more commonly used to cryopreserve mammalian oocytes (Vajta and Nagy, 2006).

Overall slow cooling methods have been unsuccessful for MII bovine oocytes, with very low blastocyst yield in vitro. Bovine oocytes are highly prone to chilling injury. Long time periods of exposure to cold temperatures is likely the major contributor to the failure of slow cooling as a methodology (Critser et al., 1997). As a result, researchers have turned their attention to rapid cooling methods to cryopreserve bovine oocytes. In 1996, Martino and colleagues (Martino et al., 1996b) demonstrated a significant improvement in the cryopreservation of bovine oocytes using a so-called “ultra-rapid cooling” method. In this report, they utilized electron microscope grids as a carrier for the oocytes and vitrification solution and plunged them directly into liquid nitrogen. Since this time, several other devices/methods to achieve rapid cooling have been developed and tested with bovine oocytes, including OPS (Vajta et al., 1998), solid surface vitrification (SSV; Dinnyes et al, 2000), gel loading pipette tips (Asada et al., 2002), glass capillaries (Rho et al., 2002), and the cryotop (Chian et al., 2004). In a series of experiments, Otoi and colleagues took a more systematic approach to develop improved vitrification solutions and methods for their addition and removal to try to account for potential osmotic damage during the procedure, and demonstrated that the use of a 0.25 ml straw could achieve results comparable to the so-called ultra-rapid cooling devices (Otoi et al., 1998). Testing various stepwise CPA addition methods, EG concentrations, and CPA removal procedures, this group achieved much better blastocysts development. They determined that a 3-step procedure was superior to a one or two-step CPA addition. Such improvements provide strong support for utilizing a fundamental approach to improving methods to cryopreserve mammalian oocytes.

The first report of a pregnancy and subsequent delivery of a human baby derived from a frozen and thawed oocyte appeared in 1986 and 1988, respectively (Chen, 1986, 1988). Several other reports appeared in the late 1980's describing additional attempts to cryopreserve human oocytes. One notable feature of these reports (and many other reports on oocyte and embryo cryobiology) is the lack of fundamental experiments designed to characterize the cryobiology of human oocytes. Instead, simple changes to a standard equilibrium protocol were made and outcomes were assessed. Changes included altering the addition and removal of the cryoprotectant (stepwise and at room temperature; (Diedrich et al., 1987)), and assessing the effects of PG vs. DMSO (Al-Hasani et al., 1987). Concerns over possible damage to the meiotic spindle during cryopreservation of oocytes slowed progress in this field during the early years. Late, in the middle of 90s, the use of low concentrations of sucrose (0.1 M) in the freezing medium became routine, and likely contributed to the increased post-thaw morphological survival of oocytes with this method. In 2001, Fabbri and colleagues (Fabbri et al., 2001) systematically studied the effects of different sucrose concentrations on oocyte survival with the equilibrium method using 1.5 M PG. Increasing the concentration of sucrose from 0.1 M to 0.3M caused a marked improvement in survival, from 33 % to 82 %. Although some investigators claimed the clinical results are nearly equivalent to the use of fresh embryos (Marina and Marina, 2003), other investigators have been more cautious in their interpretation (Coticchio et al., 2004), and in two recent reports with a very large number of cycles, the results were still rather poor (Borini et al., 2006; Levi Setti et al., 2006), especially when compared to the use of fresh embryos.

Some studies, however, have been of a more fundamental nature in which investigators have attempted to elucidate basic principles responsible for damage or death of oocytes. In such studies, intrinsic properties of oocytes, such as their permeability to water and/or to solutes, may be determined. Leibo et al. (Leibo et al., 1974) and Parkening et al. (Parkening et al., 1976) began investigation of the fundamental cryobiology of mouse oocytes in regard to intracellular freezing temperatures, effects of various low temperatures, cryoprotective agents and cooling rates on the survival, fertilizability and development. Pfaff et al reported their research on the membrane permeability characteristics to water and DMSO for in-vivo- and in-vitro-derived and cultured murine oocytes (Pfaff et al., 1998); and Agca et al on rat immature and mature oocytes (Agca et al., 2000a).

Osmotic characteristics of the plasma membrane to water and intracellular ice crystal formation kinetics of bovine oocytes from different developmental stages (GV, MII, in vitro fertilized (IVF)) have also been very well documented (Ruffing et al., 1993). Osmotic behavior in the presence of NaCl as a function of time, and intracellular ice crystal formation temperature in the presence of glycerol, ethylene glycol and propylene glycol as a function of cooling rate has been investigated. It has been determined that mature bovine oocytes have a smaller inactive cell volume fraction compared to immature oocytes. It was concluded from these experiments that differences exist in oocytes from different developmental stages and was suggested that these factors have to be considered in developing cryopreservation protocols. Later,

Agca et al published systematic studies on the effect of osmotic stress on the developmental competence of germinal vesicle and MII stage bovine cumulus oocyte complexes and its relevance to cryopreservation, the effect of developmental stage on bovine oocyte plasma membrane water and cryoprotectant permeability characteristics and temperature dependence (Agca et al., 1999; Agca et al., 1998b; Agca et al., 2000b).

The first (Hunter et al., 1992a; Hunter et al., 1992b) examined the water permeability of both "fresh" and failed-to-fertilize oocytes and found that human oocytes have oolemma water permeability characteristics very similar to mouse oocytes (0.48 μm/min/atm at 20°C) with an activation energy of 9.5 kcal/mol. Others (Fuller et al., 1992) examined the permeability of mouse and human oocytes to 1,2-propanediol and water simultaneously. The results of this study indicated that human oocytes are about twice as permeable to 1,2-propanediol as mouse oocytes. McWilliams et al. (McWilliams et al., 1995) studied osmotic and physiological responses of human oocytes to concentrated solutions of mono and disaccharides and found that non-permeating saccharides can serve as a great osmotic buffer and promotes the recovery of human oocytes. Recently, osmotic responses and tolerance limits to changes in external osmolalities, and oolemma permeability characteristics, of human in vitro matured MII oocytes was reported (Van den Abbeel et al., 2007).

The establishment of long-term preservation methods for mammalian oocytes at the desired developmental stage has significant importance in improving ART for human and various animal species. However, the determination of reliable methods for oocyte cryopreservation has been challenging. The first live birth was obtained from cryopreserved MII mouse oocytes was reported nearly 32 years ago (Whittingham, 1977), in which a slow cooling in the presence of DMSO was used. Subsequent studies in other mammalian species utilizing 1.5 M DMSO or 1,2 propanediol (PROH) and cooling rates of 0.3-0.5°C/min (seeding the samples at –7°C) to –40 or –80°C have been disappointing (Bernard and Fuller, 1996; Critser et al., 1997). These attempts have shown that it is possible to obtain live births from cryopreserved human (Chen, 1986; Porcu et al., 1997), and bovine (Fuku et al., 1992; Lim et al., 1992) oocytes, but with extremely low rates of success.

1.4 COMPLICATIONS OF THE OOCYTE CRYOPRESERVATION

Difficulties in the cryopreservation of mammalian oocytes are due to their complex structures at the organelle/subcellular level (Friedler et al., 1988; Arav et al., 1993). Furthermore, the oocyte's cytoskeleton structure can be sensitive to cooling. At the time of ovulation, in most species oocytes are in metaphase stage of the second division (MII). The dichromatid chromosomes aligned on the equatorial axis are bound to the microtubules in the meiotic spindle. This stage can be problematic for cryopreservation with temperature and CPA sensitivity of the spindle and microtubules (Watson and Holt, 2001). Cooling oocytes to low temperatures substantially disrupts cytoskeletal elements (e.g., spindle fiber integrity), causes depolymerization of the spindle and microtubules (Songsasen et al., 2002; Wu et al., 1999; Zenzes et al.,

2001). As a result, fertilization may not take place because normal separation of chromatids might be disturbed, resulting in aneuploidy following extrusion of the second polar body. Zona pellucida hardening due to premature cortical granule release can be triggered by some CPA and eventually can prevent normal fertilization (Fabbri, 2006). Additionally, a recent study indicated that irreversible oolemma lipid-phase changes occur during cooling. The large size of oocytes with consequent low surface-to-volume ratios make it more difficult for water and cryoprotectants to enter or leave the cells across plasma membranes, thus increasing the chances of ice crystal formation and CPA toxicity (Leibo and Songsasen, 2002).

Since the effects of chilling on the developmental potential of oocytes from many species are widely recognized, ultra-rapid cooling methods, first introduced by Rall and Fahy (1985), have been used to cryopreserve mouse (Isachenko and Nayudu, 1999; Nakagata, 1989; Shaw et al., 1992; Valojerdi and Salehnia, 2005), human (Kuwayama, 2007; Kuwayama et al., 2005; Yoon et al., 2003), and bovine (Cetin and Bastan, 2006; Vajta et al., 1998) oocytes with varying levels of success. Recent trends in mammalian oocyte cryopreservation have lead to the use of various devices for vitrification such as such as open-pulled straws (Vajta et al., 1998), electron microscope copper grids (Martino et al., 1996b), cryo-loops (Lane et al., 1999), cryotops (Kuwayama et al., 2005), and by solid-surface vitrification (Dinnyes et al., 2000). However, the vitrification method requires a high concentration of permeable and/or non-permeable CPAs loaded into cells before plunging into LN. Introducing this relatively high solute concentration into cells exposes the cells to extreme osmotic stresses and chemical toxicity, and is also a procedural challenge in practice (Huang et al., 2006; Stachecki and Cohen, 2004). In addition, most of these novel technologies require direct exposure of samples to liquid nitrogen in order to achieve sufficiently rapid cooling rates, and this usually precludes effective biocontainment (Mortimer, 2004).

1.5 DEVELOPMENTS OF OPTIMIZED CRYOPRESERVATION METHODS VIA FUNDAMENTAL APPROACH AND THEORETICAL ANALYSIS

Currently used oocyte cryopreservation protocols have been direct, or slight modifications of the methods developed for mouse embryos. These were primarily developed by trial and error adjustments of cooling and warming rates, and choice of CPA and CPA concentration. However, because there are a large number of protocol variables potentially affecting cell viability, an exhaustive experimental search for the optimal combination of these parameters would be prohibitively expensive in terms of time and resources. Recently, it has been realized that a fundamental understanding of the nature of damage to oocytes during the multiple steps involved in the cryopreservation procedure, such as CPA addition/removal, cooling, and intracellular ice formation temperature, is crucial. The ability for successful cryopreservation of mammalian oocytes is highly dependant upon an understanding of the fundamental cryobiological factors that determine viability or death post-thaw.

The cryopreservation process causes significant changes in the thermal, chemical, and physical environment in the tissue, with attendant risks of biological damage. Temperature changes are mainly due to heat-transfer boundary conditions imposed by the cooling and warming methods, but can also be affected

by the latent heat of fusion of ice in the cell suspension. The chemical environment may be altered prior to cryopreservation by addition of cryoprotectant agents, and the intracellular and extracellular CPA concentration changes phase in the suspending medium occurs during cryopreservation. The growth of this ice phase removes water from the remaining unfrozen solution, thus enriching the medium in solutes, and lowering the chemical potential of the unfrozen water. Consider now the development of a cryopreservation procedure. If there are n steps in the chemical-processing protocol, and m steps in the temperature profile, there will be at least p = 3n + 2m protocol parameters to optimize. Because there is interaction between the various processing steps (e.g., the effect of cooling rate depends on the cryoprotectant concentration; the effect of the warming procedure depends on the preceding freezing protocol), all p parameters should be simultaneously optimized. Whereas in the simplest case, n = 2 (a single cryoprotectant addition step and a single dilution step) and m = 2 (linear cooling and linear warming), optimization using a full factorial design with only two levels for each parameter would require 2^p=1024 experiments. Clearly, the number of experiments required for rigorous optimization of cryopreservation procedures is prohibitively large, even for the simplest class of protocols (Karlsson and Toner, 2000).

Developing protocols that optimize the survival, fertilization and developmental rates of fully grown GV and MII stage oocytes following exposure to the extreme chemical and physical stresses associated with cryopreservation has proven to be a major challenge. Cryopreservation of biological specimens causes complex changes in structure and cellular composition, and no single approach has yet proved to be universally effective. In addition, there are significant stage- and species-specific differences between freezing oocytes and embryos.

The use of mathematical models to predict the effect of cryopreservation on cells was pioneered by Mazur (1963). Rational design of freezing protocols has become possible in the wake of advances in the theoretical modeling of intracellular ice formation, a major mechanism of freezing injury (Muldrew and McGann, 1994; Pitt et al., 1992; Toner et al., 1993). Pitt (1992) has demonstrated the power of mathematical models in the optimization of non-linear freezing protocols, using a hypothetical cell type as an example. Muldrew predicted an optimal protocol for the cryopreservation of particular cartilage to -80°C using the osmotic rupture model (Muldrew and McGann, 1994), but has not attempted to test this protocol experimentally. Toner et al (1993) have used their intracellular ice formation model to optimize a protocol for the rapid freezing of 1-cell mouse embryos to -45°C in the absence of cryoprotectants, obtaining good agreement between experimental results and model predictions. The model has recently been extended to include cryoprotectants, as well as the effects of intracellular crystal growth (Karlsson et al., 1994). Theoretical predictions by Karlsson et al have been shown to be consistent with the results of an experimental protocol optimization, thus demonstrating the feasibility of using the model for the rational design of freezing protocols. Model predictions are then tested experimentally, resulting in the recovery of >80% morphologically normal oocytes after cryopreservation to -196°C. The rates of fertilization and

development of these oocytes were comparable with values obtained using current cryopreservation techniques for mouse oocytes.

1.6 OUTLINE OF THE STUDY

In this Ph.D. thesis, starting from basic cryobiology principles, following the establishment of comprehensive theoretical modeling are presented.

Chapter 1 presents an overview of the current state of oocyte cryopreservation, and the summary of the developments of optimized cryopreservation methods via fundamental approach and theoretical analysis. In Chapter 2, typical biophysical events that occur during a procedure of cryopreservation are discussed in details. Based on the classic membrane transportation equations (Kedem and Katchalsky formulism) for a ternary solution, a theoretical model that includes the movement of cryoprotectant across the plasma membrane during cooling and warming and the ternary phase diagram is derived for the first time. All equations that govern these biophysical events are presented, along with oocyte related parameters and their relevance to cryopreservation.

In Chapter 3, one stand-alone published manuscript presents the method of theoretically optimizing an ISF protocol. In this study, rat zygote was chosen as the model cell and DMSO was chosen as the permeable CPA because the most complete set of information exists for this combination. Theoretically, these calculations may be conducted for any cell type and CPA provided the appropriate information regarding the fundamental membrane permeability parameters and phase diagram solution characteristics are known. While the procedures described in this chapter focused upon rat zygotes, the cryobiological principle and the methodology would apply directly to other species and other cell types; including mammalian oocytes.

In Chapter 4, one stand-alone manuscript presents an accumulative osmotic damage model for oocyte cryopreservation. The objective of the this study was to experimentally determine osmotic characteristics of rabbit oocytes, such as the osmotically inactive volume (V_b), isotonic oocyte volume (V_{iso}), and the values of membrane permeability coefficients for water (hydraulic conductivity, L_p), and permeating cryoprotectants (P_s) . Investigation of the rabbit oocyte volume responses during the cryoprotectant agent (CPA) addition and dilution procedures was conducted and compared to the ability of the parthenogenetically activated oocytes to develop to blastocysts in culture. The results of this comparison led to the establishment of a new model to describe the accumulative osmotic damage (AOD) associated with the processes of the addition/dilution.

In Chapter 5, the research on the development of a novel cryopreservation three-step method for mammalian oocyte is presented. Cryopreservation of metaphase II oocytes requires that they pass through a critical temperature range rapidly enough to prevent chilling injury associated with the depolymerization of the metaphase spindle fibers. In order to accomplish this, a “three-step freezing” method was designed. The first step is a non-equilibrium cooling step, which reduces the sample temperature from ambient

temperature to an intermediate temperature (Tp) at a high rate. The second step involves maintaining the cells at Tp for a specific time (th) allowing the CPA to reach a critical concentration intracellularly. The third step involves rapidly cooling the cells by plunging the sample into liquid nitrogen. Using biophysical characteristics that were experimentally determined previously, such as the membrane permeability coefficient(s) for water (Lp), CPAs (P_{CPA}) and their activation energies (E_a of L_p and Ea of P_{CPA}) , and intracellular ice formation (IIF) kinetic parameters, the current model allows the investigation of the relationships among the initial CPA concentration, Tp and th at Tp. The calculation results would eliminate the conditions that lead to a high probability of intracellular ice formation (P_{IIF}) both during the holding period or the plunge into LN_2, the latter occurring if an insufficient intracellular concentration to achieve intracellular vitrification during the holding period is attained. Calculation results are presented in contour plots, from which cryopreservation protocols can be created by identifying conditions that could be used from the plots. The model was quite accurate in predicting the likelihood of intracellular ice formation, with 3 of the 4 combinations having 95 percent confidence intervals containing the value of the model's prediction for mouse oocytes.

The overall goal of the work is to develop rational design approach to cryopreservation protocols for mammalian oocyte, in which a theoretical model is used to efficiently optimize a freezing protocol for oocytes. This may be critical in developing successful cryopreservation methods for human or endangered species/breeds oocytes by drastically reducing the number of oocytes and experiments required for optimization. In addition, theoretical models can be the basis for the researchers to improve their understanding on the complex behavior of cells during cryopreservation.

CHAPTER 2. THEORY OF FUNDAMENATAL CRYOBIOLOGY AND EQUATION DERIVATION

2.1 BIOPHYSICAL EVENTS DURING CRYOPRESERVATION

Current cryopreservation protocols consist of a series of biophysical events that subject cells to major anisosmotic conditions which result in potentially damaging changes in cell volume. Cells shrink transiently upon the addition of cryoprotective agents (CPA) and then re-swell as the cryoprotectant permeates. Cells undergo a second shrinkage when cooled at rates low enough to preclude intracellular freezing as growing extracellular ice concentrates the solutes in the diminishing volume of non-frozen water, causing exosmosis. The cells return once again to their normal volume during warming and thawing. Finally, cells undergo a potentially damaging osmotic volume excursion during the removal of the cryoprotectant (Mazur, 1984, 1990). The direction and magnitude of the volume excursion depends on the manner of the addition or removal of cryoprotectant and on the inherent permeability of the cell to both cryoprotectant and water (Gao et al., 1995; Levin and Miller, 1981). These osmotically driven volume changes (at constant or varying temperatures) can be described theoretically using biophysical equations (Kedem and Katchalsky, 1958) if these transport parameters describing the permeability of the cell to water and solute are known, namely: (1) the hydraulic conductivity of water (L_p), (2) the permeability coefficient of the solute (P_S). Mazur *et al*. (1972) first proposed a "two-factor" hypotheses of cell damage during cooling and warming, based primarily on the rate of cooling. In Mazur's model, cells lose viability at supraoptimal cooling rates due to intracellular ice formation (IIF) and at suboptimal rates by a prolonged exposure to high solute concentrations. Numerous attempts have been made to correlate observations of cell injury at supraoptimal cooling rates with predictions of intracellular ice nucleation using physicochemical theory. Mazur (1960) suggested that intracellular ice formation (IIF) was caused by the growth of ice crystals through aqueous channels in the plasma membrane. Toner *et al* (1990) introduced a two-factor mechanism of IIF: volume catalyzed nucleation (VCN) and surface catalyzed nucleation (SCN) to investigate the IIF induced by heterogeneous nucleators in cell solution (VCN) and the internal surface of the membrane (SCN). Muldrew and McGann (1990) proposed a mechanism of intracellular ice formation resulting from membrane damage caused by exceeding a critical gradient in osmotic pressure. Pitt *et al* (1992) introduced a stochastic model to calculate the probability of IIF based on the extent of supercooling of the cytoplasm. For the "solution effects" caused by suboptimal cooling, Fahy (1981) and Pegg and Diaper (1988) studied the solute loading and susceptibility of slowly cooled cells to rapid warming. A quantitative investigation of any of the above theories, to different extents, requires knowledge of: (1) the change in cell water volume vs. temperature during cooling and warming, (2) the change in intracellular solute concentration vs. temperature, (3) the change in extracellular solute concentration vs. temperature, and (4) the degree of supercooling vs. temperature.

It is possible to determine these changes provided that: (1) the cell acts as an ideal osmometer (a plot of cell volume vs. 1/osmolality is linear), (2) the above transport parameters and their respective activation energies (E_a) are known, and (3) the phase diagram of the CPA solution is known. In order to accurately calculate the changes that occur during cryopreservation, one must ensure that the parameters are accurately determined and that the theoretical model is as complete as possible. Mazur (1963) first introduced a model to examine the kinetics of water loss from cells at subzero temperatures, which permitted the calculation of cell water content as a function of temperature and cooling rate, and the variability of these parameters with cell volume, surface area, hydraulic conductivity and its temperature coefficient. In his model, Mazur assumed that the plasma membrane was impermeable to the cryoprotectant at temperatures below 0^{o}C, and used the Clausius-Clapeyron equation describing the vapor pressure change as a function of temperature.

2.2 MATHEMATICAL FORMULATION OF THE MEMBRANE PERMEABILITY COEFFICIENTS

The Kedem and Katchalsky formulism was used in present dissertation as the theoretical model of the permeability of cell membranes to nonelectrolytes (Kedem and Katchalsky, 1958). Briefly, for a ternary solution consisting of a permeable solute (cryoprotectant, subscript "s") and an impermeable solute (NaCl, subscript "*n*"), the total transmembrane volume flux (J_V) and permeable solute flux (J_S) are presented as:

$$\frac{1}{A}\frac{dV}{dt} = J_v = L_p\left[(P^e - P^i) - RT(M_n^e - M_n^i) - \sigma RT(M_s^e - M_s^i)\right] \quad (2.1)$$

$$\frac{1}{A}\frac{dn_s^i}{dt} = J_s = (1-\sigma)\overline{m}_s J_v + P_s(a_s^e - a_s^i), \quad (2.2)$$

where V is cell volume and n^i_S is the number of moles of CPA inside the cell, P is the hydrostatic pressure, and M is osmolality and a is activity (explanations for descriptions, units and values of the symbols are summarized in Table A). In the term $\overline{m}_s = \dfrac{m_s^e - m_s^i}{\ln m_s^e - \ln m_s^i}$, m is the concentration in molal. The superscripts "*i*" and "*e*" refer to the intra- and extracellular cell compartment, respectively. The terms L_p, P_S and σ are parameters for the hydraulic conductivity of water, the permeability coefficient of the CPA, and the reflection coefficient, respectively. The temperature and universal gas constant are given by T and R, respectively. Equations 2.1 and 2.2 may be rewritten in more convenient terms. The contribution of the CPA to the osmolality and activity of the solution may be represented as products of molality and coefficients:

$$\begin{aligned} M_s^j &= \varphi_s \nu_s m_s^j \\ a_s^j &= \gamma_s^j m_s^j \end{aligned} \quad (2.3a)$$

where φ_s is the osmotic coefficient and γ_s is the activity coefficient, and ν_S is equal to unity for the nonelectrolyte CPA. In this paper, φ_s and γ_s are set to be unity so that

$$M_s^j = m_s^j, a_s^j = m_s^j, \quad (2.3b)$$

where j = i or e for the intra or extracellular region. For the impermeable solute (NaCl), the osmotic coefficient ϕ_n was assumed to be constant. Then the intracellular osmolality of NaCl is given by:

$$M_n^i = M_n^{(o)} \frac{V^{(o)} - V_b - V_s^{(o)}}{V - V_b - V_s}, \quad (2.4)$$

where V_b is the osmotically inactive cell volume and $V_s = N_s^i \cdot \overline{V}_s$ is the CPA volume ($\overline{V}_s$ is the partial molar volume of the CPA). The superscript "(o)" represents the initial values at t = 0. In the

absence of CPA, V_S = 0, and assuming that the initial conditions are isotonic and V_{bp} is the percentage of osmotically inactive cell volume, i.e. V_b=$V_{iso}V_{bp}$., then Eq. 2.4 becomes:

$$\frac{V}{V_{iso}} = \frac{M_{iso}}{M}(1 - V_{bp}) + V_{bp} \,. \tag{2.5}$$

This equation defines the Boyle Van't-Hoff plot, in which V / V_{iso} is plotted vs. M_{iso} / M and the percentage of osmotically inactive cell volume, V_{bp}, is given by the intercept of the plot. The relation between n_s^i and m_s^i is given by:

$$n_s^i = (V - V_b - V_s)m_s^i \,, \tag{2.6}$$

where (V -V_b- V_S) denotes the volume of intracellular water.

Combining Equations 2.1, 2.2, and 2.6 and assuming the hydrostatic pressure difference across the membrane is zero, a pair of coupled nonlinear equations that describe the cell volume and amount of solute in the cell as functions of time are obtained:

$$\frac{dV}{dt} = L_p ART\left[(M_n^i - M_n^e) + \sigma(m_s^i - m_s^e)\right] \tag{2.7}$$

and

$$\frac{dm_s^i}{dt} = \frac{(1 + \overline{V}_s m_s^i)^2}{V - V_b}\left\{[\overline{m}_s(1 - \sigma) - \frac{m_s^i}{(1 + \overline{V}_s m_s^i)}]\frac{dV}{dt} + AP_s[(m_s^e - m_s^i)]\right\} \,. \tag{2.8}$$

2.3 ACTIVATION ENERGIES FOR PARAMETERS

The Arrhenius relationship was used to describe the temperature dependence of the parameters L_p and P_S (Levin et al., 1976). The value of any parameter P_a (L_p or P_S) at any temperature T can be obtained by the following formula:

$$P_a(T) = P_{ao} \cdot \exp\left[\frac{E_a}{R}\left(\frac{1}{T_o} - \frac{1}{T}\right)\right]; \tag{2.9a}$$

or in another form:

$$\ln[P_a(T)] = -\frac{E_a}{RT} + \text{Constant}, \tag{2.9b}$$

where E_a is the activation energy for the process, expressed here in Kcal/mole, R is the universal gas constant, and T the absolute temperature. The subscript "(o)" represents the values at a reference temperature T_O. From Eq. 2.9b, if the P_a data at different temperatures are plotted as ln[$P_a(T)$] vs. *1/T* , a linear plot, (Arrhenius plot), is obtained with a slope of:

$$slope = -E_a / R, \tag{2.10}$$

from which E_a can be determined.

2.4 CALCULATIONS OF INTRACELLULAR WATER VOLUME AND CPA CONCENTRATIONS DURING FREEZING AND THAWING.

By Raoult's law, the vapor pressure of a solvent is proportional to the mole fraction of solvent. The vapour pressure of water in intracellular and extracellular regions can be described by:

$$p^i = p_o x^i, \text{ and} \tag{2.11}$$

$$p^e = p_o x^e \tag{2.12}$$

where p_O is the vapor pressure of pure water, and $x^i = \frac{n_w^i}{n_w^i + n_n^i + n_s^i}$, $x^e = \frac{n_w^e}{n_w^e + n_n^e + n_s^e}$ are the mole fractions of intracellular and extracellular water, respectively. The superscripts "*i*" and "*e*" refer to the intra- and extracellular compartments, respectively; and subscripts "*n*", "*w*" and "*s*" refer to NaCl, water and solute CPA, respectively. Further, we can write the mole fractions in the following manner:

$$x^i = \frac{n_w^i}{n_w^i + n_n^i + n_s^i} = \frac{n_w^i v_{10}}{(n_w^i + n_n^i + n_s^i)v_{10}} = \frac{V_w^i}{V_w^i + (n_n^i + n_s^i)v_{10}}, \text{ and} \tag{2.13}$$

$$\frac{1}{x^e} = 1 + \frac{n_n^e + n_s^e}{n_w^e} = 1 + \frac{W_n^e / MW_n + W_s^e / MW_s}{W_w^e / MW_w}, \tag{2.14}$$

where n is the mole number, W is the weight of a substance in grams, MW is the molecular weight, and v_{10} is the molar volume of water. We define $R_t = W_s^e / W_n^e$ in this paper instead of the standard notation R to distinguish the weight ratio from the universal gas constant R. So Eq. 2.14 becomes:

$$\frac{1}{x^e} = 1 + \frac{W_s^e}{W_w^e} MW_w \left(\frac{1}{MW_n R_t} + \frac{1}{MW_s} \right) = 1 + \frac{W_s^e}{W_w^e} G , \tag{2.15}$$

where $G = MW_w \left(\frac{1}{MW_n R_t} + \frac{1}{MW_s} \right)$. Hereafter we ignore the superscript "e" for the weight of substances in extracellular region.

The melting point for DMSO/NaCl/Water ternary solution is given by (Pegg, 1986):

$$T_m = A_1 C + B_1 C^2 + C_1 C^3 \tag{2.16}$$

where coefficients A_1, B_1 , and C_1 are functions of R_t. At any temperature above the eutectic temperature, the extracellular solute concentration at temperature T can be obtained by solving for $C=C(T, R_t)$ in Eq. 2.16. By definition, C is the total solute concentration in g/100g and can be written as:

$$C = \frac{100 W_{st}}{W_{st} + W_w} = \frac{100}{1 + W_w / W_{st}}, \tag{2.17a}$$

and

$$W_{st} = W_n + W_s = W_s (1 + 1/R_t). \tag{2.17b}$$

Rearranging the above equations, we get:

$$\frac{W_w}{W_s} = \left(\frac{100}{C} - 1) \right) \left(1 + \frac{1}{R_t} \right). \tag{2.18}$$

By putting Eq. 2.18 into Eq. 2.15, we have:

$$\frac{1}{x^e} = 1 + G \frac{W_s}{W_w} = 1 + \frac{G' C}{(100 - C)}, \tag{2.19}$$

where $G' = \frac{G R_t}{(1 + R_t)}$. The rate of change of the cell water volume is given by:

$$\frac{dV_w}{dt} = A L_p(T)(\pi^i - \pi^e), \tag{2.20}$$

where $\pi = \frac{RT}{v_{10}} \ln(p_o / p)$. Considering the cooling rate $B=dT/dt$, we obtain

$$\frac{dV_w}{dT} = \frac{ARTL_p(T)}{v_{10} B} \left[\ln p^e - \ln p^i \right]. \tag{2.21}$$

Substituting Eq. 2.11 and Eq. 2.12 for p^e and p^i in Eq. 2.21, we have:

$$\frac{dV_w}{dt} = -\frac{ARTL_p(T)}{v_{10}B}\left[\ln x^i + \ln(1/x^e)\right].$$

Replacing the x^i by Eq. 2.13 and $1/x^e$ by Eq. 2.19, we now have:

$$\frac{dV_w}{dT} = -\frac{ARTL_p(T)}{v_{10}B}\left[\ln\left(\frac{V_w}{V_w + (n_n^i + n_s^i)v_{10}}\right) + \ln\left(1 + \frac{G^{'}C(T)}{100 - C(T)}\right)\right]. \tag{2.22}$$

If the transmembrane movement of CPA is taken into consideration, the following equation is used to calculate the change in intracellular CPA (assume $\sigma = 1$):

$$\frac{dn_s^i}{dt} = AP_s(T)\left(m^e - m^i\right). \tag{2.23}$$

The intracellular CPA concentration can be calculated as $m^i = n^i_S/V_W$ and the extracellular concentration is given by:

$$m^e = \frac{W_s}{MW_s}\frac{1000}{W_w} = \frac{1000R_tC}{MW_s(100 - C)(R_t + 1)}. \tag{2.24}$$

Finally we obtained two coupled equations depicting the changes of intracellular water volume and the mole number of CPA during temperature changes with cooling rate of B in the presence of extracellular ice:

$$\frac{dV_w}{dT} = -\frac{ARTL_p(T)}{v_{10}B}\left[\ln\left(\frac{V_w}{V_w + (n_n^i + n_s^i)v_{10}}\right) + \ln\left(1 + \frac{G^{'}C(T)}{100 - C(T)}\right)\right] \tag{2.25}$$

$$\frac{dn_s^i}{dT} = \frac{AP_s(T)}{B}\left(\frac{1000R_tC}{MW_s(100 - C)(R_t + 1)} - \frac{n_s^i}{V_w}\right). \tag{2.26}$$

These equations represent a theoretical model incorporating the transmembrane movement of cryoprotectant at during a cooling rate of B. The model can be used to investigate the responses of cells to established cryopreservation procedures by simulating the cell water volume, the water flux across the plasma membrane, intra- and extracellular solute concentrations, the degree of supercooling of the cytoplasm, and the probability of ice nucleation in the cytoplasm.

CHAPTER 3. A THEORETICAL MODEL FOR THE DEVELOPMENT OF INTERRUPTED SLOW FREEZING PROCEDURES

3.1 INTRODUCTION

Current mammalian oocyte and embryo cryopreservation protocols have evolved from methods that have been successful with mouse and cattle embryos (Stachecki et al., 1998). The basic strategy typically employed involves the use of a "two-step" or "interrupted slow freezing" (ISF) procedure; which is a common approach currently used to cryopreserve many different cell and tissue types (Mazur, 1990). In general, this procedure consists of an initial slow cooling period followed by rapid cooling as the sample is plunged into liquid nitrogen (LN_2) for final storage. In the initial slow cooling step, extracellular ice is induced at a temperature just below the solution freezing point, and then slow cooling continues (at a given rate defined as: B_1) in the presence of this growing ice phase, which raises the extracellular solute concentration in the unfrozen fraction and results in water being removed from the cell via exosmosis (see Table A for a complete description of terms and abbreviations). Permeating CPAs, such as GLY, DMSO, EG or PG are typically included in the suspension medium, to protect the cell against injury from the high concentrations of electrolytes (so-called solution effects) that develop as water is removed from the solution as ice. These CPAs become increasingly concentrated intracellularly as the cell dehydrates.

As this ISF procedure continues, the slow cooling step is terminated at an intermediate temperature at which plunging occurs (T_p), and is followed by a rapid cooling step (at a given rate defined as: B_2) in which the cell is usually plunged into LN_2. Provided the initial cooling step was conducted in such a way as to allow a "critical concentration" ($[CPA]_c$) of intracellular solute ($[S]_i$; in the present study defined as CPA + NaCl) to be reached within the cell, the CPA will interact with the remaining water during this rapid cooling step, resulting in the intracellular solution forming a glass-like structure (vitrification) preventing damaging intracellular ice formation (IIF). The concentration of CPA required to achieve intracellular vitrification during the subsequent rapid cooling (and to maintain the vitrified state during warming) is dependent upon the nature of the solute, the rate of rapid cooling during the plunge into LN_2, and the rate of warming during subsequent thawing (Ren et al., 1994).

The T_p at which the $[CPA]_c$ is attained during the slow cooling phase of ISF will depend upon the initial concentration of CPA present in the cells (at the onset of the slow freezing step) and the initial slow cooling rate. For a given $[CPA]_c$, this temperature could be theoretically determined for a specific initial concentration of CPA loaded into cells prior to freezing and a specific cooling rate. This suggests that theoretical determination of an ISF cryopreservation protocol is possible provided that the $[CPA]_c$ is known.

Therefore, in the context of ISF protocol development, the goal is to determine the best selection of the initial CPA concentration ($[CPA]^0$), B_1 and the T_p, which allows the $[S]_i$ to reach the $[CPA]_c$. These

determinations can be achieved by experimental and theoretical approaches. The procedures usually involve defining ranges of prospective selections of $[CPA]^0$ and B_1 for a given cell and CPA type, followed by evaluation of these ranges to determine which will yield optimal results judged by experimental or established theoretical criteria. Many models have been proposed to integrate the above aspects (to differing extents) in an attempt to quantitatively examine the biophysical events that occur during cryopreservation. Mazur (1963; 1966) first introduced a model which allowed the examination of the kinetics of water loss from cells at subzero temperatures, relating it to the effects of cooling and warming velocity on cryo-survival. Liu *et al*. (1997) established a theoretical model incorporating the transmembrane movement of cryoprotectant at low temperatures and the DMSO/NaCl/water ternary phase diagram. Karlsson *et al*. (1996) have conducted a comprehensive study in which a coupled mechanistic model was used to design and optimize a two-step cryopreservation protocol for mouse oocytes. Briefly, their method consisted of fixing a given CPA concentration (1.5 M) then optimizing the cryopreservation protocol by: (i) minimizing the time taken to reach the final temperature (to reduce injury by solution effects) and (ii) avoiding IIF. The optimization process developed by Karlsson *et al*. involved defining a cost function equivalent to the duration of the freezing protocol. The protocol was then theoretically optimized by using a sequential simplex algorithm to minimize the cost function, subject to the constraint that the predicted incidence of intracellular ice formation remains below 5%.

The objective of the present study was to theoretically optimize an ISF protocol to cryopreserve rat zygotes. In this study, DMSO was chosen as the permeable CPA because the most complete set of information exists for solutions of this permeating cryoprotectant, specifically critical concentrations/cooling and warming rates necessary for vitrification and ternary solution phase diagram information (Pegg, 1986). The basic phenomenological strategy employed in the current model was similar to Karlsson *et al*.'s (1996) studies in that the consequences of the duration of slow cooling and the probability of IIF were considered; however the current strategy employed a different theoretical method. Specifically, the current model assumed: a) that the cell membrane was permeable to CPA at any temperature (with permeability being calculated using the Arrhenius relationship); b) the actual ternary solution phase diagram was used instead of the more general Clausius-Clapeyron equation; and c) a simplified model was used to predict IIF. Essentially, development of the model followed three steps: (1) an initial range of DMSO concentrations from 0 to 4 Molal, and a range of cooling rates from 0 to 2.5^{o}C/min were evaluated theoretically to determine the selections of $[CPA]^0$ and B_1 that would allow the $[S]^i$ to reach the $[CPA]_c$; (2) using Mazur's IIF model (Mazur, 1977), the selections that could result in IIF were eliminated; and (3) the associated plunging temperatures for the combinations of $[CPA]^0$ and B_1 ranges were then calculated. The optimum set of conditions from the final range was then selected based on minimum duration of slow cooling.

3.2 MATERIALS AND METHODS

3.2.1 Theoretical Prediction of Intracellular Water Volume and Solute Mole Number at Varying Temperatures

During slow cooling, temperature is typically decreased linearly causing the intracellular solute concentration to increase monotonically as shown in Figure 3.1. For a specific cell and CPA, the change in the intracellular CPA concentration is affected by cooling conditions, i.e. the B_1 of the process and the $[CPA]^0$ loaded into cells prior to the onset of freezing. As shown conceptually in Figure 3.1, for three different cooling conditions (initial CPA concentrations and cooling rates) a, b, and c, the $[S]^i$ reaches the $[CPA]_c$ at different temperatures, A, B and C, respectively. These temperature points are defined as the plunging temperatures (T_p).

Table 3-1. Parameter values for rat zygotes

Description	**Units**	**Value**[a]
Hydraulic conductivity L_p	$\mu m \cdot atm^{-1} \cdot min^{-1}$	0.54 (at 25 ^oC)
Solute permeability P_{CPA}	$cm \cdot min^{-1}$.	1.024×10^{-3}
Isotonic cell volume	μm^3	2.3×10^5
Surface area	μm^2	1.8×10^4
Osomotic inactive volume	μm^3	4.6×10^4
Activation energy (L_p)	$Kcal \cdot mole^{-1} \cdot K^{-1}$	14.8
Activation energy (P_{CPA})	$Kcal \cdot mole^{-1} \cdot K^{-1}$	17.1
Nucleation temperature	^oC	-35
Coefficient a_0	none	40375[b]
Coefficient a_1	none	-1837[b]
Coefficient a_2	none	20.9[b]

[a](Pfaff et al., 2000)

[b]Data for DMSO, adapted from Sutton (1991)

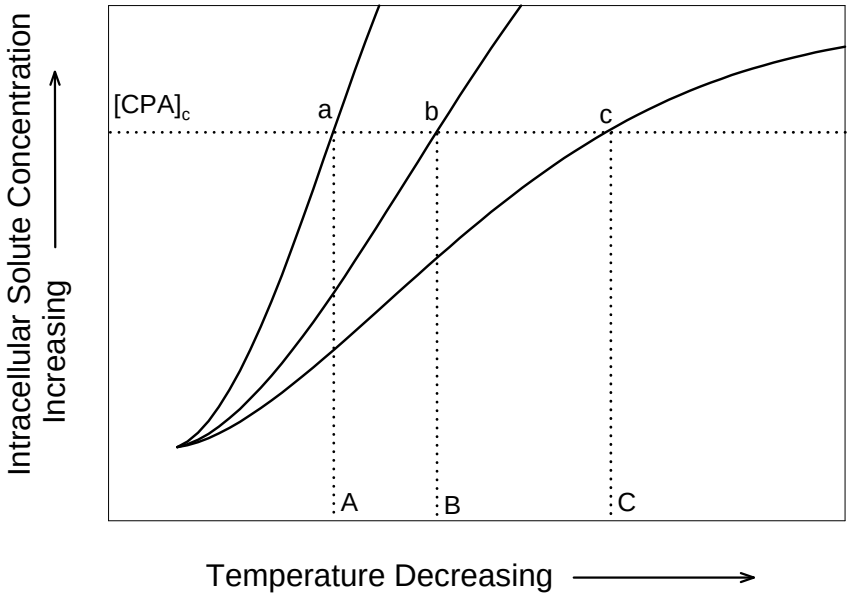

Figure 3.1. A schematic diagram showing that the intracellular solute concentration reaches the critical concentration ([CPA]c) at different temperatures (A, B and C) for different cooling conditions a, b, and c, respectively. The figure represents 3 situations where the initial CPA concentrations are the same but the cooling rates vary.

The $[S]^i$ during slow cooling can be readily calculated when the cell water volume and the number of moles of CPA are known. The changes in intracellular water volume and intracellular CPA mole number during the temperature change of rate B_1 were predicted as described by Liu *et al*. (1997) using a model consisting of the following coupled equations:

$$\frac{dV_w}{dT} = -\frac{ARTL_p(T)}{v_{10}B_1}\left[\ln\left(\frac{V_w}{V_w + (n_n^i + n_s^i)v_{10}}\right) + \ln\left(1 + \frac{G'C(T)}{100 - C(T)}\right)\right] \qquad (3.1)$$

and

$$\frac{dn_s^i}{dT} = \frac{AP_{CPA}(T)}{B_1}\left(\frac{1000R_tC}{MW_s(100 - C)(R_t + 1)} - \frac{n_s^i}{V_w}\right); \qquad (3.2)$$

where $G' = \frac{R_t}{(1 + R_t)}MW_w\left(\frac{1}{MW_nR_t} + \frac{1}{MW_s}\right)$. The values of the parameters L_p and P_{CPA} (and their associated activation energies) required for the calculations were obtained from Pfaff et al. (2000) and are listed in Table 3-1. The terms V_w and A are cell water volume and surface area, and n_s^i is the number of moles of CPA inside the cell (see Table A for a complete listing of symbols and abbreviations). The temperature and universal gas constant are given by T and R, respectively. C is the total extracellular concentration of CPA and NaCl in g/100g, MW is the molecular weight, and v_{10} is the molar volume of

water. In the current study, R_t is defined as W_s^e / W_n^e (W is the weight of a substance) instead of the standard notation R to distinguish it from the universal gas constant R.

The value of parameter $L_p(T)$ and $P_{CPA}(T)$ in equations (3.1) and (3.2) can be calculated using the following Arrhenius relationship(Levin et al., 1976):

$$P_{ara}(T) = P_{arao} \cdot \exp\left[\frac{E_a(L_p, P_{CPA})}{R}\left(\frac{1}{T_o} - \frac{1}{T}\right)\right]; \tag{3.3}$$

where $P_{ara} = L_p$ or P_{CPA} and $E_a(L_p , P_{CPA})$ is the activation energy for the process, expressed here in Kcal/mole. The subscript "o" represents the values at a reference temperature T_o.

The extracellular solute concentration, C=C (T, R_t), at temperature T can be obtained by solving the following equation of the melting point for DMSO/NaCl/Water ternary solution (Pegg, 1986):

$$T = A_1C + A_2C^2 + A_3C^3 \tag{3.4}$$

where coefficients A_1, A_2 , and A_3 are functions of R_t.

By solving these equations, it is possible to quantitatively calculate: (i) the change in cell water volume vs. temperature during cooling; (ii) the change in $[S]^i$ vs. temperature; and (iii) the change in extracellular solute concentration vs. temperature.

3.2.2 Assumptions Pertaining to Intracellular Ice Formation (IIF)

Several theories have been proposed to quantitatively study the probability of IIF (Karlsson et al., 1994; Muldrew and McGann, 1990, 1994; Pitt et al., 1992; Toner et al., 1990). These models, to some extent, require additional parameters to describe the kinetics of intracellular ice formation. These parameters are usually cell specific and are typically determined by experiments incorporating relatively high cooling rates in order to observe IIF. The present method makes assumptions based upon Mazur's "three requirements" for IIF: (1) the sample temperature has reached the ice nucleation zone, or in other words, the temperature has become lower than the nucleation temperature; (2) the intracellular water content at that time is ≥ 10% of its isotonic value; and (3) the intracellular water is 2°C or more supercooled. Based upon these criteria, IIF will not occur if any one of these requirements is not met. Cell water content can be calculated as described above while the nucleation temperature must be experimentally determined. The extent of supercooling can be calculated by taking the difference between the melting points (determined by the NaCl/DMSO/H_2O phase diagram, Equation 4) of intracellular and extracellular solutions. For any given $[CPA]^0$ and B_1, the total $[S]^i$ can be calculated at any temperature. This information enables determination of the plunging temperature T_p for specific $[CPA]^0$ and B_1 combinations, provided that the $[CPA]_c$ for a given CPA is known.

3.2.3 Source of Embryos for Ice Nucleation Experiments

Each experimental replicate consisted of five to ten postpubertal, naturally cycling female rats (8-10 weeks of age) from an outbred stock (HSD: Sprague Dawley® SD®), (Harlan Sprague Dawley, Inc., Indianapolis, IN) which were synchronized using a GnRH agonist (des-Gly^{10},[p-Ala^{6}]-Luteinizing Hormone Releasing Hormone Ethylamide (Sigma Chemical Co, St. Louis, MO). The lyophilized powder was dissolved and reconstituted using physiological saline to yield a 200 μg/ml solution. Each female rat was injected (IP) with 0.2ml (40 g) of GnRH agonist solution between 9:00 am and 10:30 am and placed in a cage with a mature male rat in the afternoon of the 4th day after synchronization. The following morning, the female rats were screened for presence of vaginal plugs, and vaginal cytology was evaluated for the presence of spermatozoa and stage of the estrous cycle. For collection and recovery of zygotes, rats were injected (IM) with 0.1 ml of a 10:2 (v/v) mixture of 100 mg/ml Ketamine (Ketaset®, Fort dodge Animal House, Fort Dodge, IA): 100 mg/ml Xylazine (Rompun®, Bayer Co., Shawnee Mission, KS) for sedation followed by cervical dislocation. The oviducts were excised and placed into a petri-dish containing phosphate buffered saline (PBS) (Life Technologies Inc., Grand Island, NY), supplemented with 1 mg/ml hyaluronidase (Sigma Chemical Co., St. Louis, MO) and 4 mg/ml bovine serum albumin (BSA) (Sigma Chemical Co., St. Louis MO). The extended, translucent oviductal ampulla was dissected to release the clutch of zygotes into the solution in the petri-dish. The zygotes were left in the petri-dish with the hyaluronidase for approximately 5 minutes to enable dissociation and removal of the cumulus cells from the zygotes. A stereo dissecting microscope (Nikon SMZ-2T) was used to evaluate the zygotes for the presence of polar bodies and pronuclei to verify fertilization. The cumulus-free zygotes were washed by transferring them through three drops of hyaluronidase-free PBS before being placed into 40 μl culture drops of Ham's F10 under oil in petri-dishes, and maintained in an incubator in humidified 5% CO_2 and air / 90% N_2 at 37°C.

3.2.4 Determination of Critical Concentration

For the purposes of this study, the $[CPA]_c$ was assumed to be the greater value between the concentration necessary to induce vitrification during cooling ($[CPA]_c$) and that required to preclude devitrification during warming ($[CPA]_c$) at rates that could be attained in the given cell containers. This concentration is defined as $[CPA]_c$, and was the value used in the optimization calculation. Using the $[CPA]_c$ ensures a conservative estimate of $[CPA]_c$ for determination of $[CPA]^0$, $B_1$and the T_p. For the plunging step, the following formula introduced by Sutton (1991) was used for calculating the critical cooling rate (B_c) for a given concentration (C) of solute (CPA and NaCl) in solution with H_2O:

$$B_c = a_o + a_1 C + a_2 C^2 \qquad (3.5)$$

where a_0, a_1 and a_2 are coefficients (Table 3-1). For the present formalism, C was based on CPA and NaCl content at a constant ratio (it should be noted that Equation 3.5 was originally developed based on

CPA only). By measuring B_c, and then solving Equation 3.5, the $[CPA]_c$ was determined. For the warming process, data published by Ren *et al*. were used to estimate the critical concentration ($[CPA]_c$).

3.2.5 Measurement of Cooling and Warming Rates Inside Straws

For the present study, standard 0.25 ml plastic straws were chosen as the freezing container. For measurement of B_2, the straws were placed in LN_2 vapor. The distance from the straws to the LN_2 surface was adjusted until the temperature stabilized at approximately -30°C, then they were plunged into the liquid phase. Data were recorded at the rate of 20 data points per second using a computer interfaced temperature measurement board (Omega, Stamford CT.). Cooling rates were calculated as $B_2 = \Delta T/\Delta t$, where ΔT is the temperature difference between two adjacent points which are apart by Δt in time (in this case, Δt=0.05 seconds). For determining B_3, the straws were transferred to a 37°C water bath directly from LN_2. Data were recorded and analyzed as described above.

3.2.6 Prediction of the Theoretically Optimized Cryopreservation Protocol

The procedure for theoretical optimization involved three steps. First, the $[CPA]_c$ was determined based on measurement of B_2 and B_3 inside the straws. Next, the initial investigation ranges for $[CPA]^0$ and B_1 were determined and these ranges were quantized into appropriate intervals for subsequent numerical calculation of $[S]^i$ and degree of supercooling. In the final step of model development, combinations of $[CPA]^0$ and B_1 values that could be used were determined and the T_p values for these combinations were calculated. To be more specific, these combinations are determined by using the criterion that intracellular dehydration must reach the $[CPA]_c$ to restrict the selections of $[CPA]^0$ and B_1 values, then using Mazur's "three requirements" IIF model to eliminate the selections that could result in IIF. The optimum set of conditions can then be selected by the minimum duration of slow cooling, which minimizes solution effects.

In this study, $[CPA]^0$ values ranging from 0 to 4 molal (4 molal ≈ 3.1 Molar) were chosen in conjunction with B_1 values ranging from 0 to -2.5°C/min. These ranges were then divided into fifty equal intervals. The calculations cover a temperature range (T_{seed} -T_{end}), where T_{seed} is the seeding temperature (the T_{seed} was set equal to the melting point) and T_{end} is the end point of the calculation. Because the T_p is unknown prior to the calculation, a lower temperature (-80°C in the current study) was set to ensure the calculated T_p would be included in the range. For each of these 2500 (50X50) combinations of $[CPA]^0$ and B_1, the intracellular CPA concentration, intracellular water volume and extent of supercooling at each temperature point were calculated. The temperature points ranged from the T_{seed} to the T_{end} at the interval of (T_{seed} -T_{end})/100.

The intracellular concentration for each combination of $[CPA]^0$ and B_1 was calculated at each temperature point starting from T_{seed} to T_{end}, and the value was compared to the $[CPA]_c$. When the predicted value became greater than the $[CPA]_c$, the calculation was terminated for this combination of $[CPA]^0$ and

B_1 and the temperature point was recorded. The extent of supercooling and intracellular water volume was then calculated for the temperature points that fell below the nucleation temperature to determine if IIF would occur based on Mazur's "three requirements". Any combination which would likely result in IIF was then ruled out. If the $[S]^i$ could not reach the $[CPA]_c$ over the entire temperature range, this combination of $[CPA]^0$ values and B_1 values were also ruled out. The remaining points were considered the optimum range for plunging in LN_2 for that particular combination of $[CPA]^0$ and B_1 values.

Because the B_1 and T_p values for the optimum region are known, the duration of slow cooling can readily be calculated as:

$$\tau_i = \frac{T_{pi} - T_{seedi}}{B_{1i}} \quad , \tag{3.6}$$

where τ_i is the time required to cool the cells from seeding temperature to plunging temperature, and T_{pi}, T_{seedi} and B_{1i} are the associated T_p, T_{seed} and B_1, for each individual combination, respectively. Each τ_i can be determined for each of the combinations of initial concentration and cooling rate.

3.3 RESULTS

3.3.1 Cooling/Warming Rates in 0.25 ml Plastic Straws

Experimental measurements of temperature during plunging of four straws (0.25 ml) are presented in Figure 3.2A and during warming in Figure 3.2B. During plunging, the cooling rate changed from 0 to a maximum of approximately $1.0x10^4$ °C/min, then decreased to 0 as the sample temperature equilibrated with LN_2 at -196 °C. During warming (in a 37°C water bath), the warming rate changed from 0 to a maximum of approximately $2.0x10^4$ °C /min, then decreased to 0 when the sample temperature equilibrated with the water bath.

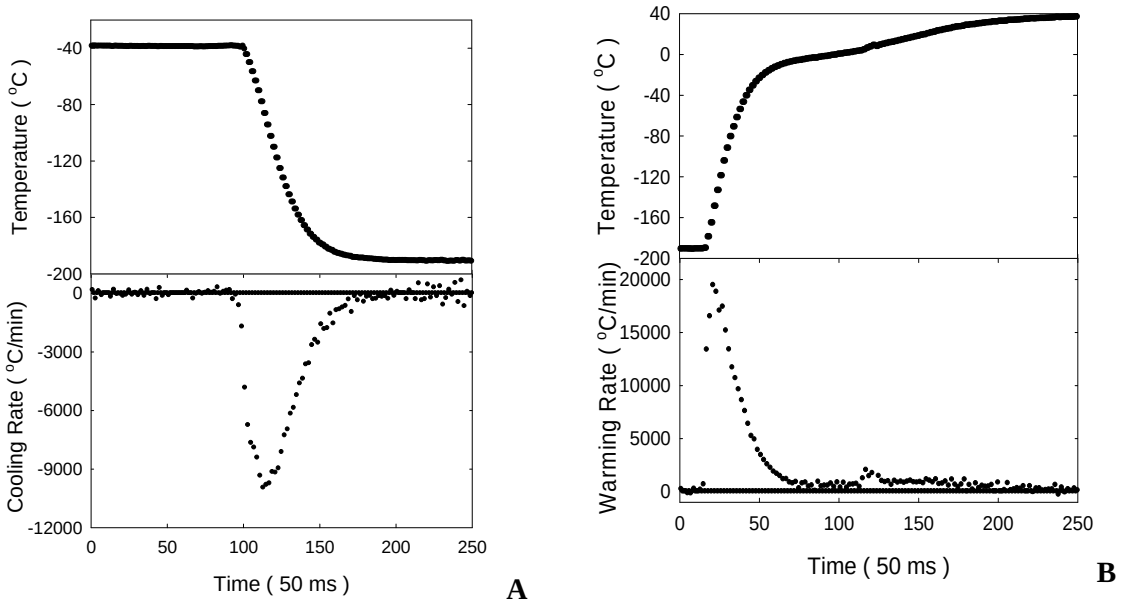

Figure 3.2. Panel A represents changes in sample temperature (top) and cooling rate (bottom) when 0.25 ml straws are plunged into LN2. Panel B represents temperature (top) and warming rate (bottom) when 0.25 ml straws are placed into a 37oC water bath .

3.3.2 *Estimation of Critical Concentration.*

To precisely calculate the $[CPA]_c$ from measured B_2 and B_3 is beyond the scope of the current study. The B_2 for 40% (w/w) DMSO and NaCl concentration was calculated using Sutton's formula (Sutton, 1991) and was determined to be 3.5 $x10^2$ °C/min, which is much lower than the actual cooling rate inside the straw during plunging. The B_3 for 45% and 47.5% (w/w) binary solutions of DMSO (e.g. DMSO without NaCl) have been determined to be 2.38 x 10^3°C/min and 1.86 x 10^3 °C/min, respectively (Ren et al., 1994), which is also much less than the actual warming rate. Considering both the cooling and warming rate requirements, the critical concentration was estimated as 40% w/w for the experimental conditions.

3.3.3 Experimental Determination of Intracellular Nucleation Temperature

Images captured from the recorded cryomicroscopy experiments were examined to determine the intracellular nucleation temperature. When rat zygotes were cooled at a rate of 10°C/min in 1.5M DMSO, IIF reached 5% when the temperature reached –36°C and all zygotes had IIF at - 46°C (no zygotes had IIF at –34°C; Figure 3.3). Based upon these measurements, the onset of nucleation was estimated to be –35°C for rat zygotes.

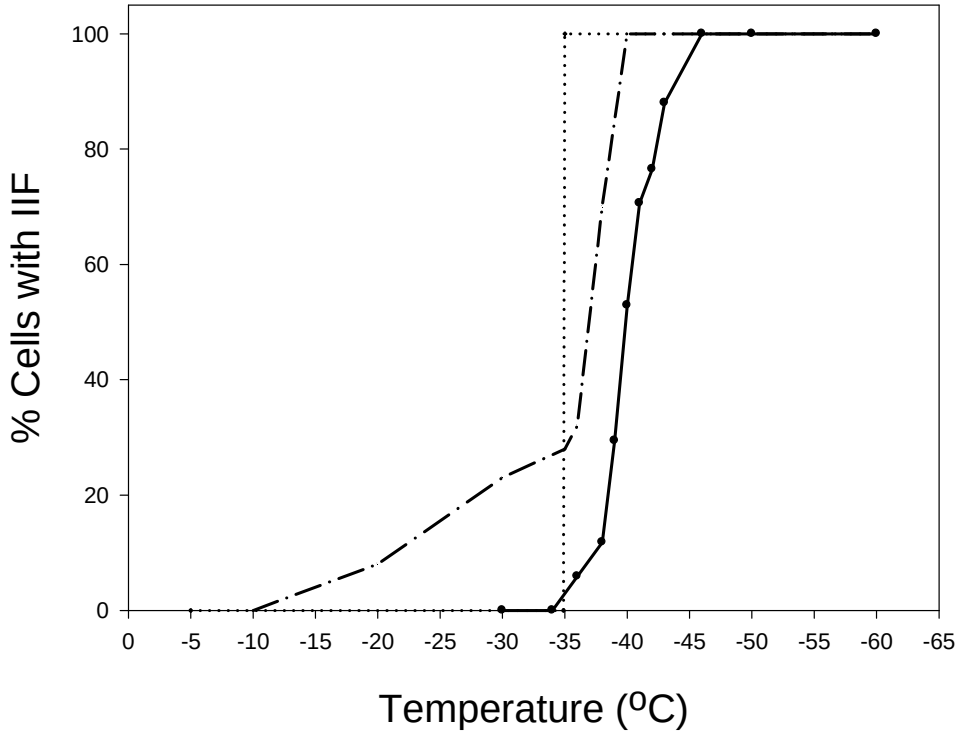

Figure3.3. The solid line shows measured intracellular nucleation temperatures of rat zygotes in 1.5 M DMSO cooled at 10°C/min. The data represent the percentage of zygotes with IIF from 3 experimental runs (total number of 28 rat zygotes). The dotted line shows the corresponding predicted values of IIF in rat zygotes calculated using Mazur's model of IIF. The dot-dash line shows the IIF predictions for mouse oocytes in the presence of glycerol for comparison.

3.3.4 Estimation of Optimal Plunging Temperature

A hypothetical rat zygote was considered suspended in 50 equally spaced $[CPA]^0$ values ranging from 0.08 to 4 molal and cooled from T_{seed} to T_{end} at one of fifty equally spaced B_1 values ranging from 0.05 to 2.5°C/min. For each of the 2500 combinations of $[CPA]^0$ and B_1 values, the model calculated $[S]^i$, water volume and supercooling at each temperature point (100 equally spaced points from T_{seed} to T_{end}). The criteria of $[CPA]_c$ exceeding 40% (w/w) and no predicted IIF were used to divide the plane of $[CPA]^0$ vs. B_1 into three regions (Figure 3.4) as follows:

Region I: in this region, no combination of $[CPA]^0$ and B_1 allows the intracellular solute concentration to reach the $[CPA]_c$ at any temperature point. This region contains the high cooling rate zone and low initial CPA concentration zone. The high cooling rates in this region (bottom of Figure 3.4) would not allow the cell to dehydrate sufficiently, and the low concentrations (left part of Figure 3.4) are simply not high enough for the intracellular solute concentration (CPA and NaCl) to reach the $[CPA]_c$. The cooling rates and concentrations in this region were rejected in the developing optimized ISF procedure.

Region II: The combinations of $[CPA]^0$ and B_1 allow the $[S]^i$ to reach $[CPA]_c$ at certain temperature points, but under these conditions there is a high probability of IIF during slow cooling. If a cell is cooled under these conditions, the cell would be supercooled more than 2°C when the temperature reaches the nucleation zone (-35°C in this case) and intracellular water content would be greater than 10% of its isotonic volume. These conditions were also rejected in developing the ISF procedure.

Region III: The combinations of $[CPA]^0$ and B_1 allow the $[S]^i$ to reach the $[CPA]_c$, and no IIF is predicted during slow cooling. Figure 3.5 shows the T_p for each $[CPA]^0$ and B_1, indicated by the points in a 3-dimensional plot (Panel A) and a 2-dimensional plot (Panel B). These points range from approximately -25°C (for points around the high concentration/low cooling rate corner) to approximately -35°C (for points around the low concentration/high cooling rate corner).

There is a minimum $[CPA]^0$ boundary below which no B_1 (in the range of 0.05 to 2.5°C/min) allows the $[S]^i$ to reach the $[CPA]_c$. There is also a maximum B_1, above which any B_1 causes the same effect. Roughly, these two limits construct a box of $[CPA]^0$ and B_1 values that are candidates for the optimized protocol. The optimum set of conditions was selected by minimizing τ_i from Equation 6 and determined to be: a $[CPA]^0$ of 1.2 M DMSO, a B_1 of 0.95°C/min and T_p of -35°C.

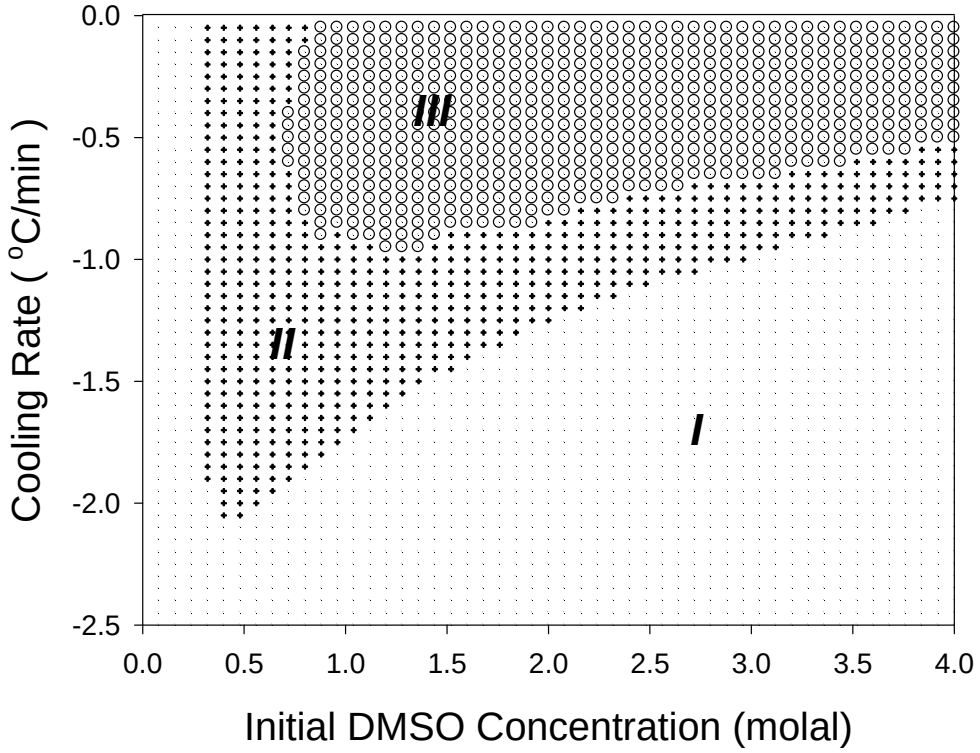

Figure 3.4. A diagram showing the plane of initial CPA concentration and cooling rate is divided into three regions. In Region I (dotted), no combination of initial CPA concentration ([CPA]0) and cooling rate (B1) allows the intracellular solute concentration ([S]i) to reach the critical concentration $[CPA]_c$, 40%) necessary for intracellular vitrification to occur during plunging into LN2. In Region II (crossed), the combinations of [CPA]0 and B1 allow the [S]i to reach 40%, but, based upon Mazur's intracellular ice formation (IIF) model [11], IIF is predicted to occur before plunging. In Region III, the combinations of [CPA]0 and B1 allow the [S]i to reach 40%, there is no IIF during slow cooling, and recrystallization is not predicted during warming.

3.4 DISCUSSION

Historically, mammalian embryo ISF procedures have further been divided into two categories based on the optimal plunging temperature and warming conditions (Rall et al., 1984). One category ("slow warming" method) utilizes slow cooling (<1°C/min) to temperatures below -60°C, followed by transfer into LN_2 (-196°C) and subsequent slow warming at rates of ~25°C/min or less (Whittingham et al., 1972; Wilmut, 1972). The second procedure ("rapid warming" method) utilizes slow cooling to an intermediate temperature, usually between –25° and -40°C, followed by transfer into LN_2 and subsequent rapid warming at rates above ~300°C/min (Whittingham et al., 1979).

The current study proposes a new method by which "rapid warming" ISF procedures may be enhanced through modeling, taking into account typical cryobiological practices, i.e. the use

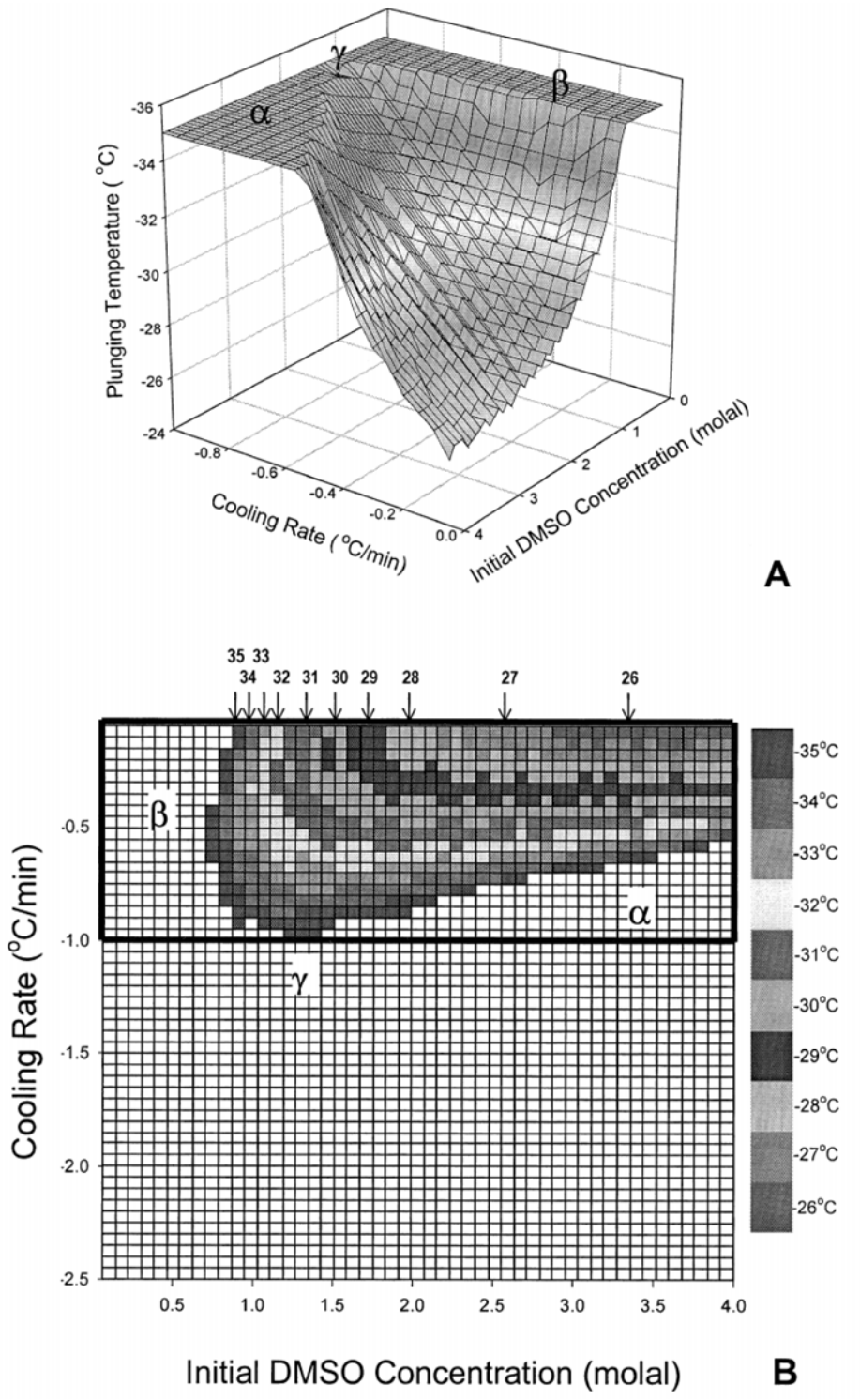

Figure 3.5. Plunging temperatures for each combination of initial CPA concentration ([CPA]0) and cooling rate (B1) in Region III of Figure 3.4. A three dimensional plot (Panel A) shows the trend of how the optimal plunging temperature changes with different [CPA]0 and B1 values. The gray level coded plot (Panel B) of plunging temperatures shows the exact values (indicated in °C). The points from Region I and II are plotted in white, and only data in the black box in Panel B were included in Panel A.

of 0.25 ml plastic straws, 0 to 4 Molal DMSO concentrations and cooling rates between 0 to 2.5°C/min. To apply this approach, specific fundamental biophysical and physical-chemical parameters must be known, including: cell membrane permeability coefficients and their activation energies, ternary solution

(NaCl/CPA/H_2O) phase diagram information and the solution's vitrification properties. This study presents a model designed to develop ISF procedures based upon two criteria: (i) the $[S]^i$ must reach a $[CPA]_c$, at which the intracellular solution can be readily vitrified during plunging and (ii) lethal IIF must be avoided. The model was applied to the rat zygote, using DMSO as the permeating CPA, and from the predicted optimal: (1) $[CPA]^0$ range, (2) B_1 range and (3) associated T_p values, a protocol consisting of: a $[CPA]^0$ of 1.2 M DMSO, a B_1 of 0.95°C/min and a T_p of -35°C was predicted by calculating which set of conditions resulted in the minimum duration of slow cooling.

Several other models have been developed to attempt to quantitatively examine the biophysical events that occur during these procedures, the most recent being those developed by Karlsson *et al*., who proposed a theoretical model of optimization and applied it to the mouse oocyte considering glycerol as the permeating CPA. In contrast to Karlsson's study, in the model described here, the changes of intracellular water volume and $[S]^i$ during cooling and warming were predicted as described by Liu *et al*. (Liu et al., 1997) considering that the cell remains permeable to CPA at low temperatures. In addition, a fixed initial CPA concentration was not a necessary constraint in the current model. This allows more flexibility in determining the set of conditions for optimum ISF protocols without needing to repeat the simulations for other fixed CPA concentrations. It also allows the possibility of considering other biological concerns that are equally crucial in cryopreservation. For example, the potential toxic effects of CPAs on cells usually become severe when CPA concentrations are high and the exposure time is long. In this regard, when the duration of slow cooling does not change greatly over a wide range of CPA concentrations, a lower CPA concentration should be chosen. This is possible using the current model, and from this point of view, the upper-right corner of Figure 3.5B (high $[CPA]^0$, low B_1) on the Initial Concentration/Cooling rate plane could be readily eliminated.

Another issue involved in ISF procedure development is IIF estimation. Lacking the necessary parameters for the rat zygote, the most current IIF models could not be used (i.e. (Karlsson et al., 1994)); however, Mazur's model (1997) agreed closely with experimental data (Figure 3.3) and was therefore considered adequate. The use of different IIF models will affect the shape of Zones II and III. However, the use of different IIF models would not fundamentally change our results because: (1) the boundary between Zones I and II (Figure 3.4) is independent of the choice of slow cooling IIF model (it is based on the $[CPA]_c$ required for vitrification during the rapid cooling step), with the boundary between Zones II and III (Figure 3.4) constrained to stay within Zone I; and (2) IIF curves from the experimental data agree closely with predictions made using Mazur's model as well as those from Karlsson's predictions for mouse oocytes (Figure 3.3).

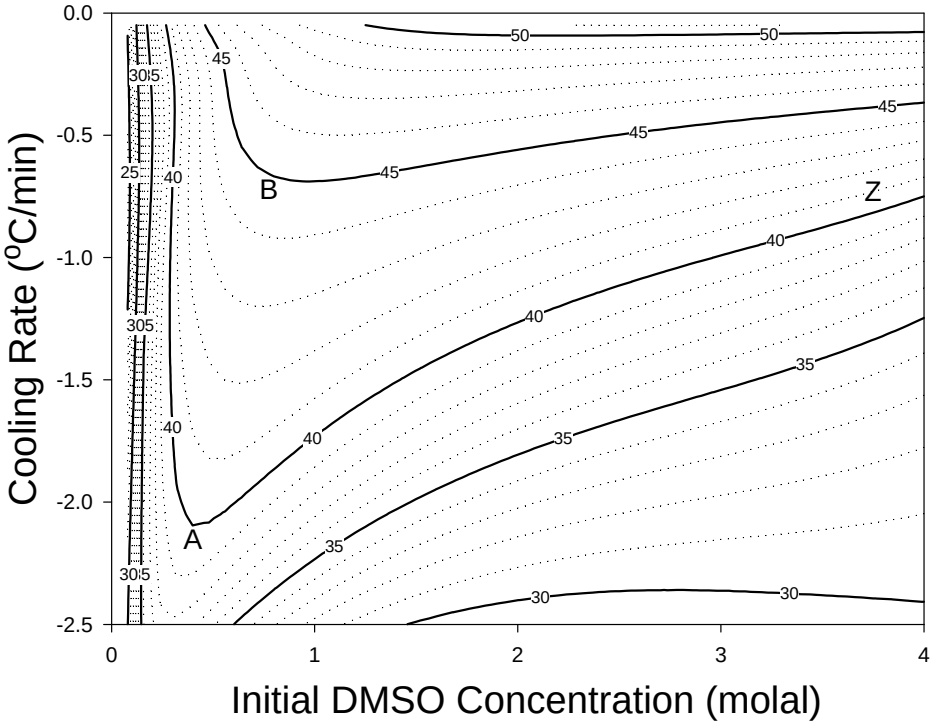

Figure 3.6. A contour graph of the maximum intracellular solute concentration the cell can achieve during slow cooling from the seeding temperature to the Tend. The numbers present the percentage of the CPA concentration.

The current model could also be used to optimize a situation in which the cell type is biologically sensitive to supercooling and not to CPA exposure time. The high $[CPA]^0$, low B_1 region of Figure 3.5 indicates that the T_p values are much higher in this section (approximately ten degrees higher). Although the cells are exposed to relatively high CPA concentrations and subzero temperatures much longer (due to lower B_1 values), the absolute temperature values are much higher and supercooling is much lower. According to Pitt (1992), two effects dominate IIF: (1) supercooling and (2) exposure time. Therefore, it would be predicted that these cells should be cooled at a lower B_1 value with a higher $[CPA]^0$ value.

The model's prediction, indicated by Figure 3.5, that a higher $[CPA]^0$ allows for a lower B_1 value is entirely consistent with previous theory and experimental data as well (Mazur et al., 1984). A contour map of maximum $[S]^i$ plotted for different $[CPA]^0$ and B_1 values is presented in Figure 3.6. For discussion purposes, the section "AZ " of the line "40%" was used as the trace of optimal combinations of $[CPA]^0$ and B_1 values. It is clear that the optimal B_1 decreases as the $[CPA]^0$ increases. There are two distinguishing aspects here that are important to note. First, as explained previously by Mazur, the introduction of CPA makes the cells susceptible to IIF at even lower cooling rates. This statement supports the current prediction, since the IIF region in Figure 3.4 has the same trend as the line of "40%" in Figure 3.6. The cause of this phenomenon is most likely that the higher $[CPA]^0$ values tend to trap more water inside the cell and thereby increase the probability of IIF (Diller, 1982). For the situation of a same cooling rate but different $[CPA]^i$, a cell with lower $[CPA]^i$ has to dehydrate more than a cell with higher $[CPA]^i$ to make its

intracellular concentration equilibrate with extracellular concentration, which increases during slow cooling in the first step. For this scenario, the IIF occurring during slow cooling could be avoided by using a lower B_1. Second, as illustrated in Figure 3.6, for a given B_1, higher $[CPA]^0$ values tend to have a lower C_{max} during slow cooling (again, most likely due to the higher intracellular CPA concentration tending to trap more water inside the cell). For this scenario, the issue is the $[CPA]_c$, and a lower $[CPA]^0$ must be chosen to ensure that the $[S]^i$ can become greater than the $[CPA]_c$.

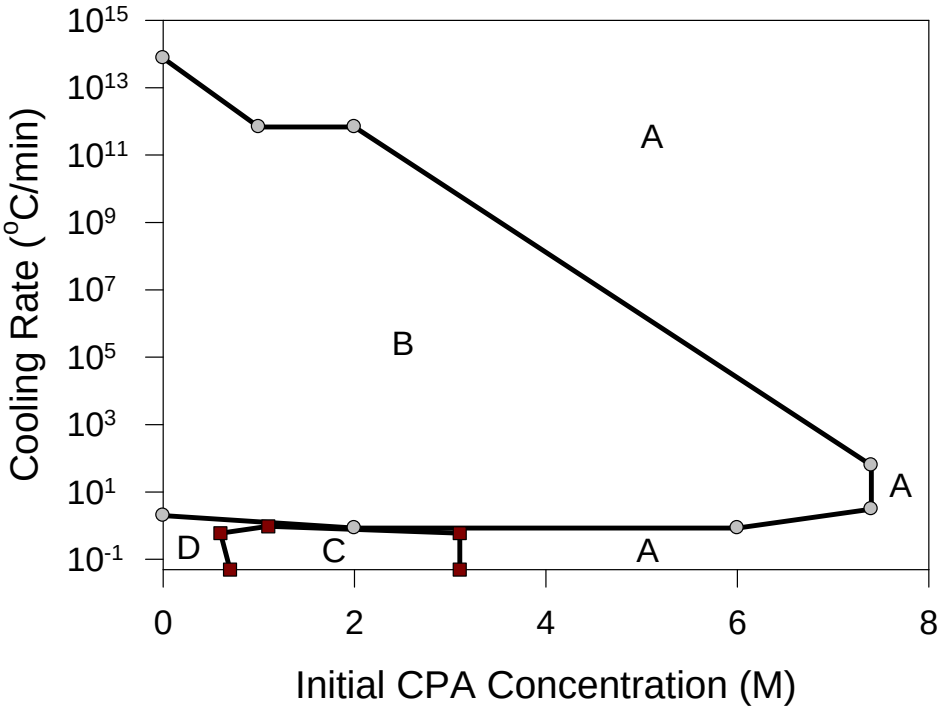

Figure 3.7. Comparison of the current model predictions of optimum combinations of initial CPA concentrations ($[CPA]^0$) and cooling rates (B_1) which would be predicted to avoid IIF in rat zygotes (Region C) shown with similar predictions from Karlsson et al. [17] for mouse oocytes in the presence of glycerol (Regions A, C and D). Region C is consistently predicted by both models. Region D is eliminated by the current model due to low $[CPA]^0$, which does not allow the intracellular solute concentration to reach the critical concentration ($[CPA]_c$). Region B is predicted (by Karlsson et al.) as a supercritical region for which the final crystallized volume fraction would exceed 10-3, indicating intracellular ice formation.

The calculation results and predicted IIF zone for mouse oocytes first presented by Karlsson et al. in 1994 are in close agreement with the results predicted in the current study for rat zygotes using DMSO. Their plot is reconstructed along with the current predictions (Fig. 3.7), and the results indicate close agreement until low $[CPA]^0$ values (less than 0.6 molal) are considered. The discrepancy in this range may be attributed to the current model's prediction that the C_{max} in this situation could not reach the required $[CPA]_c$ if these $[CPA]^0$ values were used.

In Karlsson *et al.*'s most recent study, a cost function was used to optimize the duration time of the freezing protocol, and this may be accomplished in a simplified manner in the current model by calculating the duration of slow cooling using Equation 3.6. From Figure 3.8, Panel A, it is obvious that higher B_1 values decrease τ_i dramatically, even though the corresponding T_p values are lower than those using the

lower B_1 values. Figure 3.8, Panel B indicates that there is an optimal $[CPA]^0$ for a given B_1, which minimizes the duration of the slow cooling step. For the rat zygote, this optimal $[CPA]^0$ changes slightly for different B_1 values. When the B_1 increases from 0.1°C/min to 0.95°C/min, the optimal $[CPA]^0$ decreases from 1.7 Molal to 1.2 Molal. Similar to the predictions made by Karlsson's model, these optimal conditions occur right on the border of regions where unacceptable cell damage is predicted. Therefore, though theoretically optimal, this set of conditions may actually be risky in practice, because any procedural error (e.g., fluctuation in cooling rate, error in solution preparation) or error in solution properties (e.g., error in $[CPA]_c$ estimation) could result in unexpected negative consequences. Indeed, the determination of Zone III is very sensitive to the value of $[CPA]_c$. The estimated $[CPA]_c$ values used in the model were based on published data for binary solutions (e.g. CPA and H_2O only). If this approximation resulted in an under-estimation of $[CPA]_c$, it could be detrimental because in practice the $[S]^i$ would not be high enough at T_p to ensure vitrification during plunging. By selecting a point more towards the center of Zone III, (e.g. a $[CPA]^0$ of 1.5 Molal DMSO, a B_1 of 0.5°C/min and a T_p of -30°C) a more conservative estimation can be achieved.

Consistent with the current model, Hirabayashi (1997) recently reported cryopreservation of 2-cell rat embryos using an ISF method consisting of a 0.5 °C/min B_1, a $[CPA]^0$ of 10%(v/v) DMSO (~ 1.45M), and a T_p of -30°C. Using late morula or early blastocysts obtained from naturally ovulated and mated Wistar female rats, Utsumi *et al*. (1992) investigated the effects of $[CPA]^0$ on percent survival (at a fixed B_1) and found a 0% and 20% survival rate for 0.15 M and 0.3 M DMSO, respectively. Survival increased to 60% and 59% for 1.0 M and 1.5 M. This same study also reported the effects of B_1 and T_p (at a fixed $[CPA]^0$) on embryo survival. Utsumi *et al.* concluded that survival decreased dramatically when a 5°C/min B_1 was used; while, for the same T_p, the percent survival tended to be higher if a lower B_1 was used. All of these experimental results correspond well with the current model predictions (Region III in Figure 3.4). However, it is important to note that direct comparisons cannot be made because embryo developmental stages and specific experimental conditions were different from those used to develop the model in the current study.

Figure 3.6 suggests an alternative way to optimize ISF procedures. If a discrete isoconcentration line is roughly used as the guideline for selecting $[CPA]^0$ and B_1, the "turning point" (e.g., A and B in Figure 3.6, where the curve has the smallest radius) could be considered as the optimal point for corresponding isoconcentrations since B_1 has the maximum value while $[CPA]^0$ is close to the minimum value. If a comparison is made between the turning points of 40% and 45% isoconcentration lines, we can conclude that the optimal B_1 is much higher for 40% than 45% and the $[CPA]^0$ is relatively lower. The former condition, higher B_1 and lower $[CPA]^0$, would appear to be optimal because the higher B_1 shortens the duration of slow cooling (therefore potentially reducing solution effects injury), and the lower $[CPA]^0$ lowers the osmotic stress and lessens the potential CPA toxicity.

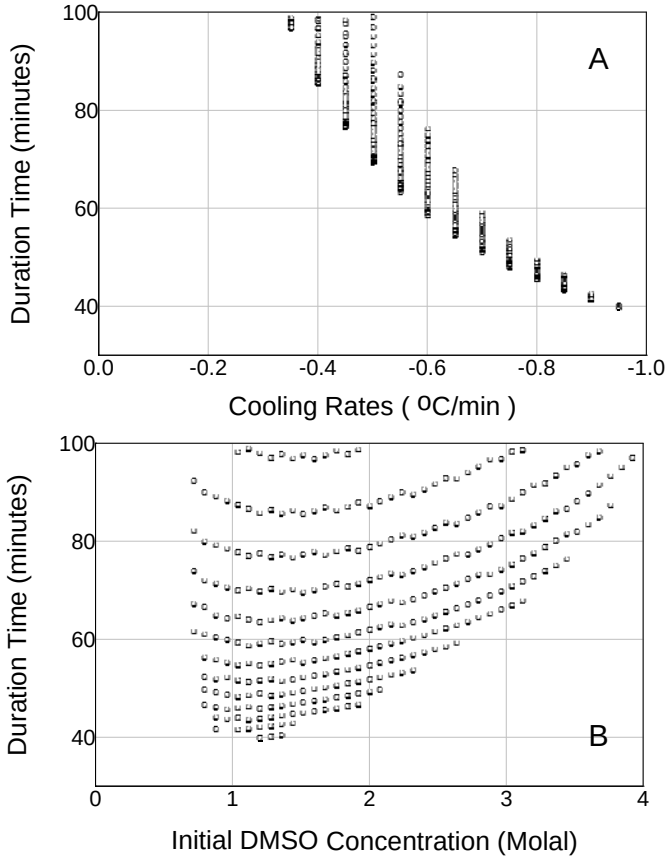

Figure 3.8. Duration of the slow cooling step for different cooling rates (B_1) and initial CPA concentrations ($[CPA]_0$). Duration decreases as the cooling rate increases (panel A). For each B1, there is a corresponding $[CPA]_0$, which minimizes the duration (panel B).

The $[CPA]_c$ is constrained by the B_2 during plunging and B_3 during thawing for a given solution. It is important to note that if these rates could be increased by using a thinner container, or material with higher heat transfer properties, then $[CPA]_c$ may be reduced. This would result in situations where equilibrium cooling could be performed much more efficiently since higher B_2 values and lower $[CPA]^0$ values could be applied. The positive results reported by investigators who use thermal-pulled, thin straws may be due to these reasons (Vajta et al., 1997).

CHAPTER 4. ACCUMULATIVE OSMOTIC DAMAGE MODEL FOR OOCYTE CRYOPRESERVATION

4.1 INTRODUCTION

Oocyte cryopreservation can also provide more efficient treatment for individuals needing oocytes from donors and those wishing to preserve fertility before cancer treatments. While advances have been made in oocyte cryopreservation as measured by the delivery of healthy babies in recent years (Gook and Edgar, 2007), continued optimization of human oocyte cryopreservation techniques is challenging due to the scarcity of material for experimentation. Cryopreservation consists of several steps including adding and removing cryoprotectants and cooling and warming. Each of the steps can be conducted in a large number of ways. Furthermore, recent trends in mammalian oocyte cryopreservation have lead to the use of various devices for vitrification such as open-pulled straws, electron microscope copper grids, cryoloop, cryotop, or even without any containers in micro-drops (Papis et al., 2000) and by solid-surface vitrification. Therefore, testing all of the possible options for cryopreservation through experimental optimization will require a very large number of oocytes. Conducting such trials with human oocytes would be very challenging for many reasons (de Melo-Martin and Cholst, 2007). As a result, rapid advances in the understanding of mammalian oocyte cryobiology will require the use of animal models.

The rabbit has been used as a model organism for studying mammalian reproduction for decades (Chang et al., 1970; Heape, 1891; Pincus, 1939); in particular it was instrumental in the development of techniques such as in vitro fertilization, embryo culture, and embryo transfer that are essential components of modern assisted reproductive medicine (Betteridge, 1981; Chang, 1948, 1959). Experimental evidence suggests that the extreme sensitivity of cattle and pig oocytes to cooling in comparison to oocytes from humans may make them relatively poor models (Hunter et al., 1991; Liu et al., 2003; Martino et al., 1996a).

Optimization of cryopreservation procedures can be pursued by a wholly empirical approach, or by using fundamental cryobiology theory and testing the theoretical results experimentally (Leibo, 2007). Taking a theoretical approach with the use of computer modeling requires the knowledge of several biophysical parameters of the cells under study, including the cell volume (which includes the proportion of osmotically-active and non-active components), the cell surface area, and the permeability of the cell to water and cryoprotectants. Using computer modeling, we investigated the rabbit oocyte volume responses during the cryoprotectant agent (CPA) addition and dilution procedures, and compared these responses to the ability of the oocytes to develop to blastocysts in culture. The results of this comparison led to the establishment of a new model to describe the accumulative osmotic damage (AOD) associated with the processes of the addition/dilution. This new model more accurately describes the viability loss seen compared to a simpler maximum volume excursion model which has been described in the past.

4.2 MATERIALS AND METHOD

4.2.1 Oocyte collection

Mature (20-22 weeks old) Hycole hybrid female rabbits were superovulated by intramuscular injection of 120 IU pregnant mare serum gonadotrophin (PMSG, Folligon, Intervet International B.V., Boxmeer, Holland) and 180 IU human chorionic gonadotrophin (hCG, Choragon, Ferring GmbH, Kiel, Germany) intravenously 72 h later. Mature oocytes were flushed from the oviducts 13–14 h post-hCG injection with mM199. The cumulus cells were removed from the oocytes by mechanical pipetting in 5 mg/mL hyaluronidase in mM199 at 37°C. The oocytes were kept in 50-µl drops of mEBSS in a Petri dish covered with mineral oil inside an incubator with a humidified atmosphere (appx. 90%) of 5% CO_2 in air at 39°C. Oocyte perfusion and image acquisition

The method for microperfusion of oocytes has been described previously (Gao et al., 1994). Briefly, one cover of a 10 cm Petri dish was placed on the stage of an Olympus (IX-71) inverted microscope. Two oocytes were placed in a 50-µl droplet of mM199 in the center of the dish cover. Two holding micropipettes were mounted on Narishige micromanipulators to immobilize these oocytes by negative pressure applied to the outer zona pellucida by two Narishige IM-5A injectors, and the oocytes were carefully placed inside the view field of the microscope. One mL of the CPA solution (either Me_2SO, EG, GLY or SU) was added to the mM199 droplet on the perfusion dish to perfuse the held oocytes at the room temperature (23-24°C). To minimize the evaporation from the mM199 droplet, the time taken between placing the oocyte in the 50-µl droplet and flushing it with the perfusate was limited to 30 seconds. The osmotic induced volumetric changes of the oocytes during perfusion were observed using 40X objective magnification and videotaped for image analysis. Videotaping was started before the perfusion and the image of the oocyte prior to perfusion was used to calculate the initial volume. For Me_2SO, EG, GLY and SU, the durations of perfusion were 10, 10, 20 and 6 minutes, respectively.

The videotaped images were digitalized (AverMedia Technologies, Inc., Taipei, Taiwan) into a series of still images of the oocytes at the given time points. These images were used to acquire the data of volume change history during the perfusion. For the experiments at room temperature, images were captured every 3 seconds from real-time video for the first 3 minutes of the perfusion. In the presence of GLY, volume changes became very slow after the first fast shrinkage phase; thus additional images were captured every 5 seconds for an additional 5 minutes.

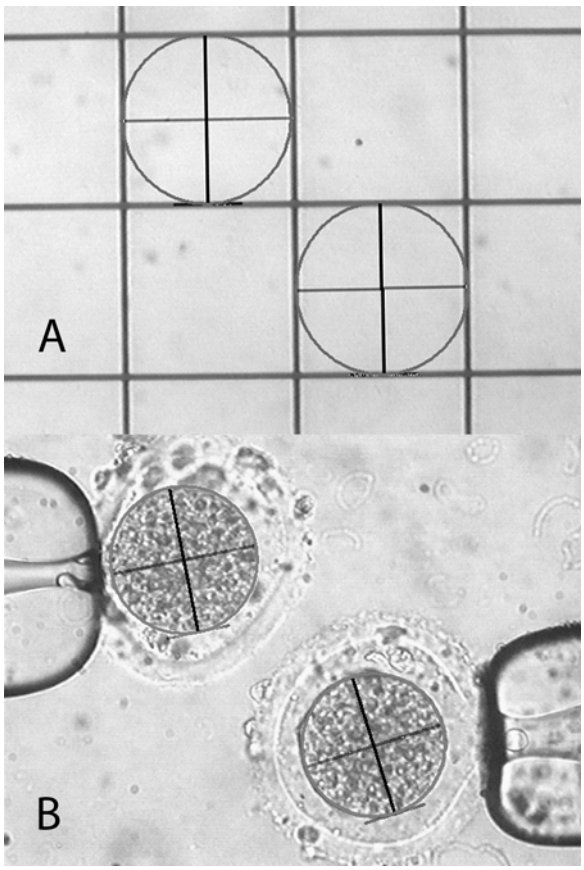

Figure 4.1. The images that were digitized from the videotape at the given time points were measured by customized software. Under the same measurement configuration, a calibration factor was determined by the measurement of a cover of Makler chamber with grids of 0.1 mm by 0.1 mm (Panel A); the sizes of the oocytes were determined as the diameter of the overlapping circle that enclosed the oocyte, assuming spherical geometry (Panel B).

Image analysis was performed using customized image analysis software. Only the oocytes that remained nearly spherical during the volume excursions were used to estimate the permeability parameters. Briefly, the captured images were displayed on the computer screen. One point on the edge of the oocyte was selected by left-clicking the mouse button. A circle, whose diameter changes as the cursor moves, was created by dragging the cursor across the oocyte to the other side. When the created circle enclosed the oocyte, judged by overlapping the circle over the edge of oocyte, the mouse button was released and the diameter of the circle was recorded as the diameter of the measured oocyte. The calibration factor was determined by the measurement of a cover of a Makler chamber with grids of 0.1 mm by 0.1 mm under the same measurement configuration. The volume and surface area of the oocyte were calculated from this diameter, assuming spherical geometry.

4.2.2 Determination of the permeability coefficients

For our study, we used a two-parameter model to describe the passive coupled membrane transport dynamics. This model uses a pair of coupled differential equations to describe the change in cell volume (dV_c/dt) and moles of intracellular permeating solute (dN^i_s/dt) when the cell is exposed to a ternary solution consisting of a permeable solute (CPA) and an impermeable solute (NaCl) and solvent (water).

$$\frac{dV_c}{dt} = L_p ART[(M_n^i - M_n^e) + (\frac{N_s^i}{V_c - V_b - N_s \cdot \overline{V}_s} - m_s^e)] + \overline{V}_s \cdot \frac{dN_s^i}{dt} \quad (4.1)$$

$$\frac{dN_s^i}{dt} = AP_s(m_s^e - \frac{N_s^i}{V_c - V_b - N_s \cdot \overline{V}_s}) . \quad (4.2)$$

where V_c is the rabbit oocyte volume and N_s^i is the number of moles of CPA that has permeated the oocyte (see Table A for explanations and definitions of terms).

MLAB was used to solve equations 4.1 and 4.2 using the Gear method. The Marquard-Levenberg curve-fitting method (MLAB user manual), as implemented in MLAB, was used to fit the experimental data and determine the values of L_p and P_s. A fixed value for V_{bp}, determined independently from the Boyle van't Hoff plot, was used in the fitting calculation. As explicitly shown by the terms in equations 4.1 and 4.2, several assumptions were used as commonly employed in previous cryobiology studies: [i] the extracellular space is assumed to be infinite; [ii] the surface area of the cell is changing as the volume changes assuming a spherical geometry; [iii] the intracellular and extracellular solutions are assumed to be ideal and dilute. We also assumed that the osmotic coefficients for the solutes were equal to 1, such that molalities and osmolalities are equivalent, and the additivity of solute osmolalities are linear.

4.2.3 Parthenogenetic activation and development

At the end of the perfusions, the oocytes were released from the holding pipettes, and collected. These oocytes were then placed into a 1mol/L sucrose solution to dilute the permeating CPAs from the cytoplasm at room temperature. The durations of the dilutions were 10, 10, and 15 minutes for Me_2SO, EG, and GLY, respectively. For oocytes only exposed to sucrose, oocytes were directly washed in mM199 before being put into culture drops. The oocytes were incubated for 30 minutes after two brief washes in mM199, then were parthenogenetically activated by electrical stimulation with three 20 µs 3.2 kV cm^{-1} DC pulses in activation medium and incubated in mEBSS drops. After 1.5 hours another identical electrical stimulation was applied to the oocytes followed by one hour incubation with 2 mmol/L 6-dimethylaminopurine and 5 µg $mmol/L^{-1}$ cycloheximide. The oocytes were finally cultured in mEBSS for 4.5 days until the expanded or hatching blastocyst stage, and cleavage, morulae and blastocyst developmental rates were recorded.

4.2.4 Theoretical simulations and accumulative osmotic damage model

During the processes of cryopreservation, cells experience several stresses due to the exposure to CPAs such as osmotic volume excursions from physiological status and chemical toxicity. The effects of these challenges can be experimentally assessed by examining the developmental potential of the oocytes after parthenogenetic activation. Regarding the osmotic volume excursions, it is reasonable to hypothesize that the damages are dictated by the magnitude of the volume excursion, the rates of the changes and the direction of the changes (shrinkage or swelling); for the CPA toxicity, it can be hypothesized that damage is dictated by the CPA concentration and the duration of exposure. To investigate all these factors and possible interactions among them is beyond the scope of the current study. However, we have investigated one of these hypotheses; namely that cell damage due to CPA exposure is directly related to the total degree of osmotic volume excursion (both magnitude and duration were assessed to give a measure of osmotic damage).

During cryopreservation, the magnitude and duration of the volume excursions are determined by elements that are intrinsic to biological cells such as membrane permeability parameters and cellular dimensions, and by elements that are set by experimental conditions such as CPA concentration and duration of exposure. To systematically investigate these types of damages, it is helpful to build a theoretical model. We propose one simple model to calculate the accumulative osmotic damage (AOD) caused by volume excursion as described by the following equation

$$\mathrm{AOD} = \int_{start}^{end} abs\left[\frac{V_c - V_{iso}}{V_{iso}}\right] \cdot dt\,, \qquad (4.3)$$

where (V_c - V_{iso}) is the volume excursion; The integration is calculated over the whole duration of the procedure. This model treats the shrinkage and swelling equally by taking the absolute value into account. The AOD values were calculated from the start points of additions to the end points of dilutions for all CPAs, excluding the washing step, during the CPA perfusion process associated with the determination of the membrane permeability values in the earlier experiment. AODs were not calculated for the step of washing for 2 reasons: (i) washing is very short; (ii) for all cases, AOD value will be the same for each CPAs during the washing.

4.2.5 Statistical analyses

Permeability data for water and CPAs were compared using ANOVA with SAS for Windows version 9, using the Tukey multiple comparison correction. Differences between the treatments were only considered significant if the P-value was less than 0.05. Regression and correlation analyses were conducted using Microsoft Excel for Windows.

4.3 RESULTS

4.3.1 Rabbit oocyte CPA permeabilities

Membrane permeability data for rabbit oocytes in the presence of different CPAs at room temperature are summarized in Table 4-1. There were no significant differences among L_P mean values in the presence of the different CPAs ($p>0.05$) at the experimental temperature (23°C). There were no significant differences between the P_s values of Me_2SO and EG. However, these values were significantly higher than the value of P_s for GLY. The correlation coefficients for L_p and P_s were 0.82, 0.54, and 0.23 for Me_2SO, EG, and GLY, respectively.

In the presence of sucrose, however, we could not determine the value of the hydraulic conductivity due to non-spherical shrinkage of oocytes. We estimated the value to be close to 0.8 μm $min^{-1} \cdot atm^{-1}$ by examining the time required to reach equilibrium in the presence of the 1mol/L sucrose solution.

Table 4-1. Permeability Parameters for Rabbit Oocytes in the presence of Different CPAs (mean ± SD)

CPA type	Number of Oocytes	L_p ($\mu m \cdot min^{-1} \cdot atm^{-1}$)	P_s ($\times 10^{-3}$ $cm \cdot min^{-1}$)
Me_2SO	26	0.79 ± 0.26	2.9 ± 1.3
EG	23	0.82 ± 0.22	2.7 ± 1.3
GLY	27	0.64 ± 0.16	0.27 ± 0.18*

* Indicates a significant difference compared to values within the same column.

4.3.2 Blastocyst Development and AOD

The results for the development of activated oocytes after the CPA addition and removal are summarized in the Table 4-2.

Table 4-2. In Vitro development of the parthenogenetic activated rabbit oocytes following addition (15% v/v concentration) and dilution of different CPAs in the presence of 1M sucrose.

	Number of oocytes	Cleaved to 2-8 Cell stages		Morulae development		Blastocyst development	
Me_2SO	37	26	70%	24	65%	18	49%
EG	37	30	81%	26	70%	14	38%
GLY	37	6	19%	0	0%	0	0%
SU *	38	30	79%	28	74%	22	58%
CONTROL	39	38	97%	34	87%	27	69%

*Note: Sucrose Concentration was 1mol/L. Oocytes were placed directly into culture drops after a brief wash in mM199.

Using the experimentally-determined permeability coefficients, we simulated the volume excursions for rabbit oocytes during the process of CPA addition, and dilution in the presence of sucrose during the permeability experiment using equations 4.1 and 4.2 (Figure 4.2). We calculated the values of AODs associated with these CPA additions and dilutions by Equation 4.3. The normalized percentages of blastocyst development after exposure to different CPAs were plotted in relation to the AODs (Table 4-3).

These values were strongly correlated (r = -0.98; Figure 4.3). In Figure 4.2, the volume excursions for the isotonic washing step for Me_2SO, EG, GLY and SU were omitted; in the calculations for AODs, the washing step for Me_2SO, EG, GLY and SU were omitted as well.

Table 4-3. In Vitro Normalized Blastocyst development of the rabbit oocytes following addition (15% v/v) and dilution of different CPAs in the presence of 1M sucrose and the calculated Accumulative Osmotic Damage (AOD).

	CPA addition duration (min)	CPA Dilution duration (min)	AOD	Normalized Blastocyst Development (%)
Me_2SO	10	10	407	71
EG	10	10	427	55
GLY	20	15	864	0
Sucrose	6	0	214	84
CONTROL	n/a	n/a	0	100

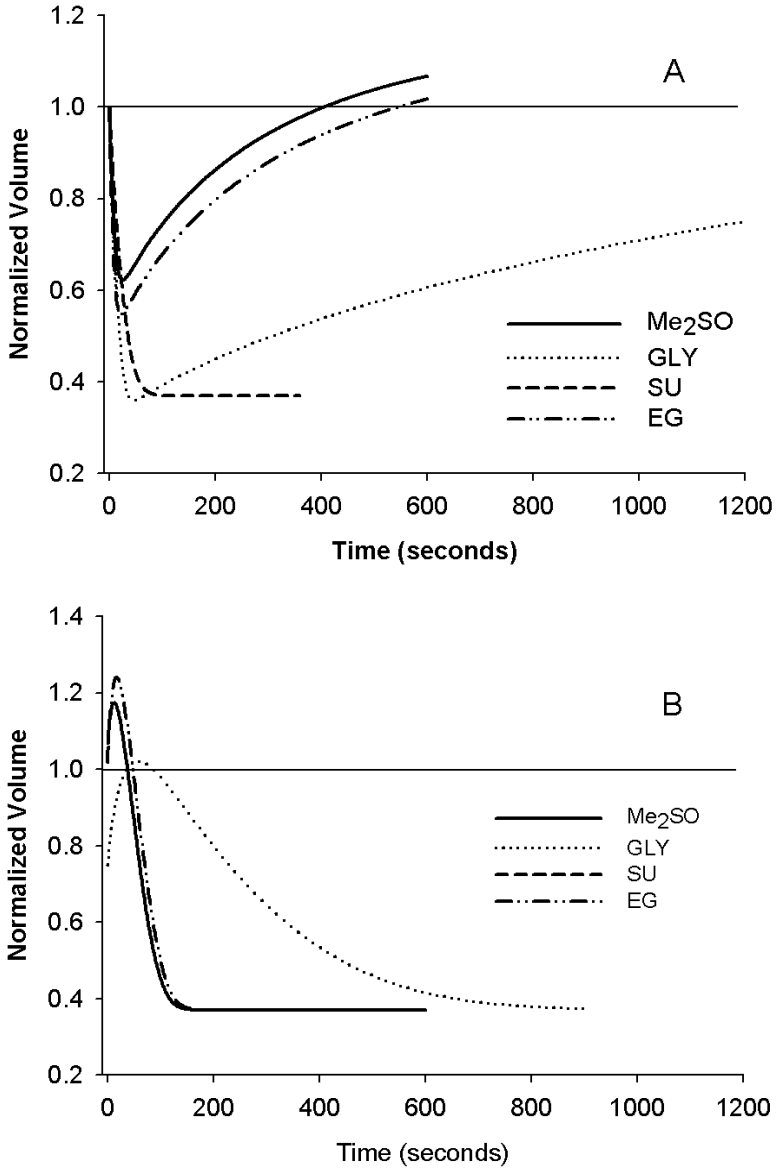

Figure 4.2. Volume changes in the normalized scale as a function of time following CPA additions and dilutions at the room temperature. The durations of addition and dilution in the presence of each CPA are the same as the oocyte experienced in the experiments. There is no dilution for sucrose. Isotonic volume lines are given in the addition and dilution plots by two horizontal solid lines at the unit normalized volume.

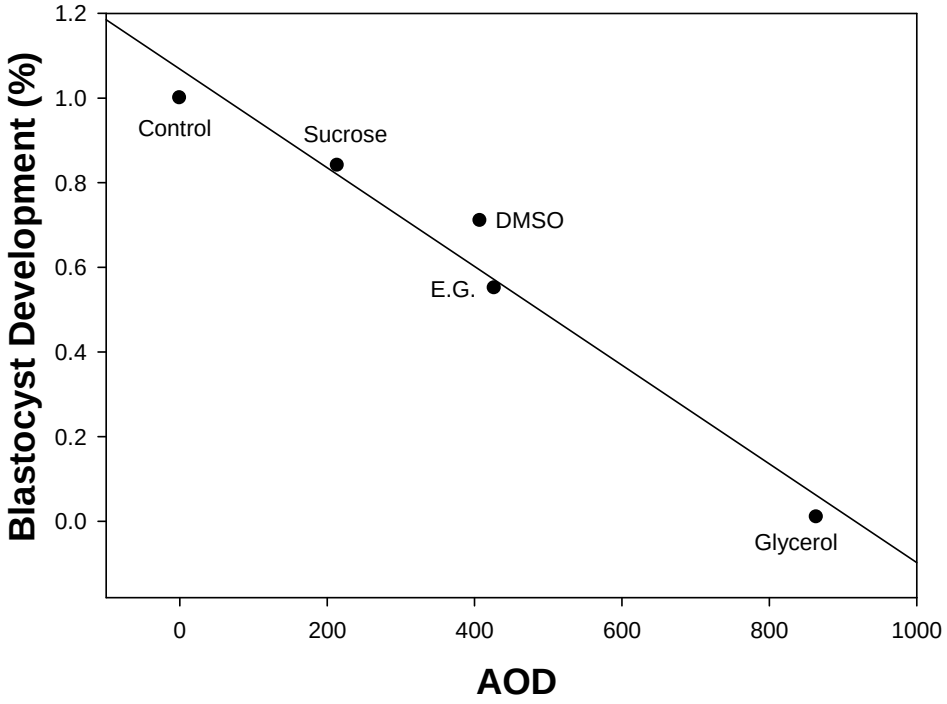

Figure 4.3. Accumulative osmotic damage vs. the normalized blastocyst development percentage of in vitro cultured rabbit oocytes following addition (15% v/v concentration) and dilution of different CPAs in the presence of 1mol/L sucrose. Accumulative Osmotic Damage (AOD) values were calculated by Equation 4. The AOD for the control is zero and normalized development is 1 by definition.

4.4 DISCUSSION

Cryopreservation of oocytes is one of the greatest challenges in the assisted reproduction technologies (ARTs) today. Currently, there are two basic methods for oocyte cryopreservation: slow freezing and vitrification. Slow freezing has the advantage of using low concentrations of CPAs; vitrification is a rapid method, which decreases chilling injury (cold shock), however it requires a high concentration of CPAs (Zeron et al., 2002). A typical vitrification requires concentrations of cryoprotectants in the medium of around 40 to 50 % (compared to 5-10% for slow-freezing) at cooling and warming rates easily achievable in conventional laboratory conditions. Such high CPA concentrations are often detrimental to cells, causing lethal osmotic injury and toxic effects (Fahy et al., 1984). In oocyte cryopreservation, a combination of Me_2SO and EG are frequently used in the vitrification solution to reduce chemical toxicity. In addition, it is possible to lower the critical permeable CPA concentration by adding non-permeable high molecular weight compounds such as disaccharides, e.g. sucrose or trehalose (Fahy, 1986a, 1986b; Fahy et al., 1984). Some of the deleterious osmotic effects of exposure to CPAs can be diminished by optimizing the strategy of multiple-step addition and removal (Gao et al., 1995; Katkov et al., 1998; Mullen et al., 2007), and precise control of concentration of CPA and/or non-permeable additives and timing. Optimization of cryopreservation procedures by a theoretical approach requires the knowledge

of several biophysical parameters of the cells under study, including the cell volume (which includes the proportion of osmotically-active and non-active components), the cell surface area, and the permeability of the cell to water and cryoprotectants (Mazur, 2004). In addition, it requires the knowledge of tolerable levels of osmotic stress.

4.4.1 CPA permeabilities

The hydraulic conductivity and CPA permeability results obtained in this study are summarized in the Table 4.1. The hydraulic conductivity in the presence of Me_2SO is slightly higher to those described for mouse (0.63 μm min $^{-1}$ ·atm^{-1} at 24 ^{o}C (Agca et al., 1998a), human (0.7 μm min $^{-1}$ ·atm^{-1} at 24 ^{o}C (Paynter et al., 1999). In the presence of EG, the hydraulic conductivity obtained in this study is similar to or slightly higher than those described for mouse (0.73 μm min $^{-1}$ ·atm^{-1} at 24 ^{o}C (Paynter et al., 1999), and human (0.64 μm min $^{-1}$ atm^{-1} at 24 ^{o}C, (Mullen, 2007); 0.82 μm min $^{-1}$ ·atm^{-1} (De Santis et al., 2007).

The CPA permeability in the presence of Me_2SO obtained in this study is higher than those described for mouse (1.69 x 10^{-3} cm min^{-1} at 24°C (Agca et al., 1998a) and human oocytes (1.5 x 10^{-3} cm min^{-1} at 24 ^{o}C (Paynter et al., 1999). In the presence of EG, the CPA permeability obtained in this study is also higher than those described for mouse (0.85 x 10^{-3} cm min^{-1} at 24°C (Paynter et al., 1999), human (0.81 x 10^{-3} cm min^{-1} at 24 ^{o}C, (Mullen, 2007) and 0.6 x 10^{-3} cm min^{-1} (De Santis et al., 2007).

4.4.2 AOD model

During CPA addition and dilution procedures, cells experience osmotically-induced volumetric changes. These changes can cause irreversible damage to cells when critical volume excursion limits (swelling and shrinkage) are reached (Mazur and Schneider, 1986). To our best knowledge, no quantitative model has been developed to describe the associated damage. Historically, osmotic damage during CPA addition and removal has been equated solely to the magnitude of the volume changes experienced (Meryman, 2007). As a result, attempts to mitigate this damage have focused on preventing cells from exceeding a specified volume range. On the contrary, the results from the present study suggest that the magnitude of the volume excursion is not the sole predictor of osmotic damage, at least for mammalian oocytes. This idea is also supported by recently published reports describing attempts to improve vitrification of mammalian oocytes which include a brief exposure to the vitrification solution prior to cooling (Bos-Mikich et al., 1995; Kuwayama et al., 2005; Nakagata, 1989; Shaw et al., 1992; Somfai et al., 2006). In some studies, experimental treatments where cells were only exposed to the solution conditions and not subjected to cooling have shown relatively good survival, particularly if the exposure time to the most concentrated solution was short (Fuku et al., 1995; Hotamisligil et al., 1996) and reports cited above). These results, along with those from the present study suggest that there is a kinetic component to osmotic damage.

Using cell permeability parameters and computer modeling enables simulation of volume changes in various situations of CPA addition and dilution. In the typical volume vs. time plot of cellular volume change (e.g. Figure 4.2), the result of the integration calculation of AOD will be proportional to the area of the curves between the volume line and isotonic volume line. This provides a way to visually estimate the magnitude of AOD. In this study, we developed a straightforward quantitative osmotic volume excursion model that incorporates both magnitude and duration of volume excursions that are associated with the procedure of cryoprotectant addition and removal. As a first test of the validity of this model, we have assessed the correlation between the in vitro development potential of the parthenogenetically- activated oocytes and the associate AOD (equation 4.4) resulting from the CPA addition and dilution procedures used in the permeability study (Table 4-3). During CPA dilutions in the presence of sucrose, we used the estimated value of hydraulic conductivity 0.8 μm $min^{-1} \cdot atm^{-1}$. The correlation between these two data sets is strong (r = -0.98). The hypothesis that both the magnitude and duration of the osmotic volume excursions is responsible for loss of cell viability is supported by comparing the volume excursions for exposure to sucrose and glycerol in Figure 4.4. If the magnitude of the volume excursion was the only factor responsible for cell injury, the developmental potential of cells exposed to these 2 treatments should be very similar (since the absolute cell volume excursion which cells experienced during these treatments was similar). Examination of Figure 4.5 shows this not to be the case, however; oocytes exposed only to sucrose survived very well compared to those exposed to glycerol, despite the magnitude of volume changes being similar. We acknowledge that chemical toxicity of glycerol cannot be completely discounted as a possible cause of the difference in the viability seen between these two treatments, nor can the possibility of a stabilization effect of sucrose. The cell permeability values for glycerol suggest that only a small amount of this compound would have entered the oocytes during the exposure. Therefore, we feel that chemical toxicity is not a likely explanation for the degree of viability loss seen with GLY exposure.

In the procedures of CPA addition/dilution, one will always encounter the dilemma of the magnitude versus duration issue: multiple step addition/dilution that decreases the magnitude prolongs the duration. A more accurate model for describing the effects of both factors should allow the development of improved cryopreservation procedures. Here we propose the AOD model as a first step toward the development of a more comprehensive description of osmotic damage to cells during CPA addition and removal. Future attempts at model development should include the inclusion of a chemical toxicity effect, which could help to resolve the uncertainty described above.

CHAPTER 5. DEVELOPMENT OF A NOVEL CRYOPRESERVATION THREE-STEP METHOD FOR MAMMALIAN OOCYTE

5.1 INTRODUCTION

The establishment of long-term preservation methods for mammalian oocytes will provide an alternative to embryo cryopreservation. However, the determination of reliable methods for mammalian oocyte cryopreservation has been challenging. Mature oocytes exposed to sub-physiologic temperatures experience a substantial degree of disruption of their metaphase II spindles (Aman and Parks, 1994; Pickering et al., 1990), cortical granules (Vincent and Johnson, 1992) and plasma membrane (Arav et al., 1996). Chilling and cryopreservation of germinal vesicle (GV) oocytes causes reduction in maturation rates, resulting in reduced developmental potential following fertilization (Martino et al., 1996a; Pickering et al., 1990; Zenzes et al., 2001). Many studies indicate that cryopreservation of either GV or MII oocytes using current slow cooling protocols will result in reduction in cell viability for different reasons (Critser et al., 1997). Since the effects of chilling on the developmental potential of oocytes from many species are widely recognized, ultra-rapid cooling methods, introduced by Rall and Fahy (Fahy, 1986b; Rall et al., 1987), have been used to cryopreserve mouse (Nakagata, 1989; Rayos et al., 1994; Wood et al., 1993), human (Yoon et al., 2000) and bovine (Martino et al., 1996b; Vajta et al., 1998) oocytes with varying levels of success. However, the vitrification method requires a high concentration of CPA (e.g. 6M) loaded into cells before plunging into LN_2. Introducing this high solute concentration into cells exposes the cells to extreme osmotic stresses and chemical toxicity, and is also a procedural challenge (Agca, 2000; Fahy, 1986b; Hotamisligil et al., 1996).

Rapid freezing by a so-called "two-step" procedure has been studied for several types of cells (Landa, 1990; Lopez-Bejar et al., 1994; McGann and Farrant, 1976; Rapatz and Luyet, 1973; Wood and Farrant, 1980). This approach, in fact, consists of three steps: first, CPA loading followed by a fast cooling step, which reduces sample temperature from physiologic temperature to a subzero holding temperature (T_p, *e.g.* –25°C) at a high rate. The second step involves maintaining the cells at T_p for a specific period. The third step involves plunging the sample into liquid nitrogen (LN_2). Basically, intracellular CPA concentration increases during the second step as a result of dehydration. When the intracellular CPA concentration reaches a critical concentration (C_c) sufficient to allow intracellular vitrification, the oocytes are plunged into LN_2 (third step), concluding a "three-step freezing" method. The procedure could overcome these problems that are associated with the cryopreservation of oocytes by: (a) loading oocytes with a moderate concentration of CPA (*e.g.* 2.5 M) (b) using a very fast cooling rate to cool oocytes to T_p where the chilling effects on spindle depolymerization and developmental potential may be reduced (Aigner et al., 1992).

This procedure puts cells in highly supercooled situation. Theoretically, as a cell is progressively supercooled, there is an associated increase in the probability of intracellular ice formation (P_{IIF}). The kinetics of this ice formation is dependent on conditions of supercooling, temperature and intracellular

solution content. In a cryopreservation procedure, these conditions can be controlled in two ways: (1) by controlling the thermal history and (2) by controlling the initial solution conditions.

The difficulties in application of this approach lie in the determination of cryopreservation conditions (holding temperature, T_p and holding time, t_h) for a given cell type, CPA type, and initial CPA concentrations. All these parameters are interactive, thus make it impractical to empirically design a cryopreservation protocol.

Using experimentally determined biophysical characteristics such as membrane permeability coefficients and their activation energies (Agca et al., 1998a) and previously developed models (Karlsson et al., 1996; Liu et al., 2000), we can calculate intracellular solute concentration and probability of intracellular ice formation (P_{IIF}) for an oocyte that is undergoing cryopreservation under specific cooling and initial solution conditions. In this thesis, the enhanced and integrated model was developed and applied the to a three-step cooling procedure for mouse oocytes. Calculation results are presented in novel contour plots, from which cryopreservation protocols can be created by identifying conditions that could be used from the plots.

5.2 METHOD

5.2.1 Physical events involved in "three-step" cryopreservation

First Step: Initially, cells are loaded with CPA at physiologic temperature by introducing them to a solution containing the appropriate concentration and allowing an appropriate equilibration time. Then the sample is rapidly cooled by touching a pre-cooled object (*e.g.* a hemostat) to the cell container (*e.g.* a straw) at room temperature, initiating the formation of ice in the solution. Then the container is plunged into a preset cooling bath at T_p. We assume ice has formed at the freezing point of the solution, and a constant cooling rate of B for this period when the temperature changes from the freezing point to T_p. The extracellular solute concentration increases from the initial concentration to the value $C(T_p, R_t)$, which is dictated by the phase diagram relationship (Pegg, 1986). Intracellularly, cell water volume decreases and the intracellular CPA concentration increases. These values can be quantitatively determined using Equation (5.1) and (5.2) (Liu et al., 2000)

$$\frac{dV_w}{dT} = -\frac{ARTL_p(T)}{v_{10}B}\left[\ln\left(\frac{V_w}{V_w + (n_n + n_s)v_{10}}\right) + \ln\left(1 + \frac{G'C(T)}{100 - C(T)}\right)\right] \tag{5.1}$$

$$\frac{dn_s}{dT} = \frac{AP_s(T)}{B}\left(\frac{1000R_tC(T)}{MW_s(100 - C(T))(R_t + 1)} - \frac{n_s}{V_w}\right), \tag{5.2}$$

where $G' = \frac{R_t}{(1 + R_t)} MW_w\left(\frac{1}{MW_n R_t} + \frac{1}{MW_s}\right)$. (All symbols and parameters are defined in Table A.)

Since the cooling rate B is very high (B≈300 ^oC/min) for this step, the cell will experience little dehydration during the short time period (≈10 seconds) that elapses during seeding. Therefore, the initial

intracellular solute concentration is just slightly higher than C^0 (Fig 5.1 B). However the extracellular solute concentration has been reached at a relative high level due to the relative low T_p.

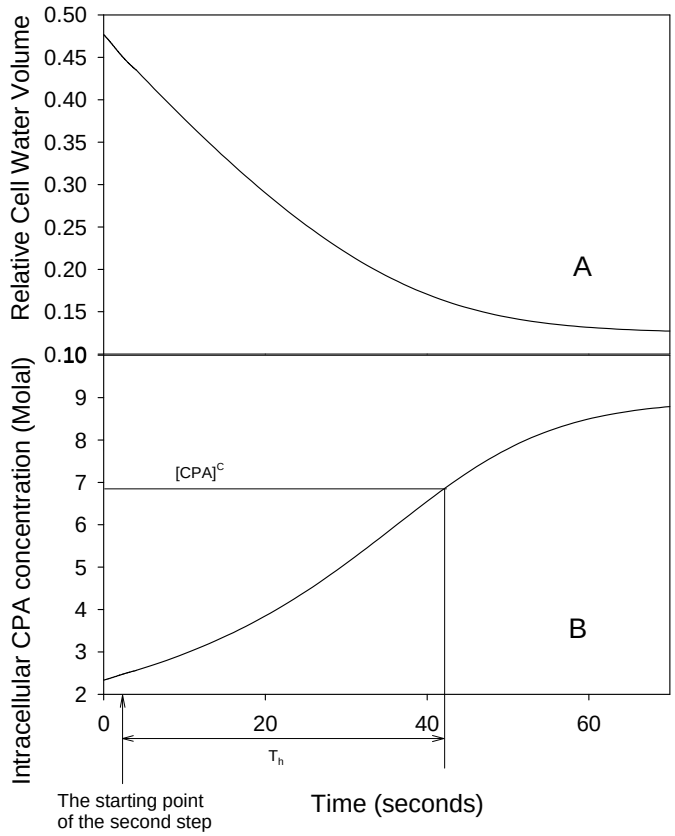

Figure 5.1. A schematic diagram showing bovine oocyte cell water volume change and intracellular CPA concentration change in the first and second step. For a given critical concentration [CPA]c, the intracellular CPA concentration reaches the value when the cell has been hold at T_p for a period of Th. The figure represents a situation where the initial CPA concentration is 2 Molar and holding temperature is –30 ^oC.

Second Step: When the cell suspension reaches, and is held at T_p, the cooling rate becomes zero, so the extracellular CPA concentration remains constant. Its value can be calculated using the phase diagram equation (Eq. 5.6, see below). Since the extracellular concentration is much higher than the intracellular concentration, the cell water will undergo exosmosis, driven by the gradient of chemical potential. We can use the following equations to calculate the rate of dehydration and increase in the number of moles of intracellular CPA concentration:

$$\frac{dV_w}{dt} = -\frac{ART_pL_p(T_p)}{v_{10}}\left[\ln\left(\frac{V_w}{V_w + (n_n + n_s)v_{10}}\right) + \ln\left(1 + \frac{G'C(T_p)}{100 - C(T_p)}\right)\right] \qquad (5.3)$$

$$\frac{dn_s}{dt} = AP_s(T)\left(\frac{1000R_tC(T_p)}{MW_s(100 - C(T_p))(R_t + 1)} - \frac{n_s}{V_w}\right). \qquad (5.4)$$

As the cells dehydrate, their intracellular CPA concentration approaches the extracellular value. In order to reach the C_c intracellularly through dehydration, the T_p must be low enough such that the

corresponding extracellular solute concentration will be higher than C_c. If the holding time of the second step is sufficiently long, the cell is able to lose enough water via exosmosis to concentrate the intracellular CPA to exceed the C_c. By using the above equations, we can calculate how long the holding time should be, provided we know the value of the critical concentration required for cytoplasmic vitrification.

Third Step: When the intracellular concentration exceeds C_c, the holding period is terminated by plunging the sample into LN_2.

5.2.2 Additional Equations

It is assumed that the value of the permeability parameters P_a (L_p or P_s) at any temperature T can be calculated by the Arrhenius relationship (Levin et al., 1976):

$$P_a(T) = P_{ao} \cdot \exp\left[\frac{E_a(L_p \text{ or } P_s)}{R}\left(\frac{1}{T_o} - \frac{1}{T}\right)\right] \tag{5.5}$$

where T_o is a reference temperature point and P_{ao} is the permeability value at the T_o. E_a is the activation energy for L_p or P_s.

The extracellular solute concentration at temperature T can be calculated by solving for $C=C(T, R_t)$ from the following melting point for DMSO/NaCl/Water ternary solution (Pegg, 1986):

$$T_m = A_1 C + B_1 C^2 + C_1 C^3, \tag{5.6}$$

where coefficients A_1, B_1, and C_1 are functions of R_t. This equation was also applied to the situations where sucrose has been added in the DMSO/NaCl/Water ternary solution.

5.2.3 Calculation of the probability of intracellular ice formation (P_{IIF})

We assume that seeding has been accomplished at the freezing point of the cell suspension. From this point, and as the holding proceeds, the intracellular solution has an increased likelihood of experiencing ice nucleation. Toner introduced a model to investigate the ice formation inside biological cells during freezing (Toner et al., 1990). Karlsson improved the model by introducing the treatment for CPA (Karlsson et al., 1993; Karlsson et al., 1994; Karlsson et al., 1996). The probability of intracellular ice formation can be calculated considering the three mechanisms of homogeneous nucleation (HOM), surface-catalyzed nucleation (SCN), and volume-catalyzed nucleation (VCN):

$$P_{IIF} = 1 - \left(1 - PIIF^{HOM}\right) \cdot \left(1 - PIIF^{SCN}\right) \cdot \left(1 - PIIF^{VCN}\right) \tag{5.7}$$

where

$$PIIF^{HOM} = 1 - \exp\left\{\int_{to}^{tf} \Omega_{HOM} \exp\left[-\frac{\kappa_{HOM} \cdot T_m^5}{(T_m - T)^2 \cdot T^3}\right] \cdot V \cdot dt\right\} \tag{5.8}$$

$$PIIF^{VCN} = 1 - \exp\left\{\int_{to}^{tf} \Omega_{VCN} \exp\left[-\frac{\kappa_{VCN} \cdot T_m^5}{(T_m - T)^2 \cdot T^3}\right] \cdot V \cdot dt\right\} \tag{5.9}$$

$$PIIF^{SCN} = 1 - \exp\left\{\int_{to}^{tf} \Omega_{SCN} \exp\left[-\frac{\kappa_{SCN} \cdot T_m^5}{(T_m - T)^2 \cdot T^3}\right] \cdot A \cdot dt\right\} \quad (5.10)$$

and these integration limits (to and tf) are referred to the starting and ending points of the period, during which the P_{IIF} is calculated. Here we use this improved model to determine the ice formation parameters by fitting the theoretical P_{IIF} to the actual observation of intracellular ice formation (described below). The model was then used to predict the P_{IIF} from seeding to the end of the second step in all experimental conditions that were investigated. The values of the parameters required for these calculations can be determined by fitting equations (5.7) and (5.8 – 5.10) to the experimental data of P_{IIF}.

5.2.4 Determination of P_{IIF} parameters

A cryomicroscope system (Hoxan Corporation, Japan) was used to determine the probability of ice nucleation at different temperatures. Mature mouse oocytes were collected from superovulated females using standard procedures (see below). They were placed into a customized glass cell, which was mounted on the cooling chamber of the system with a temperature probe. The chamber was fixed on the stage of an inverted microscope (Nikon, Japan). Cooling was controlled by the system and was set at the rate of - 40 ^{o}C/min, the maximum control cooling rate the system can achieve. The images of oocytes during the cooling process were videotaped and captured by a computer for further analysis later. The incidence of intracellular ice formation can be detected when a sudden refractive index change occurs in the cytoplasm, causing the oocyte to become very dark or opaque when viewed using phase-contrast optics (Figure 5.2). Temperature dependence of the P_{IIF} was determined by counting the numbers of cells that had IIF in serial images at different temperatures (T), as follows:

P_{IIF} (T) = (the number of cells that had IIF at T) / (the number of total cells)

The P_{IIF} data then were used in a fitting calculation to determine the IIF parameters.

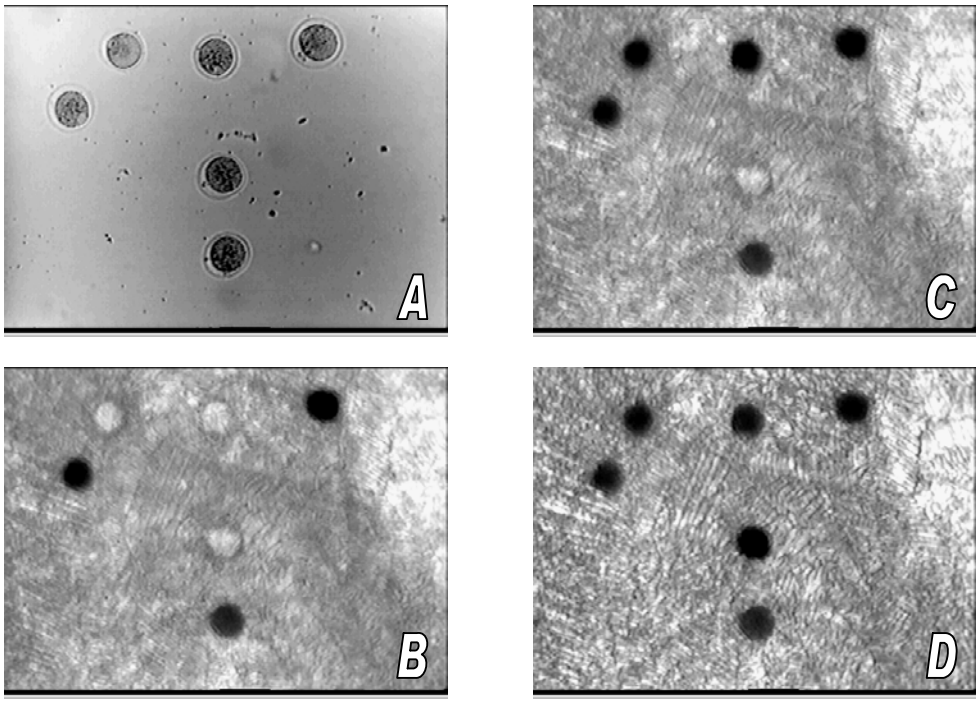

Figure 5.2. Sequence of images captured from a video tape demonstrated the kinetics of IIF for mouse oocytes cooled at -40 ^{o}C/min in a 1.5 M DMSO solution. A) before extracellular ice formation at –4 oC ; B) Three of six oocytes with intracellular ice formation (IIF) characterized by blackening of the cytoplasm; C) Five of six oocytes with IIF; D) All oocytes have IIF at – 41 ^{o}C.

5.2.5 Presentation of calculation results

From a practical point of view, we restricted our investigation on the T_p in the range of –20 to –35 ^{o}C, and C^0 in the range of 1 M to 4 M. These ranges were divided into appropriate intervals for subsequent numerical calculation of P_{IIF} and t_h. Our simulation results can be represented by two contour plots. The first is a contour plot for IIF (called P_{IIF}-Plot hereafter). The P_{IIF}-Plot shows the P_{IIF} in a percentage scale for each combination of T_p and C^0 for the corresponding t_h from t_h-Plot (see below). It represents the accumulated probability of IIF during the first and the second step, i.e. the seeding and holding periods. The second contour plot is for the holding time (called t_h-Plot hereafter). t_h-Plot shows the time, in seconds, that would be required to hold the cells at the given T_p and C^0 so that the intracellular CPA concentration can reach the C_c. If a combination of holding temperature and C^0 will not allow the intracellular solute concentration to reach the C_c, this combination will have its IIF value assigned to 100%, because intracellular ice formation will occur during plunging into LN_2.

5.2.6 Experiments to validate the theoretical predictions.

To validate the model's prediction of IIF we selected 4 points on the contour plots that had differing combinations of C^0 and T_p, and consequently differing values of P_{IIF}, and performed 3-step freezing experiments using these conditions. The factor levels for C_0 were 1.5 and 2.5 M; and for Tp, -25 and -30 °C. The t_h was 30 minutes for all treatments. Six replicates were completed. The cells that had lysed during

the experiment were scored as having experienced IIF. A 95% confidence interval for the experimental mean percent IIF value was calculated and compared with the theoretically predicted value as a measure of the model's accuracy. All chemicals used in this experiment were from Sigma chemical company (St. Louis MO, USA) unless otherwise noted. Four to five week old B6C3/F1 mice (Harlan Sprague Dawly, Indianapolis IN USA) were superovulated with 5 IU PMSG (Sioux Biochemicals, Sioux Center, IA USA), and 5 IU hCG 48 hours later. Oocytes were collected 12.5 - 13 hours after the hCG injection by dissecting out the oviduct and expelling the clutch of cumulus oocyte complexes into HEPES buffered Tyrode's Lactate (TL-HEPES, Bavister 1983) with hyaulronidase (1 mg per ml). All TL-HEPES solutions contained bovine serum albumin (Fraction V) at a concentration of 3 mg per ml. Cumulus cells were removed during this incubation by pipetting. The oocytes were maintained at near physiologic temperature (~37 °C) during the entire processing period. For each experimental replicate, 6 animals were superovulated. Oocytes exhibiting normal size, cytoplasmic granularity, and the presence of the first polar body were chosen for inclusion into the experiment. Oocytes from each animal were randomly and evenly distributed to all experimental conditions for each replicate. For each experimental condition, a 0.25 cc freezing straw was loaded with alternating solutions of 0.6M sucrose in TL-HEPES and the appropriate CPA solution (DMSO in TL-HEPES + 10% fetal calf serum + 0.29M Sucrose) which were separated by an air bubble. The volumes of CPA solution and sucrose solution in the straws were roughly equivalent. Oocytes were loaded into the CPA solution within the straw, the straw was heat sealed, and the oocytes were held for 2 minutes to equilibrate with the CPA solution prior to seeding. The solutions of CPA were maintained near 37° C until seeding commenced. After the 2 minute equilibration time, ice was induced in the CPA column by holding the straw with a large hemostat that had been pre-cooled in liquid nitrogen. When ice formation was visualized, the straw was placed into a test-tube filled with methanol which was held in a cooling bath (Neslab Instruments Inc., Model RTE140, Newington, NH USA) filled with ethylene glycol and equilibrated at the experimental temperature. The experimental treatment consisting of a C^0 of 1.5M and T_p of -25 was determined from the model to have insufficient conditions to bring the intracellular concentration to C_c, thus the model predicts that all of the cells will experience IIF during the LN2 plunge (as discussed in the previous paragraph). After the 30 minute holding time, the straws for this treatment were plunged quickly into liquid nitrogen prior to thawing. All other treatments were thawed after the holding step due to the prediction that Cc would be reached by this time. Straws plunged into liquid nitrogen were held there for at least one minute prior to thawing. Thawing was accomplished by plunging the straws directly into a water bath at 37° C for ~15 seconds. After this time the contents of the straw were expelled into a 400 microliter drop of TL-HEPES with 0.6M sucrose at 37° C. The oocytes were maintained in this solution for at least 2 minutes and visualized for evidence of osmotic activity. Those oocytes showing evidence of osmotic activity (reduction in cell volume) were scored an intact. After the holding period in the sucrose solution the oocytes were returned to an isotonic medium and osmotic activity was confirmed in the intact oocytes. All oocytes scored as intact after expulsion in the sucrose solution

experienced rehydration after being placed into the isotonic solution. In each replicate, the percent of oocytes having a ruptured oolemma of the total recovered from the straw were used for the statistical analysis.

5.3 RESULTS

5.3.1 IIF Observation and Determination of IIF Parameters

The observation data points of the cryomicroscopy experiment on mouse oocytes are plotted in Fig. 5.3 (open circles). The ice formation parameters were determined by fitting the model (Equation 5.5 - 5.10) to these experimental observations. The fitted parameters are listed in Table 5-1.

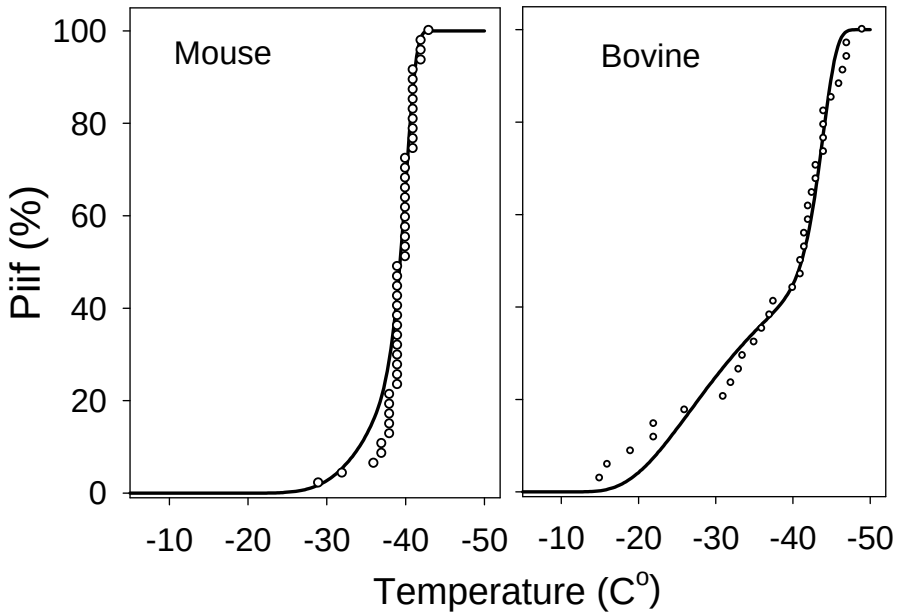

Figure 5.3. Curve fitting to determine the nucleation parameters for mouse and bovine oocytes. The experimental observation (open circle) were conducted at cooling rate of 40 °C/min in the presence of 1.5 M DMSO.

Table 5-1. Parameter values used in the current paper

Description	Units	Mouse Oocyte[a]	Bovine Oocyte[b]
hydraulic conductivity L_p	$\mu m \cdot atm^{-1} \cdot min^{-1}$	0.40 (at 20 °C)	1.16 (at 20 °C)
solute permeability P_s	$cm \cdot min^{-1}$.	1.07×10^{-3}	2.6×10^{-3}
Isotonic Cell Volume	μm^3	1.96×10^5	8.34×10^5
Surface Area	μm^2	1.63×10^4	4.28×10^4
Osomotic inactive volume	percentage	20%	20%
Activation Energy (L_p)	$Kcal \cdot mole^{-1} \cdot K^{-1}$	16.4	8.46
Activation Energy (P_s)	$Kcal \cdot mole^{-1} \cdot K^{-1}$	23.2	21.1
Ω_o for VCN	$\mu m^{-3} \cdot sec^{-1}$	1.993 x 10^4	2.032×10^3
κ_o for VCN	K^5	3.611 x 10^{11}	3.263×10^{11}
Ω_o for SCN	$\mu m^{-2} \cdot sec^{-1}$	3.062×10^{-4}	3.916×10^{-5}
κ_o for SCN	K^5	5.404×10^{10}	1.885 x 10^9

[a] Agca et al (1998a)

[b] Agca et al (1999)

5.3.2 Determination of the P_{IIF} values for different combinations of T_p, C^0, and t_h

The calculation results were represented by the P_{IIF}-Plot showing the P_{IIF} in a percentage scale and corresponding t_h for each combination of T_p and C^0, over the investigation on the T_p in the range of –20 to –35 °C, and C^0 in the range of 1 M to 4 M (Fig. 5.4). We assumed that 40% was the C_c of DMSO for mouse oocytes, and 0.29M sucrose was present in this extracellular solution. The area of 100% P_{IIF} (the area without contour lines in Fig. 5.4), which was assigned to 100% due to insufficient intracellular concentration, divided the plane of T_p/C^0 roughly in one third diagonally. The remaining section of the plots are divided by contour lines that show the P_{IIF} values and holding times for the associated C^0 and T_p values listed on the axes.

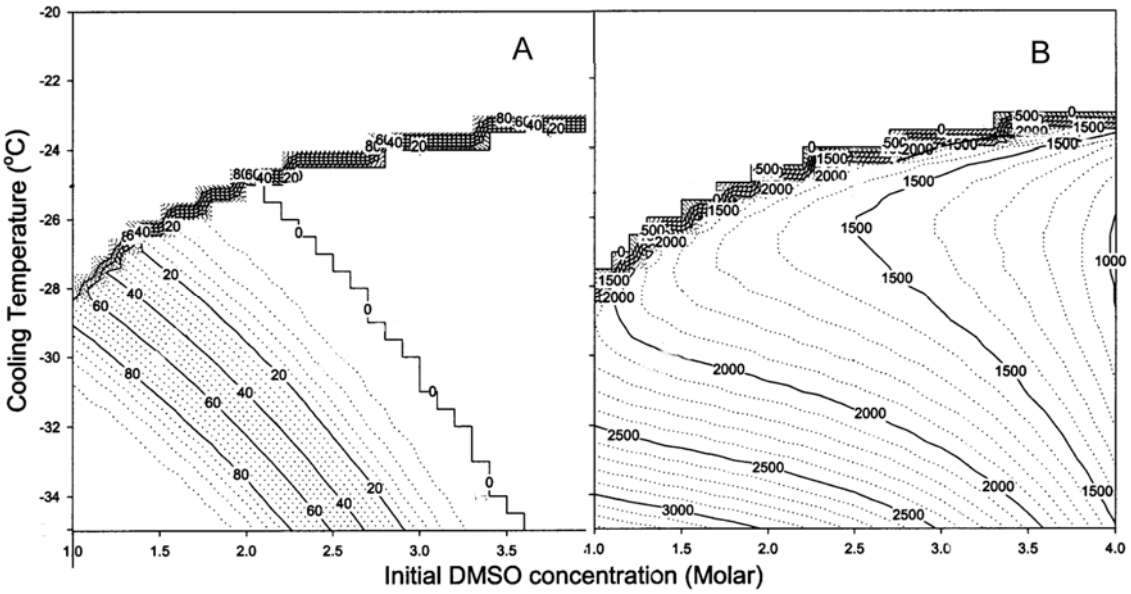

Figure 5.4. Contour graphs of the probability of intracellular ice formation and holding time for mouse MII oocyte. The numbers present the percentage of P_{iif} in Plot-P_{iif} and seconds of holding time. The critical concentration [CPA]c was assumed to be 40% and the extracellular nonpermeating solute osmolality was 600 mOsm.

5.3.3 Experimental results versus the theoretical predictions

During preliminary experiments, we determined that IIF did not occur during the seeding period using this method (data not shown). is listed in the last column. Figure 5.5 compares the theoretically predicted probability of IIF with the 95% confidence interval for the experimentally-predicted probability for each condition. Three of the four experimental conditions had the theoretically predicted value of P_{IIF} fall within the confidence interval range. The condition where the predicted IIF and experimental IIF values differ was in the area of the contour plot where it was determined that the intracellular CPA would fail to reach C_c after the holding period. These data suggest that our assumption of C_c needs to be re-evaluated, for some of the cells had intact membrane upon thawing.

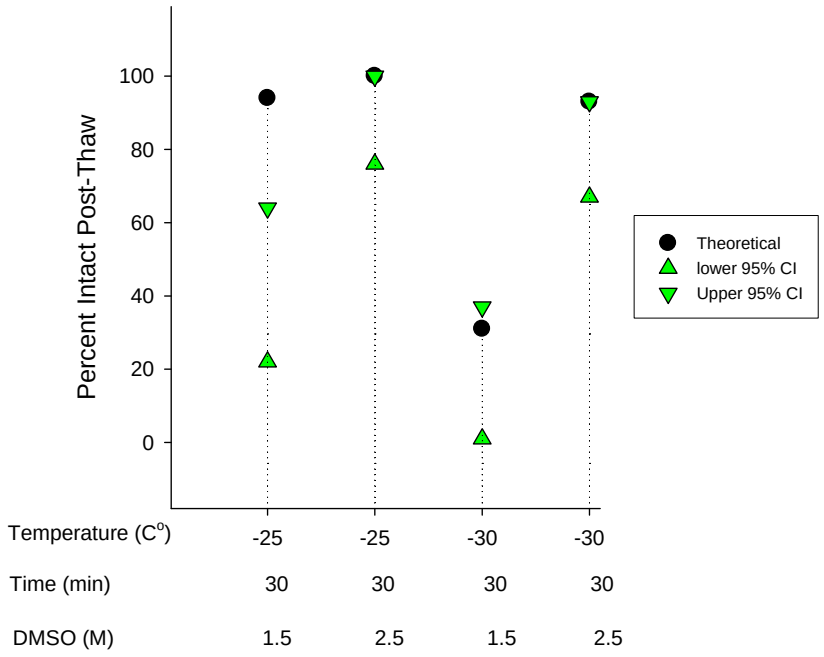

Figure 5.5. Comparison of experimental results to theoretical prediction at various conditions. The experimental survival is estimated as morphology integrity. The theoretical survival is assumed as (100-Piif).

5.3.4 Optimization of an oocyte freezing protocol

From a practical point of view in regards to the 3-step procedure, C^0 and T_p are two aspects an investigator has to consider and decide upon before the cryopreservation experiment. In the context of protocol development mouse oocytes presented here, we determined what the holding time for a given C^0 and a given T_p would need to be to reach C_c. However, during this procedure, intracellular ice formation, which is one of main factors of cryoinjury, can occur during the first 2 steps of rapid non-equilibrium cooling and holding for some experimental conditions (T_p and C^0). Or it could occur at the third step if the cytoplasmic concentration has not increased sufficiently through exosmosis. In this case, plunging the cells into LN_2 results in the IIF instead of vitrification. Therefore, the optimal first and second steps (cooling from T_a to T_p and holding the samples at T_p until the CPA concentration reaches the C_c) will: (1) utilize a value of C^0 that the cell can tolerate; (2) prevent intracellular ice formation; and (3) allow the concentration of the intracellular solution to become sufficient to achieve vitrification during the third step (plunging into LN_2) and prevent devitrification during warming.

We can determine a protocol for 3-step mouse oocyte cryopreservation from these contour plots as follows. First, the acceptable C^0 must be determined. It is clear from P_{IIF}-Plot panel A that there is an inverse relationship between the value of C^0 and the minimum P_{IIF} attainable. Thus tolerance of the CPA should be known to optimize this procedure. Assuming that an initial DMSO concentration of 2.5M is acceptable, draw a vertical line from the X-axis at this point on panel A up to the point on the contour plot

where the P_{IIF} is acceptable (in this instance we can achieve a predicted P_{IIF} value of 0). Then the appropriate holding temperature may be determined by referring to the Y-axis at this point, which is -25 ^{o}C in this instance. The holding time for this combination can be determined by locating the same point on panel B and identifying the contour line which crosses this point. In this case is it about 1700 seconds. Therefore, the appropriate procedure would be to load the cells with 2.5M DMSO, plunge the straw into a cooling bath set to –25 ^{o}C after seeding, hold the straw in this bath for 1700 seconds, and then plunge the straw into liquid nitrogen.

5.4 DISCUSSION

5.4.1 General discussion of P_{IIF}-Plot

In the area with the absence of contour bars, the values for P_{IIF} were assigned to be 100% as stated above. This area encompasses almost all points that have holding temperatures above –24 ^{o}C. This can be readily explained by examining the phase diagram for a solution of 2.5 M DMSO plus 0.32M NaCl, the solute concentrations will not reach 40% when the temperature is –24 ^{o}C or above. During the cooling process, the concentration of the extracellular solution will follow the phase diagram, the value being solely determined by temperature for the given solution. The intracellular solute concentration approaches the extracellular concentration during the holding step, but will never exceed it. Therefore, the T_p must be low enough so that the extracellular solute concentration at the T_p is great than C_c.

From the P_{IIF}-Plot, the effects of C^0 and T_p on P_{IIF} are explicitly shown. For a given T_p, the values of P_{IIF} decrease as the C^0 increases. Higher intracellular CPA concentrations tend to reduce the extent of supercooling, which is the major factor of P_{IIF}. For a given C^0, the values of P_{IIF} increase as the T_p decreases. Lower holding temperatures increase the extent of supercooling and decrease membrane permeabilities (L_p and P_s) and dehydration. Consequently, this results in a higher P_{IIF}.

The iso-P_{IIF} contour lines lay approximately diagonally on the plane of C^0 and T_p. When we have to select conditions for a freezing protocol, we can readily choose values from the uppermost-left section along the iso-P_{IIF} line, assuming that this value of P_{IIF} is acceptable. The holding time can be determined by checking the time in seconds for the same condition (C^0 and T_p) from the t_h-plot.

5.4.2 IIF Observations and Prediction

The kinetics of intracellular ice formation are dependent upon the conditions of supercooling, temperature and intracellular content. The probability of IIF at different temperatures under a specific cooling condition can be determined by cryo-microscopy experiments, hence the ice formation parameters can be calculated. A model can be constructed which uses these parameters to estimate the P_{IIF} under different experimental conditions, and these values can be compared with experimental results. As shown in Figure 3, the theoretical prediction from our model matched the experimental results quite well, with the exception of the point in the range where P_{IIF} was set to 100%. We assumed that the intracellular DMSO

concentration needed to reach a value of 40% to achieve vitrification upon plunging into liquid nitrogen. This was based upon previous work with oocyte vitrification. Many studies have used a final CPA concentration near this value and achieved vitrification. To improve the model, this assumption will have to be investigated further. Lowering this requirement would likely allow improvements in this method of cryopreservation by allowing a broader range of C^0, T_p, and t_h values to be used, which could reduce CPA exposure or time factors and lead to less stress on the cells during the procedure.

CHAPTER 6. NEW SCIENTIFIC RESULTS

1. New coupled equations have been developed to examine the changes of intracellular water volume and the mole number of CPA during temperature changes with cooling rate of *B* in the presence of extracellular ice. Two significant improvements have incorporated into this enhanced theoretical model. It includes the movement of CPA across the plasma membrane during cooling and warming. The actual ternary phase diagram was used instead of the idealized Clausius-Clapeyron equation to calculate the extracellular solute concentration.

2. The novel methodology has been established to utilize theoretical models for the development of cryopreservation protocols by designing specific cooling profiles and selecting appropriate external conditions to optimize the cryopreservation survivals. It has been utilized to very practical cryopreservation conditions for rat zygotes in the presence of DMSO as the CPA. The optimum protocol has been determined to be: a $[CPA]^0$ of 1.2 M DMSO, a B_1 of 0.95°C/min and T_p of -35°C, based on minimum duration of slow cooling.

3. Systematic simulation calculates have been conducted for 2500 cryopreservation conditions and the novel concept of the regions and their cryopreservation relevance have been presented. These regions can be served as the guideline for cryobiologists to design new cryopreservation protocols.

4. The accumulative osmotic damage (AOD) has been proposed for the first time to systematically investigate effects of osmotic stress. It calculates an integration of the relative volume excursion of the oocyte over the whole duration of the procedure. It incorporates both magnitude and duration of volume excursions that are associated with the procedure of cryoprotectant addition and removal.

5. The hydraulic conductivity and CPA permeability in the presence of Me2SO, GLY and EG were experimentally measured in this study for rabbit oocytes. Results from the current study indicates that the GLY permeability is an order of magnitude lower than that of Me2SO and EG. These parameters were used to calculate the values of AODs. The AODs show a very strong correlation to the normalized percentages of blastocyst development after exposure to corresponding CPAs.

6. A novel cryopreservation protocol (three-step) has been designed to overcome problems that are associated with the cryopreservation of oocytes via a theoretical model that has been enhanced by integrating the ice formation kinetics of three mechanisms of nucleation. For the first time, the ice

formation parameters were determined by fitting the model to experimental observations for mouse and bovine oocytes. For mouse oocytes, the protocol was established via the theoretical calculation as the following: to load the cells with 2.5M DMSO, plunge the straw into a cooling bath set to –25 ^{o}C after seeding, hold the straw in this bath for 1700 seconds, and then plunge the straw into liquid nitrogen.

CHAPTER 7. CONCLUSION

Cryopreservation methods can be developed by theoretically examining biophysical events during the processes of the cryopreservation. These events include the movement of intracellular water and permeating cryoprotectant across the plasma membrane prior to, during and after freezing, ice formation, vitrification and thawing. During a cryopreservation procedure, cellular status such as cell water volume and intracellular solute concentration can be calculated by established equations along with corresponding parameters. The kinetics of these statuses are dependent on the intrinsic cellular characteristics, such as membrane permeability coefficients and related activation energies, and external conditions applied, such as equilibrated CPA concentrations, cooling rates and warming rates, and they are intimate related to the probability of intracellular ice formation (cell damage). This thesis presents the methodology of utilizing theoretical models for the development of cryopreservation protocols by designing specific cooling profiles and selecting appropriate external conditions to optimize the cryopreservation survivals.

Based on the classic membrane transportation equations (Kedem and Katchalsky formulism) for a ternary solution, a theoretical model that includes the movement of cryoprotectant across the plasma membrane during cooling and warming and the ternary phase diagram was established in the first time. This thesis provides the detailed derivation steps for the final coupled equations that describe the changes of intracellular water volume and the mole number of CPA during temperature changes with cooling rate of *B* in the presence of extracellular ice. These equations allow us to investigate the responses of cells during cryopreservation procedures by simulating the cell water volume, the water flux across the plasma membrane, intra- and extracellular solute concentrations, the degree of supercooling of the cytoplasm, and the probability of ice nucleation in the cytoplasm. This work had constructed a firm foundation for a comprehensive framework that was established later to optimize one cryopreservation procedure so called the interrupted slow freezing, the prevalent method for oocyte and embryo cryopreservation.

The interrupted slow freezing (ISF) consists of an initial controlled slow cooling period, which is terminated at an intermediate temperature (T_p), followed by rapid cooling as the sample is plunged into liquid nitrogen (LN_2) for final storage. In the context of ISF protocol development, the goal is to determine the best selection of the initial CPA concentration ($[CPA]^0$), B_1 and the T_p. In this study, rat zygotes was the model cell and DMSO was chosen as the permeable CPA because the most complete set of information exists for solutions of this permeating cryoprotectant, specifically critical concentrations/cooling and warming rates necessary for vitrification and ternary solution phase diagram information(Pegg, 1986). Cooling rates and warming rates were measured inside 0.25ml plastic straw and the values of these rates were used to estimate the $[CPA]_c$ based on Stton's formulism.

Essentially, the development of the model followed these steps: (1) an initial range of DMSO concentrations from 0 to 4 Molal, and a range of cooling rates from 0 to 2.5^{o}C/min were evaluated theoretically to determine the selections of $[CPA]^0$ and B_1 that would allow the $[S]^i$ to reach the $[CPA]_c$

during the controlled slow cooling (2) using Mazur's IIF model (Mazur, 1977), the conditions that could result in IIF were eliminated; and (3) the associated plunging temperatures for the combinations of $[CPA]^0$ and B_1 ranges were then calculated; (4) The optimum set of conditions from the final range was then selected based on minimum duration of slow cooling.

For the purpose of the numerical calculations, the above ranges of $[CPA]^0$ and cool rate B_1 are divided into 50 points each. For every combination of $[CPA]^0$ and B_1 value (50X50=2500 total), the established model calculated $[S]^i$, water volume and supercooling at each temperature point (100 equally spaced points from T_{seed} to T_{end}). The criteria of the critical concentration $[CPA]_c$ exceeding 40% (w/w) and no predicted IIF were used to select the candidates of $[CPA]^0$ and B_1 for the protocol.

When the obtained results for 2500 combinations are plotted on the plane of $[CPA]^0$ and B_1, three regions appear with their own characteristics. Region I: in this region, no combination of $[CPA]^0$ and B_1 allows the intracellular solute concentration to reach the $[CPA]_c$ at any temperature point. This region contains the high cooling rate zone and low initial CPA concentration zone. The logic is obviously: the high cooling rates in this region would not allow the cell to dehydrate sufficiently, and the low concentrations are simply not high enough for the intracellular solute concentration to reach the $[CPA]_c$ Region II: The combinations of $[CPA]^0$ and B_1 allow the $[S]^i$ to reach $[CPA]_c$ at certain temperature points, but there is a high probability of IIF during slow cooling. Region III: The combinations of $[CPA]^0$ and B_1 allow the $[S]^i$ to reach the $[CPA]_c$, and no IIF is predicted during slow cooling.

The concept of the regions and their relevance to cryopreservation was novel. Empirical trial-and-error methodology can hardly achieve this due to limited study points. These regions can be served as the guideline for cryobiologists to design cryopreservation protocol for new cell type. In the current system (rat zygote, 0.25 ml plastic straw and DMSO as CPA), the region plot (Figure 4.4) shows that there is a minimum $[CPA]^0$ boundary below which no B_1 (in the range of 0.05 to 2.5°C/min) allows the $[S]^i$ to reach the $[CPA]_c$; there is also a maximum B_1, above which any B_1 causes the same effect. Roughly, these two limits construct a box of $[CPA]^0$ and B_1 values that are candidates for the optimized protocol. The optimum set of conditions was selected by minimizing τ_i from Eq 3.6 and determined to be: a $[CPA]^0$ of 1.2 M DMSO, a B_1 of 0.95°C/min and T_p of -35°C.

The current research results suggest an alternative way to cryopreservate mammalian oocytes. The $[CPA]_c$ is constrained by the B_2 during plunging and B_3 during thawing for a given solution. It is important to note that if these rates could be increased by using a thinner container, or material with higher heat transfer properties, then $[CPA]_c$ may be reduced. This would result in situations where controlled cooling could be performed much more efficiently by applying higher B_1 values and lower $[CPA]^0$ values. These conditions would appear to be optimal because the higher B_1 shortens the duration of slow cooling (therefore potentially reducing solution effects injury), and the lower $[CPA]^0$ lowers the osmotic stress and lessens the potential CPA toxicity.

Theoretically, these calculations may be conducted for any cell type and CPA provided the appropriate information regarding the fundamental membrane permeability parameters and phase diagram solution characteristics are known. While the procedures described here focused upon rat zygotes, the cryobiological issues apply directly to other species and other cell types; including mammalian oocytes. In this regard, optimization of ISF methods for human oocytes and preimplantation embryos would address current concerns in ART programs related to the increasing number of available oocytes and embryos per cycle; combined with the growing concern for avoiding multiple gestation rates. However, to use these types of optimization procedures, basic knowledge of the fundamental cryobiology of these cells is required; since different species oocytes and embryos have different cryobiological characteristics (e.g., membrane permeability coefficients).

In oocyte cryopreservation, typical vitrification procedure requires concentrations of cryoprotectants in the medium of around 40 to 50 % (compared to 5-10% for slow-freezing) at cooling and warming rates easily achievable in conventional laboratory conditions. Such high CPA concentrations are often detrimental to cells, causing lethal osmotic injury. Some of the deleterious osmotic effects of exposure to CPAs can be diminished by optimizing the strategy of multiple-step addition and removal, and precise control of concentration of CPA and/or non-permeable additives and timing. Optimization of cryopreservation procedures by a theoretical approach requires the knowledge of the biophysical parameters of the oocytes, it also requires the knowledge of effects of osmotic stress (both magnitude and duration) on the developmental potential of oocytes.

To systematically investigate effects of osmotic stress, one simple model was proposed to calculate the accumulative osmotic damage (AOD) caused by volume excursion as described by the following Eq. 4.4. Basically, AOD is an integration of the relative volume excursion of the oocyte over the whole duration of the procedure. This model treats the shrinkage and swelling equally by taking the absolute value into account. It incorporates both magnitude and duration of volume excursions that are associated with the procedure of cryoprotectant addition and removal.

The hydraulic conductivity and CPA permeability in the presence of Me_2SO and EG were obtained in this study for rabbit oocytes. Results from the current study indicates that the GLY permeability is an order of magnitude lower than that of Me_2SO and EG. This explains the fact that nobody utilizes GLY as CPA for oocyte cryopreservation.

Using the experimentally-determined permeability coefficients, the volume excursions for rabbit oocytes during the process of CPA addition, and dilution in the presence of sucrose were simulated as conducted during the permeability experiment. The values of AODs associated with these CPA additions and dilutions were calculated. The AOD values were used to assess the correlation between the in vitro development potential of the parthenogenetically- activated oocytes and the associate AOD resulting from the CPA addition and dilution procedures used in the permeability study. The normalized percentages of blastocyst development after exposure to different CPAs were plotted in relation to the AODs. These values

were strongly correlated (r = -0.98; Figure 4.3). It could be concluded that the osmotic damage associated with CPA addition and removal is accurately described by both a magnitude and duration using an accumulated osmotic damage model.

In the procedures of CPA addition/dilution, one will always encounter the dilemma of the magnitude versus duration issue: multiple step addition/dilution that decreases the magnitude prolongs the duration. Historically, osmotic damage during CPA addition and removal has been focused on the magnitude of the volume changes experienced. As a result, attempts to mitigate this damage have focused on preventing cells from exceeding a specified volume range. The current more accurate AOD model for describing the effects of both factors should allow the development of improved cryopreservation procedures.

Recently, CPA dilution condition in the procedure of oocyte cryopreservation has been given more attention (Coticchio et al., 2007). Currently, applied dilution conditions are generally derived from the protocols designed for cleavage-stage embryos and are likely to be rather inappropriate. For human oocyte cryopreservation, there are two popular dilution approaches: one is multiple steps of sucrose only dilution with decreasing sucrose concentrations; another is multiple steps of CPA + sucrose dilution with decreasing CPA + sucrose concentrations. The current AOD model should be a useful tool to examine these approaches, or even optimize these approaches.

This AOD model is a first step toward the development of a more comprehensive description of osmotic damage to cells during CPA addition and removal. Future attempts at model development should include the inclusion of a chemical toxicity effect. Future studies should independently test this model to determine if it is more broadly applicable.

Since the effects of chilling on the developmental potential of oocytes from many species are widely recognized, vitrification and ultra-rapid vitrification methods were applied to cryopreserve mammalian oocyte with varying levels of success. However, the vitrification requires high concentrations of CPAs loaded into cells before plunging into LN_2. Introducing high solute concentrations into oocytes exposes the oocytes to extreme osmotic stresses and chemical toxicity, and is also facing procedural difficulties. In addition, many of these novel technologies use direct exposure of samples to LN, which might cause contamination from/to other biomaterials in the same container.

It is the objective of this thesis to design novel cryopreservation protocol to overcome these problems that are associated with the cryopreservation of oocytes by: (a) loading oocytes with a moderate concentration of CPA (*e.g.* 2.5 M); (b) using a very fast cooling rate to cool oocytes to T_p where the chilling effects on spindle depolymerization and developmental potential may be reduced; (c) plunging the oocyte into LN for final storage in a conventional cryopreservation straw. However, these procedures put an oocyte in a highly supercooled situation. Theoretically, as a cell is progressively supercooled, there is an associated increase in the probability of intracellular ice formation (P_{IIF}). The difficulties in application of this approach lie in the determination of cryopreservation conditions (holding temperature, T_p and holding time,

t_h) for an oocyte, CPA type, and initial CPA concentrations. All these parameters are interactive, thus make it impractical to empirically design a cryopreservation protocol.

In this thesis, the theoretical model introduced in the previous chapter was enhanced by integrating the ice formation kinetics that includes three mechanisms of homogeneous nucleation (HOM), surface-catalyzed nucleation (SCN), and volume-catalyzed nucleation (VCN). IIF observation was conducted on a cryomicroscope system to determine the probability of ice nucleation at different temperatures. The ice formation parameters were determined by fitting the model to these experimental observations for mouse and bovine oocytes.

P_{IIF} and t_h were calculated for different T_ps and initial CPA concentrations (C^0). The calculation results can be used to eliminate the conditions that lead to a high probability of intracellular ice formation during the holding period or the plunge into LN_2, the latter occurring if an insufficient intracellular concentration to achieve intracellular vitrification during the holding period is attained.

The calculation results were represented by the P_{IIF}-Plot showing the P_{IIF} in a percentage scale and corresponding t_h for each combination of T_p and C^0, over the investigation on the T_p in the range of –20 to –35 ^oC, and C^0 in the range of 1 M to 4 M. For mouse oocytes, the protocol was established via the theoretical calculation as the following: to load the cells with 2.5M DMSO, plunge the straw into a cooling bath set to –25 ^oC after seeding, hold the straw in this bath for 1700 seconds, and then plunge the straw into liquid nitrogen.

The calculation results show that the T_p must be low enough so that the extracellular solute concentration at the T_p should be great than $[CPA]_c$. This value can be readily calculated from the phase diagram of the extracellular solution. From the P_{IIF}-Plot, the effects of C^0 and T_p on P_{IIF} are explicitly shown. For a given T_p, the values of P_{IIF} decrease as the C^0 increases. Higher intracellular CPA concentrations tend to reduce the extent of supercooling, which is the major factor of P_{IIF}. For a given C^0, the values of P_{IIF} increase as the T_p decreases. Lower holding temperatures increase the extent of supercooling and decrease membrane permeabilities (L_p and P_s) and dehydration. Consequently, this results in a higher P_{IIF}. This information provides the principle of selecting C^0 and T_p for a 3-step cryopreservation protocol:

- T_p should be as high as possible but low enough so that the extracellular solute concentration at the T_p should be great than $[CPA]_c$.
- C^0 should be as high as possible but within the toxicity and osmotic tolerance of the oocyte.

The kinetics of intracellular ice formation are dependent upon the conditions of supercooling, temperature and intracellular content. The constructed model can estimate the P_{IIF} under different experimental conditions, and these values can be compared with experimental results. Figure 5.5 compares the theoretically predicted probability of IIF with the 95% confidence interval for the experimentally-predicted probability for each condition. Seventy five percent of experimental conditions had the theoretically predicted value of P_{IIF} fall within the confidence interval range.

As shown in Arrenius relationship, one parameter, E_a, dictates how permeability changes while temperature changes. Because of the exponential relationship, the value of E_a has huge impact on the permeability value. The current method aims at cryopreservation of oocytes. It applies a high cooling rate at the first step to decrease the temperature from a physiological level to a relative low level (T_p, e.g. -25), hoping that depolymerization would not become severe during this short period. At the end of this period (first step), the cell water volume would not change too much from its initial value due to short time and dramatically reduction of the membrane permeability, which is highly dependent on temperature. Most cell water was driven out of cells during the holding period at a constant temperature T_p. Because of high E_a value for P_s, the value of P_s at Tp is so low that cross-membrane CPA movement is negligible at this holding period. So cells response just like that they were placed in a hypertonic solution, which composed of just nonpermeating solute (i.e. NaCl, or sucrose). For this case, L_p value dominates the dehydration process.

We should consider the P_{IIF} from two aspects: IIF kinetic parameters and membrane permeabilities, which are highly dependent on their activation energies. As stated before, three-step is not best strategy to freeze cells. It has been designed to minimize the spindle depolymerization. Applicability of this method to a specific cell type will be determined by the inherent permeability parameters AND IIF parameters. Different cell types have different value for these parameters. We found in our recent parallel studies that bovine oocyte have relatively high tendency to have IIF compared to mouse oocyte. On the other hand, they have less values of activation energies (Agca et al., 1999).

This characteristics permits bovine oocytes relatively great dehydration at low temperature, hence reduces the probability of IIF. Compared to bovine oocyte, mouse oocytes have higher activation energies; they have relative lower values of kinetic parameters. This characteristics provides cells relative slower dehydration at low temperature, but lower values of kinetic parameters predicts low probability of IIF as well. So the three-step method can be applied to bovine and mouse oocytes. If a kind of cell has high activation energies and high value of kinetic parameters, then the method can not be applied.

The values of activation energy for L_p are 16.4 and 8.5 Kcal/mole/K for mouse and bovine, respectively. Reflected onto the plots of P_{IIF}-Plot and t_h-Plot, a bovine oocyte dehydrated very quickly, water volume and supercooling decreased readily, so P_{IIF} was much lower, and holding time was much shorter than a mouse oocyte assumed the same experimental condition applied. This demonstrated that there is huge difference exist between different species. Different protocols should be applied accordingly.

The present report outlines a process whereby fundamental principles of cryobiology have been applied to the design of a cryopreservation procedure intended to overcome challenges unique to a specific cell type. Chilling injury at temperatures between 25 and 0º C has long been understood to have detrimental effects on the viability of mature mammalian oocytes. By rapidly traversing this temperature range, it has been suggested that these effects can be overcome. However, holding a cell suspension at a high sub-zero temperature makes cytoplasmic water crystallization likely, resulting in lethal rupture of the cell membrane.

By integrating theoretical concepts and experimental observations, a model was developed to predict the likelihood of intracellular ice formation for combinations of DMSO concentrations, holding times, and holding temperatures in a 3-step freezing design. The model was quite accurate in predicting the likelihood of intracellular ice formation, with 3 of the 4 combinations having 95 percent confidence intervals containing the value of the model's prediction. It remains to be seen if this approach will also preserve the developmental potential of the oocytes.

CHAPTER 8. SUMMARY

This thesis presents the methodology of utilizing theoretical models for the development of cryopreservation protocols by designing specific cooling profiles and selecting appropriate external conditions to optimize the cryopreservation survivals of mammalian oocytes. Based on the classic membrane transportation equations, a theoretical model that has integrated the movement of cryoprotectant across the plasma membrane during cooling and warming and the ternary phase diagram has been established. The model was used to optimize one cryopreservation procedure so called the interrupted slow freezing (ISF), which is the prevalent method for oocyte and embryo cryopreservation. Rat zygote was the model cell and DMSO was chosen as the permeable CPA. Cooling rates and warming rates were measured inside 0.25ml plastic straw and the values of these rates were used to estimate the $[CPA]_c$. A range of DMSO concentrations from 0 to 4 Molal, and a range of cooling rates from 0 to 2.5°C/min were evaluated theoretically for the probability of IIF by using Mazur's IIF model. The simulation results are plotted on the plane of $[CPA]^0$ and B_1, three regions appear with their own characteristics. $[CPA]^0$ and B_1 that are in Region I Region II should not be used as the cryopreservation conditions due to high probability of IIF during plunging or during slow cooling respectively. In Region III, the combinations of $[CPA]^0$ and B_1 allow the $[S]^i$ to reach the $[CPA]_c$, and no IIF is predicted during slow cooling, could be used as cryopreservation conditions. The optimum set of conditions has been established by minimizing the duration of ISF and determined to be: a $[CPA]^0$ of 1.2 M DMSO, a B_1 of 0.95°C/min and T_p of -35°C. The thesis warns of the risk that associated with this condition and advises conservative selections. The concept of the regions and their relevance to cryopreservation could be served as the guideline for designing new cryopreservation protocols. This thesis also suggests of using thinner containers, or material with higher heat transfer properties so that higher slow cooling rate and lower $[CPA]^0$ could be utilized to enhance cryosurvival.

In oocyte cryopreservation, typical vitrification procedure requires high concentrations of cryoprotectants that are often detrimental to cells, causing lethal osmotic injury. To systematically investigate effects of osmotic stress, one novel model was proposed to calculate the accumulative osmotic damage (AOD) caused by volume excursion. Basically, AOD is an integration of the relative volume excursion of the oocyte over the whole duration of the procedure. It incorporates both magnitude and duration of volume excursions that are associated with the procedure of cryoprotectant addition and removal. Using the experimentally determined permeability coefficients, the volume excursions for rabbit oocytes during the process of CPA addition and dilution in the presence of sucrose were simulated as conducted during the permeability experiment. The values of AODs associated with these CPA additions and dilutions were calculated. The AOD values were then used to assess the correlation between the in vitro development potential of the parthenogenetically activated oocytes and the associated AOD values. The normalized percentages of blastocyst development after exposure to different CPAs were plotted in relation

to the AODs, and they are strongly correlated, indicating that the osmotic damage associated with CPA addition and removal is accurately described by both a magnitude and duration using an accumulated osmotic damage model. Future studies are needed to independently test this model to determine if it is more broadly applicable.

In order to design a novel cryopreservation protocol to overcome problems that are associated with the cryopreservation of oocytes, the previous theoretical model has been enhanced by integrating the ice formation kinetics that includes three mechanisms of homogeneous nucleation (HOM), surface-catalyzed nucleation (SCN), and volume-catalyzed nucleation (VCN). IIF observation was conducted on a cryomicroscope system to determine the probability of ice nucleation at different temperatures. The ice formation parameters were determined by fitting the model to these experimental observations for mouse and bovine oocytes. By integrating theoretical concepts and experimental observations, this model predicts the likelihood of intracellular ice formation for combinations of DMSO concentrations, holding times, and holding temperatures in a 3-step freezing design. The calculation results were represented by two novel plots: the P_{IIF}-Plot showing the P_{IIF} in a percentage scale and corresponding t_h in t_h-Plot for each combination of T_p and C^0, over the investigation on the T_p in the range of –20 to –35 ^oC, and C^0 in the range of 1 M to 4 M. For mouse oocytes, the protocol was established via the theoretical calculation as the following: to load the cells with 2.5M DMSO, plunge the straw into a cooling bath set to –25 ^oC after seeding, hold the straw in this bath for 1700 seconds, and then plunge the straw into liquid nitrogen. The model was quite accurate in predicting the likelihood of intracellular ice formation, with 3 of the 4 combinations having 95 percent confidence intervals containing the value of the model's prediction. Further research should be focused on examining the developmental potential of the oocytes preserved by this approach.

CHAPTER 9. LIST OF PUBLICATIONS

1. Glazar AI, Mullen SF, **Liu J**, Benson JD, Critser JK, Squires EL, et al. Osmotic tolerance limits and membrane permeability characteristics of stallion spermatozoa treated with cholesterol. Cryobiology 2009;59(2):201-6.
2. Meng Q, Polgar Z, **Liu J**, Dinnyes A. Live birth of somatic cell-cloned rabbits following trichostatin A treatment and cotransfer of parthenogenetic embryos. Cloning Stem Cells 2009;11(1):203-208.
3. **Liu J**, Mullen S, Meng Q, Critser J, Dinnyes A. Determination of oocyte membrane permeability coefficients and their application to cryopreservation in a rabbit model. Cryobiology 2009;59(2):127-34.
4. Van den Abbeel E, Schneider U, **Liu J**, Agca Y, Critser JK, Van Steirteghem A. Osmotic responses and tolerance limits to changes in external osmolalities, and oolemma permeability characteristics, of human in vitro matured MII oocytes. Hum Reprod 2007;22(7):1959-72.
5. Dinnyes A, **Liu J**, Nedambale TL. Novel gamete storage. Reprod Fertil Dev 2007;19(6):719-31.
6. Chaveiro A, Liu J, Engel B, Critser JK, Woelders H. Significant variability among bulls in the sperm membrane permeability for water and glycerol: possible implications for semen freezing protocols for individual males. Cryobiology 2006;53(3):349-59.
7. Agca Y, Mullen S, **Liu J**, Johnson-Ward J, Gould K, Chan A, et al. Osmotic tolerance and membrane permeability characteristics of rhesus monkey (Macaca mulatta) spermatozoa. Cryobiology 2005;51(1):1-14.
8. Agca Y, **Liu J**, Mullen S, Johnson-Ward J, Gould K, Chan A, et al. Chimpanzee (Pan troglodytes) spermatozoa osmotic tolerance and cryoprotectant permeability characteristics. J Androl 2005;26(4):470-7.
9. Chaveiro A, **Liu J**, Mullen S, Woelders H, Critser JK. Determination of bull sperm membrane permeability to water and cryoprotectants using a concentration-dependent self-quenching fluorophore. Cryobiology 2004;48(1):72-80.
10. Woods EJ, **Liu J**, Pollok K, Hartwell J, Smith FO, Williams DA, et al. A theoretically optimized method for cord blood stem cell cryopreservation. J Hematother Stem Cell Res 2003;12(3):341-50.
11. Guthrie HD, **Liu J**, Critser JK. Osmotic tolerance limits and effects of cryoprotectants on motility of bovine spermatozoa. Biol Reprod 2002;67(6):1811-6.
12. Agca Y, Gilmore J, Byers M, Woods EJ, **Liu J**, Critser JK. Osmotic characteristics of mouse spermatozoa in the presence of extenders and sugars. Biol Reprod 2002;67(5):1493-501.
13. **Liu J**, Christian JA, Critser JK. Canine RBC osmotic tolerance and membrane permeability. Cryobiology 2002;44(3):258-68.

14. Woods EJ, **Liu J**, Derrow CW, Smith FO, Williams DA, Critser JK. Osmometric and permeability characteristics of human placental/umbilical cord blood CD34+ cells and their application to cryopreservation. J Hematother Stem Cell Res 2000;9(2):161-73.
15. Agca Y, **Liu J**, Critser ES, Critser JK. Fundamental cryobiology of rat immature and mature oocytes: hydraulic conductivity in the presence of Me(2)SO, Me(2)SO permeability, and their activation energies. J Exp Zool 2000;286(5):523-33.
16. Agca Y, **Liu J**, Rutledge JJ, Critser ES, Critser JK. Effect of osmotic stress on the developmental competence of germinal vesicle and metaphase II stage bovine cumulus oocyte complexes and its relevance to cryopreservation. Mol Reprod Dev 2000;55(2):212-9.
17. Gilmore JA, **Liu J**, Woods EJ, Peter AT, Critser JK. Cryoprotective agent and temperature effects on human sperm membrane permeabilities: convergence of theoretical and empirical approaches for optimal cryopreservation methods. Hum Reprod 2000;15(2):335-43.
18. **Liu J**, Woods EJ, Agca Y, Critser ES, Critser JK. Cryobiology of rat embryos II: A theoretical model for the development of interrupted slow freezing procedures. Biol Reprod 2000;63(5):1303-12.
19. Pfaff RT, Agca Y, **Liu J**, Woods EJ, Peter AT, Critser JK. Cryobiology of rat embryos I: determination of zygote membrane permeability coefficients for water and cryoprotectants, their activation energies, and the development of improved cryopreservation methods. Biol Reprod 2000;63(5):1294-302.
20. Woods EJ, **Liu J**, Zieger MA, Lakey JR, Critser JK. Water and cryoprotectant permeability characteristics of isolated human and canine pancreatic islets. Cell Transplant 1999;8(5):549-59.
21. Agca Y, **Liu J**, Critser ES, McGrath JJ, Critser JK. Temperature-dependent osmotic behavior of germinal vesicle and metaphase II stage bovine oocytes in the presence of Me2SO in relationship to cryobiology. Mol Reprod Dev 1999;53(1):59-67.
22. Zieger MA, Woods EJ, Lakey JR, **Liu J**, Critser JK. Osmotic tolerance limits of canine pancreatic islets. Cell Transplant 1999;8(3):277-84.
23. Phelps MJ, **Liu J**, Benson JD, Willoughby CE, Gilmore JA, Critser JK. Effects of Percoll separation, cryoprotective agents, and temperature on plasma membrane permeability characteristics of murine spermatozoa and their relevance to cryopreservation. Biol Reprod 1999;61(4):1031-41.
24. Woods EJ, **Liu J**, Zieger MA, Lakey JR, Critser JK. The effects of microencapsulation on pancreatic islet osmotically induced volumetric response. Cell Transplant 1999;8(6):699-708.
25. Woods EJ, **Liu J**, Gilmore JA, Reid TJ, Gao DY, Critser JK. Determination of human platelet membrane permeability coefficients using the Kedem-Katchalsky formalism: estimates from two- vs three-parameter fits. Cryobiology 1999;38(3):200-8.

26. Pfaff RT, **Liu J**, Gao D, Peter AT, Li TK, Critser JK. Water and DMSO membrane permeability characteristics of in-vivo- and in-vitro-derived and cultured murine oocytes and embryos. Mol Hum Reprod 1998;4(1):51-9.
27. Woods EJ, Lakey JR, Zieger MA, **Liu J**, Critser JK. Osmotic responses of isolated canine islets to novel cryoprotectants. Transplant Proc 1998;30(2):388-9.
28. Agca Y, **Liu J**, McGrath JJ, Peter AT, Critser ES, Critser JK. Membrane permeability characteristics of metaphase II mouse oocytes at various temperatures in the presence of Me2SO. Cryobiology 1998;36(4):287-300.
29. Agca Y, **Liu J**, Peter AT, Critser ES, Critser JK. Effect of developmental stage on bovine oocyte plasma membrane water and cryoprotectant permeability characteristics. Mol Reprod Dev 1998;49(4):408-15.
30. Gilmore JA, **Liu J**, Peter AT, Critser JK. Determination of plasma membrane characteristics of boar spermatozoa and their relevance to cryopreservation. Biol Reprod 1998;58(1):28-36.
31. **Liu J**, Zieger MA, Lakey JR, Woods E, Critser JK. Water and DMSO permeability at 22 degrees C, 5 degrees C, and -3 degrees C for human pancreatic islet cells. Transplant Proc 1997;29(4):1987.
32. Woods EJ, Lakey JR, Zieger MA, **Liu J**, Nelson D, Critser JK. Permeability characteristics of microencapsulated pancreatic islets. Transplant Proc 1997;29(4):2148.
33. Woods EJ, Zieger MA, Lakey JR, **Liu J**, Critser JK. Osmotic characteristics of isolated human and canine pancreatic islets. Cryobiology 1997;35(2):106-13.
34. Lakey JR, Zieger MA, Woods EJ, **Liu J**, Critser JK. Hypoosmotic exposure of canine pancreatic digest as a means to purify islet tissue. Cell Transplant 1997;6(4):423-8.
35. Gilmore JA, **Liu J**, Gao DY, Critser JK. Determination of optimal cryoprotectants and procedures for their addition and removal from human spermatozoa. Hum Reprod 1997;12(1):112-8.
36. **Liu J**, Zieger MA, Lakey JR, Woods EJ, Critser JK. The determination of membrane permeability coefficients of canine pancreatic islet cells and their application to islet cryopreservation. Cryobiology 1997;35(1):1-13.
37. Gao DY, **Liu J**, Liu C, McGann LE, Watson PF, Kleinhans FW, et al. Prevention of osmotic injury to human spermatozoa during addition and removal of glycerol. Hum Reprod 1995;10(5):1109-22.
38. Gilmore JA, McGann LE, **Liu J**, Gao DY, Peter AT, Kleinhans FW, et al. Effect of cryoprotectant solutes on water permeability of human spermatozoa. Biol Reprod 1995;53(5):985-95.

CHAPTER 10. REFERENCE

Agca, Y. (2000). Cryopreservation of oocyte and ovarian tissue. *Ilar Journal* **41**, 207-20.

Agca, Y., Liu, J., Critser, E. S., and Critser, J. K. (2000a). Fundamental cryobiology of rat immature and mature oocytes: hydraulic conductivity in the presence of Me(2)SO, Me(2)SO permeability, and their activation energies. *Journal of Experimental Zoology* **286**, 523-33.

Agca, Y., Liu, J., Critser, E. S., McGrath, J. J., and Critser, J. K. (1999). Temperature-dependent osmotic behavior of germinal vesicle and metaphase II stage bovine oocytes in the presence of Me2SO in relationship to cryobiology. *Molecular Reproduction & Development* **53**, 59-67.

Agca, Y., Liu, J., McGrath, J. J., Peter, A. T., Critser, E. S., and Critser, J. K. (1998a). Membrane permeability characteristics of metaphase II mouse oocytes at various temperatures in the presence of Me2SO. *Cryobiology* **36**, 287-300.

Agca, Y., Liu, J., Peter, A. T., Critser, E. S., and Critser, J. K. (1998b). Effect of developmental stage on bovine oocyte plasma membrane water and cryoprotectant permeability characteristics. *Molecular Reproduction & Development* **49**, 408-15.

Agca, Y., Liu, J., Rutledge, J. J., Critser, E. S., and Critser, J. K. (2000b). Effect of osmotic stress on the developmental competence of germinal vesicle and metaphase II stage bovine cumulus oocyte complexes and its relevance to cryopreservation. *Molecular Reproduction & Development* **55**, 212-9.

Aigner, S., Van der Elst, J., Siebzehnrubl, E., Wildt, L., Lang, N., and Van Steirteghem, A. C. (1992). The influence of slow and ultra-rapid freezing on the organization of the meiotic spindle of the mouse oocyte. *Human Reproduction* **7**, 857-64.

Al-Hasani, S., Diedrich, K., van der Ven, H., Reinecke, A., Hartje, M., and Krebs, D. (1987). Cryopreservation of human oocytes. *Human Reproduction* **2**, 695-700.

Aman, R. R., and Parks, J. E. (1994). Effects of cooling and rewarming on the meiotic spindle and chromosomes of in vitro-matured bovine oocytes. *Biol Reprod* **50**, 103-10.

Andersen, A. N., Gianaroli, L., Felberbaum, R., de Mouzon, J., and Nygren, K. G. (2006). Assisted reproductive technology in Europe, 2002. Results generated from European registers by ESHRE. *Hum Reprod* **21**, 1680-97.

Arav, A., Shehu, D., and Mattioli, M. (1993). Osmotic and cytotoxic study of vitrification of immature bovine oocytes. *Journal of Reproduction & Fertility* **99**, 353-8.

Arav, A., Zeron, Y., Leslie, S. B., Behboodi, E., Anderson, G. B., and Crowe, J. H. (1996). Phase transition temperature and chilling sensitivity of bovine oocytes. *Cryobiology* **33**, 589-99.

Asada, M., Ishibashi, S., Ikumi, S., and Fukui, Y. (2002). Effect of polyvinyl alcohol (PVA) concentration during vitrification of in vitro matured bovine oocytes. *Theriogenology* **58**, 1199-208.

Benagiano, G., and Gianaroli, L. (2004). The new Italian IVF legislation. *Reprod Biomed Online* **9**, 117-25.

Bernard, A., and Fuller, B. J. (1996). Cryopreservation of human oocytes: a review of current problems and perspectives. *Human Reproduction Update* **2**, 193-207.

Betteridge, K. J. (1981). An historical look at embryo transfer. *J Reprod Fertil* **62**, 1-13.

Borini, A., Sciajno, R., Bianchi, V., Sereni, E., Flamigni, C., and Coticchio, G. (2006). Clinical outcome of oocyte cryopreservation after slow cooling with a protocol utilizing a high sucrose concentration. *Hum Reprod* **21**, 512-7.

Bos-Mikich, A., Wood, M. J., Candy, C. J., and Whittingham, D. G. (1995). Cytogenetical analysis and developmental potential of vitrified mouse oocytes. *Biology of Reproduction* **53**, 780-5.

Cetin, Y., and Bastan, A. (2006). Cryopreservation of immature bovine oocytes by vitrification in straws. *Anim Reprod Sci* **92**, 29-36.

Chang, M. C. (1948). Transplantation of fertilized rabbit ova: the effect on viability of age, in vitro storage period, and storage temperature. *Nature* **161**, 978.

Chang, M. C. (1959). Fertilization of rabbit ova in vitro. *Nature* **184(Suppl 7)**, 466-7.

Chang, M. C., Casas, J. H., and Hunt, D. M. (1970). Prevention of pregnancy in the rabbit by subcutaneous implantation of silastic tube containing oestrogen. *Nature* **226**, 1262-3.

Chen, C. (1986). Pregnancy after human oocyte cryopreservation. *Lancet* **1**, 884-6.

Chen, C. (1988). Pregnancies after human oocyte cryopreservation. *Annals of the New York Academy of Sciences* **541**, 541-9.

Chian, R. C., Kuwayama, M., Tan, L., Tan, J., Kato, O., and Nagai, T. (2004). High survival rate of bovine oocytes matured in vitro following vitrification. *J Reprod Dev* **50**, 685-96.

Coticchio, G., Bonu, M., Borini, A., and Flamigni, C. (2004). Oocyte cryopreservation: a biological perspective. *Eur J Obstet Gynecol Reprod Biol* **1**, S2-7.

Coticchio, G., Bonu, M. A., Sciajno, R., Sereni, E., Bianchi, V., and Borini, A. (2007). Truths and myths of oocyte sensitivity to controlled rate freezing. *Reprod Biomed Online* **15**, 24-30.

Critser, J. K., Agca, Y., and Gunasena, K. T. (1997). The Cryobiology of Mammalian Oocytes. *In* "Reproductive Tissue Banking, Scientific Principles" (A. M. Karow and J. K. Critser, eds.), pp. 329-357. Academic Press, San Diego.

Critser, J. K., and Russell, R. J. (2000). Genome resource banking of laboratory animal models. *Ilar Journal* **41**, 183-6.

Day, B. N. (2000). Reproductive biotechnologies: current status in porcine reproduction. *Animal Reproduction Science* **60-61**, 161-72.

de Melo-Martin, I., and Cholst, I. N. (2007). Researching human oocyte cryopreservation: ethical issues. *Fertil Steril*.

De Santis, L., Coticchio, G., Paynter, S., Albertini, D., Hutt, K., Cino, I., Iaccarino, M., Gambardella, A., Flamigni, C., and Borini, A. (2007). Permeability of human oocytes to ethylene glycol and their survival and spindle configurations after slow cooling cryopreservation. *Hum Reprod* **22**, 2776-83.

Diedrich, K., Al-Hasani, S., Van der Ven, H., and Krebs, D. (1987). Successful in vitro fertilizationof frozen-thawed rabbit and human oocytes. *Proceedings of the 5th world congress on IVF and ET*, 652-70.

Diller, K. R. (1982). Quantitative low temperature optical microscopy of biological systems. *J Microsc* **126**, 9-28.

Dinnyes, A., Dai, Y., Jiang, S., and Yang, X. (2000). High developmental rates of vitrified bovine oocytes following parthenogenetic activation, in vitro fertilization, and somatic cell nuclear transfer. *Biology of Reproduction* **63**, 513-8.

Dinnyes, A., Liu, J., and Nedambale, T. L. (2007). Novel gamete storage. *Reprod Fertil Dev* **19**, 719-31.

Fabbri, R. (2006). Cryopreservation of human oocytes and ovarian tissue. *Cell Tissue Bank* **7**, 113-22.

Fabbri, R., Porcu, E., Marsella, T., Rocchetta, G., Venturoli, S., and Flamigni, C. (2001). Human oocyte cryopreservation: new perspectives regarding oocyte survival. *Human Reproduction* **16**, 411-6.

Fahy, G. M. (1981). Simplified calculation of cell water content during freezing and thawing in nonideal solutions of cryoprotective agents and its possible application to the study of "solution effects" injury. *Cryobiology* **18**, 473-82.

Fahy, G. M. (1986a). The relevance of cryoprotectant "toxicity" to cryobiology. *Cryobiology* **23**, 1-13.

Fahy, G. M. (1986b). Vitrification: a new approach to organ cryopreservation. *Progress in Clinical & Biological Research* **224**, 305-35.

Fahy, G. M., MacFarlane, D. R., Angell, C. A., and Meryman, H. T. (1984). Vitrification as an approach to cryopreservation. *Cryobiology* **21**, 407-26.

Friedler, S., Giudice, L. C., and Lamb, E. J. (1988). Cryopreservation of embryos and ova. *Fertility & Sterility* **49**, 743-64.

Fuku, E., Kojima, T., Shioya, Y., Marcus, G. J., and Downey, B. R. (1992). In vitro fertilization and development of frozen-thawed bovine oocytes. *Cryobiology* **29**, 485-92.

Fuku, E. J., Liu, J., and Downey, B. R. (1995). In vitro viability and ultrastructural changes in bovine oocytes treated with a vitrification solution. *Mol Reprod Dev* **40**, 177-85.

Fuller, B., Hunter, J. E., Bernard, A. G., McGrath, J. J., Curtis, P., and Jackson, A. (1992). The permeability of unfertilized oocytes to 1,2-propanediol A comparison of mouse and human cells. *Cryo-Letters* **13**, 287-92.

Gao, D. Y., Liu, J., Liu, C., McGann, L. E., Watson, P. F., Kleinhans, F. W., Mazur, P., Critser, E. S., and Critser, J. K. (1995). Prevention of osmotic injury to human spermatozoa during addition and removal of glycerol. *Human Reproduction* **10**, 1109-22.

Gao, D. Y., McGrath, J. J., Tao, J., Benson, C. T., Critser, E. S., and Critser, J. K. (1994). Membrane transport properties of mammalian oocytes: a micropipette perfusion technique. *J Reprod Fertil* **102**, 385-92.

Glenister, P. H., Whittingham, D. G., and Wood, M. J. (1990). Genome cryopreservation: a valuable contribution to mammalian genetic research. *Genetical Research* **56**, 253-8.

Gook, D. A., and Edgar, D. H. (2007). Human oocyte cryopreservation. *Hum Reprod Update* **13**, 591-605.

Heape, W. (1891). Preliminary note on the transplantation and growth of mammalian ova within a uterine foster-mother. *Proc. R. Soc.* **48**, 457-8.

Hirabayashi, M., Takahashi, R., Sekiguchi, J., and Ueda, M. (1997). Viability of transgenic rat embryos after freezing and thawing. *Experimental Animals* **46**, 111-5.

Hotamisligil, S., Toner, M., and Powers, R. D. (1996). Changes in membrane integrity, cytoskeletal structure, and developmental potential of murine oocytes after vitrification in ethylene glycol. *Biology of Reproduction* **55**, 161-8.

Huang, J. H. Y., Chen, H. Y., Tan, S. L., and Chain, R. C. (2006). Effects of osmotic stress and cryoprotectant toxicity on mouse oocyte fertilization and subsequent embryonic development in vitro. *Cell Preserv Technol* **4**, 149-160.

Hunter, J., Bernard, A., Fuller, B., McGrath, J., and Shaw, R. W. (1992a). Plasma membrane water permeabilities of human oocytes: the temperature dependence of water movement in individual cells. *Journal of Cellular Physiology* **150**, 175-9.

Hunter, J. E., Bernard, A., Fuller, B., Amso, N., and Shaw, R. W. (1991). Fertilization and development of the human oocyte following exposure to cryoprotectants, low temperatures and cryopreservation: a comparison of two techniques. *Human Reproduction* **6**, 1460-5.

Hunter, J. E., Bernard, A., Fuller, B. J., McGrath, J. J., and Shaw, R. W. (1992b). Measurements of the membrane water permeability (Lp) and its temperature dependence (activation energy) in human fresh and failed-to-fertilize oocytes and mouse oocyte. *Cryobiology* **29**, 240-9.

Isachenko, E. F., and Nayudu, P. L. (1999). Vitrification of mouse germinal vesicle oocytes: effect of treatment temperature and egg yolk on chromatin and spindle normality and cumulus integrity. *Human Reproduction* **14**, 400-8.

Karlsson, J. O., Cravalho, E. G., Borel Rinkes, I. H., Tompkins, R. G., Yarmush, M. L., and Toner, M. (1993). Nucleation and growth of ice crystals inside cultured hepatocytes during freezing in the presence of dimethyl sulfoxide. *Biophys J* **65**, 2524-36.

Karlsson, J. O., Cravalho, E. G., and Toner, M. (1994). A model of diffusion-limited ice growth inside biological cells during freezing. *Journal of Applied Physiology* **75**, 4442-4450.

Karlsson, J. O., Eroglu, A., Toth, T. L., Cravalho, E. G., and Toner, M. (1996). Fertilization and development of mouse oocytes cryopreserved using a theoretically optimized protocol. *Human Reproduction* **11**, 1296-305.

Karlsson, J. O. M., and Toner, M. (2000). "Cryopreservation," Academic Press, San Diego, CA.

Karow, A. M. (1997). Implications of Tissue Banking for Human Reproductive Medicine. *In* "Reproductive Tissue Banking, Scientific Principles" (A. M. Karow and J. K. Critser, eds.), pp. 441-464. Academic Press, San Diego.

Katkov, II, Katkova, N., Critser, J. K., and Mazur, P. (1998). Mouse spermatozoa in high concentrations of glycerol: chemical toxicity vs osmotic shock at normal and reduced oxygen concentrations. *Cryobiology* **37**, 325-38.

Kedem, O., and Katchalsky, A. (1958). Thermodynamic analysis of the permeability of biological membranes to non-electrolytes. *Biochimica et Biophysica Acta* **27**, 229-246.

Kola, I., Kirby, C., Shaw, J., Davey, A., and Trounson, A. (1988). Vitrification of mouse oocytes results in aneuploid zygotes and malformed fetuses. *Teratology* **38**, 467-74.

Kuwayama, M. (2007). Highly efficient vitrification for cryopreservation of human oocytes and embryos: The Cryotop method. *Theriogenology* **67**, 73-80.

Kuwayama, M., Vajta, G., Kato, O., and Leibo, S. P. (2005). Highly efficient vitrification method for cryopreservation of human oocytes. *Reprod Biomed Online* **11**, 300-8.

Landa, V. (1990). "Two-step" freezing of individual blastomeres from mouse eight-cell embryos. *Folia Biologica* **36**, 51-6.

Lane, M., Schoolcraft, W. B., and Gardner, D. K. (1999). Vitrification of mouse and human blastocysts using a novel cryoloop container-less technique. *Fertility & Sterility* **72**, 1073-8.
Leibo, S. P. (2007). Cryopreservation of oocytes and embryos: Optimization by theoretical versus empirical analysis. *Theriogenology*.
Leibo, S. P., DeMayo, F. J., and O'Malley, B. (1991). Production of transgenic mice from cryopreserved fertilized ova. *Molecular Reproduction & Development* **30**, 313-9.
Leibo, S. P., Mazur, P., and Jackowski, S. C. (1974). Factors affecting survival of mouse embryos during freezing and thawing. *Exp Cell Res* **89**, 79-88.
Leibo, S. P., and Songsasen, N. (2002). Cryopreservation of gametes and embryos of non-domestic species. *Theriogenology* **57**, 303-26.
Levi Setti, P. E., Albani, E., Novara, P. V., Cesana, A., and Morreale, G. (2006). Cryopreservation of supernumerary oocytes in IVF/ICSI cycles. *Hum Reprod* **21**, 370-5.
Levin, R. L., Cravalho, E. G., and Huggins, C. E. (1976). A membrane model describing the effect of temperature on the water conductivity of erythrocyte membranes at subzero temperatures. *Cryobiology* **13**, 415-29.
Levin, R. L., and Miller, T. W. (1981). An optimum method for the introduction or removal of permeable cryoprotectants: isolated cells. *Cryobiology* **18**, 32-48.
Lim, J. M., Fukui, Y., and Ono, H. (1992). The post-thaw developmental competence of bovine oocytes frozen at various maturation stages followed by in vitro maturation and fertilization. *Theriogenology* **37**, 351-61.
Liu, J., Woods, E. J., Agca, Y., Critser, E. S., and Critser, J. K. (2000). Cryobiology of rat embryos II: A theoretical model for the development of interrupted slow freezing procedures. *Biology of Reproduction* **63**, 1303-12.
Liu, J., Zieger, M. A., Lakey, J. R., Woods, E. J., and Critser, J. K. (1997). The determination of membrane permeability coefficients of canine pancreatic islet cells and their application to islet cryopreservation. *Cryobiology* **35**, 1-13.
Liu, R. H., Sun, Q. Y., Li, Y. H., Jiao, L. H., and Wang, W. H. (2003). Effects of cooling on meiotic spindle structure and chromosome alignment within in vitro matured porcine oocytes. *Mol Reprod Dev* **65**, 212-8.
Lopez-Bejar, M., Lopez-Gatius, F., Camon, J., Rutllant, J., and Labernia, J. (1994). Development in vitro of rabbit embryos after freezing by two-step or ultra-rapid cooling methods. *Zentralblatt fur Veterinarmedizin - Reihe A* **41**, 780-90.
Marina, F., and Marina, S. (2003). Comments on oocyte cryopreservation. *Reproductive Biomedicine Online* **6**, 401-2.
Martino, A., Pollard, J. W., and Leibo, S. P. (1996a). Effect of chilling bovine oocytes on their developmental competence. *Molecular Reproduction & Development* **45**, 503-12.
Martino, A., Songsasen, N., and Leibo, S. P. (1996b). Development into blastocysts of bovine oocytes cryopreserved by ultra-rapid cooling. *Biology of Reproduction* **54**, 1059-69.
Mazur, P. (1963). Kinetics of water loss from cells at subzero temperatures and the likelihood of intracellular freezing. *Journal of General Physiology* **47**, 47-69.
Mazur, P. (1966). Theoretical and experimental effects of cooling and warming velocity on the survival of frozen and thawed cells. *Cryobiology* **2**, 181-92.
Mazur, P. (1977). The role of intracellular freezing in the death of cells cooled at supraoptimal rates. *Cryobiology* **14**, 251-72.
Mazur, P. (1984). Freezing of living cells: mechanisms and implications. *Am J Physiol* **247**, C125-42.
Mazur, P. (1990). Equilibrium, quasi-equilibrium, and nonequilibrium freezing of mammalian embryos. *Cell Biophysics* **17**, 53-92.
Mazur, P. (2004). Principles of Cryobiology. *In* "Life in the Frozen State" (B. J. Fuller, N. Lane and E. E. Benson, eds.), pp. 3-65. CRC Press, Boca Raton.
Mazur, P., Rall, W. F., and Leibo, S. P. (1984). Kinetics of water loss and the likelihood of intracellular freezing in mouse ova. Influence of the method of calculating the temperature dependence of water permeability. *Cell Biophysics* **6**, 197-213.
Mazur, P., and Schneider, U. (1986). Osmotic responses of preimplantation mouse and bovine embryos and their cryobiological implications. *Cell Biophys* **8**, 259-85.

McGann, L. E., and Farrant, J. (1976). Survival of tissue culture cells frozen by a two-step procedure to -196 degrees C. I. Holding temperature and time. *Cryobiology* **13**, 261-8.
McWilliams, R. B., Gibbons, W. E., and Leibo, S. P. (1995). Osmotic and physiological responses of mouse zygotes and human oocytes to mono- and disaccharides. *Human Reproduction* **10**, 1163-71.
Meryman, H. T. (2007). Cryopreservation of living cells: principles and practice. *Transfusion* **47**, 935-45.
Michelmann, H. W., and Nayudu, P. (2006). Cryopreservation of human embryos. *Cell Tissue Bank* **7**, 135-41.
Mortimer, D. (2004). Current and future concepts and practices in human sperm cryobanking. *Reprod Biomed Online* **9**, 134-51.
Muldrew, K., and McGann, L. E. (1990). Mechanisms of intracellular ice formation. *Biophysical Journal* **57**, 525-32.
Muldrew, K., and McGann, L. E. (1994). The osmotic rupture hypothesis of intracellular freezing injury. *Biophysical Journal* **66**, 532-41.
Mullen, S. F. (2007). Advances in the fundamental cryobiology of mammalian oocytes, University of Missouri, Columbia.
Mullen, S. F., Rosenbaum, M., and Critser, J. K. (2007). The effect of osmotic stress on the cell volume, metaphase II spindle and developmental potential of in vitro matured porcine oocytes. *Cryobiology* **54**, 281-9.
Nakagata, N. (1989). High survival rate of unfertilized mouse oocytes after vitrification. *Journal of Reproduction & Fertility* **87**, 479-83.
Otoi, T., Yamamoto, K., Koyama, N., Tachikawa, S., and Suzuki, T. (1998). Cryopreservation of mature bovine oocytes by vitrification in straws. *Cryobiology* **37**, 77-85.
Papis, K., Shimizu, M., and Izaike, Y. (2000). Factors affecting the survivability of bovine oocytes vitrified in droplets. *Theriogenology* **54**, 651-8.
Parkening, T. A., Tsunoda, Y., and Chang, M. C. (1976). Effects of various low temperatures, cryoprotective agents and cooling rates on the survival, fertilizability and development of frozen-thawed mouse eggs. *J Exp Zool* **197**, 369-74.
Paynter, S. J., Cooper, A., Gregory, L., Fuller, B. J., and Shaw, R. W. (1999). Permeability characteristics of human oocytes in the presence of the cryoprotectant dimethylsulphoxide. *Human Reproduction* **14**, 2338-42.
Pegg, D. E. (1986). Equations for obtaining melting points and eutectic temperatures for the ternary system dimethylsulphoxide/sodium chloride/water. *Cryo-Letters* **7**, 387-394.
Pegg, D. E., and Diaper, M. P. (1988). On the mechanism of injury to slowly frozen erythrocytes. *Biophys J* **54**, 471-88.
Pfaff, R. T., Agca, Y., Liu, J., Woods, E. J., Peter, A. T., and Critser, J. K. (2000). Cryobiology of rat embryos I: determination of zygote membrane permeability coefficients for water and cryoprotectants, their activation energies, and the development of improved cryopreservation methods. *Biology of Reproduction* **63**, 1294-302.
Pfaff, R. T., Liu, J., Gao, D., Peter, A. T., Li, T. K., and Critser, J. K. (1998). Water and DMSO membrane permeability characteristics of in-vivo- and in-vitro-derived and cultured murine oocytes and embryos. *Molecular Human Reproduction* **4**, 51-9.
Pickering, S. J., Braude, P. R., Johnson, M. H., Cant, A., and Currie, J. (1990). Transient cooling to room temperature can cause irreversible disruption of the meiotic spindle in the human oocyte. *Fertil Steril* **54**, 102-8.
Pincus, G. (1939). The development of fertilized and artificially activated eggs. *Journal of Experimental Zoology* **82**, 85-130.
Pitt, R. E., Chandrasekaran, M., and Parks, J. E. (1992). Performance of a kinetic model for intracellular ice formation based on the extent of supercooling. *Cryobiology* **29**, 359-73.
Porcu, E., Fabbri, R., Seracchioli, R., Ciotti, P. M., Magrini, O., and Flamigni, C. (1997). Birth of a healthy female after intracytoplasmic sperm injection of cryopreserved human oocytes. *Fertility & Sterility* **68**, 724-6.
Presicce, G. A., Jiang, S., Simkin, M., Zhang, L., Looney, C. R., Godke, R. A., and Yang, X. (1997). Age and hormonal dependence of acquisition of oocyte competence for embryogenesis in prepubertal calves. *Biol Reprod* **56**, 386-92.

Rall, W. F., and Fahy, G. M. (1985). Ice-free cryopreservation of mouse embryos at -196 degrees C by vitrification. *Nature* **313**, 573-5.

Rall, W. F., Reid, D. S., and Polge, C. (1984). Analysis of slow-warming injury of mouse embryos by cryomicroscopical and physiochemical methods. *Cryobiology* **21**, 106-21.

Rall, W. F., Wood, M. J., Kirby, C., and Whittingham, D. G. (1987). Development of mouse embryos cryopreserved by vitrification. *J Reprod Fertil* **80**, 499-504.

Rapatz, G., and Luyet, B. (1973). The cryopreservation of blood by the method of two-step freezing. *Biodynamica* **11**, 169-79.

Rayos, A. A., Takahashi, Y., Hishinuma, M., and Kanagawa, H. (1994). Quick freezing of unfertilized mouse oocytes using ethylene glycol with sucrose or trehalose. *Journal of Reproduction & Fertility* **100**, 123-9.

Ren, H. S., Wei, Y., Hua, T. C., and Zhang, J. (1994). Theoretical Prediction of Vitrification and Devitrification Tendencies for Cryoprotective Solutions. *Cryobiology* **31**, 47-56.

Rho, G. J., Kim, S., Yoo, J. G., Balasubramanian, S., Lee, H. J., and Choe, S. Y. (2002). Microtubulin configuration and mitochondrial distribution after ultra-rapid cooling of bovine oocytes. *Mol Reprod Dev* **63**, 464-70.

Ruffing, N. A., Steponkus, P. L., Pitt, R. E., and Parks, J. E. (1993). Osmometric behavior, hydraulic conductivity, and incidence of intracellular ice formation in bovine oocytes at different developmental stages. *Cryobiology* **30**, 562-80.

Rutledge, J. J., Monson, R. L., Northey, D. L., and Leibfried-Rutledge, M. L. (1999). Seasonality of cattle embryo production in a temperate region. *Theriogenology* **51**, 330 (Abstract).

Schnorr, J. A., Muasher, S. J., and Jones, H. W., Jr. (2000). Evaluation of the clinical efficacy of embryo cryopreservation. *Molecular & Cellular Endocrinology* **169**, 85-9.

Shaw, P. W., Bernard, A. G., Fuller, B. J., Hunter, J. H., and Shaw, R. W. (1992). Vitrification of mouse oocytes using short cryoprotectant exposure: effects of varying exposure times on survival. *Molecular Reproduction & Development* **33**, 210-4.

Somfai, T., Dinnyes, A., Sage, D., Marosan, M., Carnwath, J. W., Ozawa, M., Kikuchi, K., and Niemann, H. (2006). Development to the blastocyst stage of parthenogenetically activated in vitro matured porcine oocytes after solid surface vitrification (SSV). *Theriogenology* **66**, 415-22.

Songsasen, N., Yu, I. J., Ratterree, M. S., VandeVoort, C. A., and Leibo, S. P. (2002). Effect of chilling on the organization of tubulin and chromosomes in rhesus monkey oocytes. *Fertil Steril* **77**, 818-25.

Stachecki, J. J., and Cohen, J. (2004). An overview of oocyte cryopreservation. *Reprod Biomed Online* **9**, 152-63.

Stachecki, J. J., Cohen, J., and Willadsen, S. M. (1998). Cryopreservation of unfertilized mouse oocytes: the effect of replacing sodium with choline in the freezing medium. *Cryobiology* **37**, 346-54.

Surrey, E. S., and Quinn, P. J. (1990). Successful ultrarapid freezing of unfertilized oocytes. *Journal of in Vitro Fertilization & Embryo Transfer* **7**, 262-6.

Sutton, R. L. (1991). Critical cooling rates to avoid ice crystallization in solutions of cryoprotective agents. *J. Chem. Soc. Faraday Trans.* **87**, 101-105.

Todorow, S. J., Siebzehnrubl, E. R., Spitzer, M., Koch, R., Wildt, L., and Lang, N. (1989). Comparative results on survival of human and animal eggs using different cryoprotectants and freeze-thawing regimens. II. Human. *Human Reproduction* **4**, 812-6.

Toner, M., Cravalho, E. G., and Huggins, C. E. (1990). Thermodynamics and kinetics of intracellular ice formation during freezing of biological cells. *Journal of Applied Physiology* **69**, 1582-1593.

Toner, M., Cravalho, E. G., and Karel, M. (1993). Cellular response of mouse oocytes to freezing stress: prediction of intracellular ice formation. *Journal of Biomechanical Engineering* **115**, 169-74.

Utsumi, K., Hochi, S., and Iritani, A. (1992). Cryoprotective effect of polyols on rat embryos during two-step freezing. *Cryobiology* **29**, 332-41.

Vajta, G., Booth, P. J., Holm, P., Greve, T., and Callesen, H. (1997). Successful vitrification of early stage bovine in vitro produced embryos with the open pulled straw (OPS) method. *Cryo-Letters* **18**, 191-195.

Vajta, G., Holm, P., Kuwayama, M., Booth, P. J., Jacobsen, H., Greve, T., and Callesen, H. (1998). Open Pulled Straw (OPS) vitrification: a new way to reduce cryoinjuries of bovine ova and embryos. *Molecular Reproduction & Development* **51**, 53-8.

Vajta, G., and Nagy, Z. P. (2006). Are programmable freezers still needed in the embryo laboratory? Review on vitrification. *Reprod Biomed Online* **12**, 779-96.

Valojerdi, M. R., and Salehnia, M. (2005). Developmental potential and ultrastructural injuries of metaphase II (MII) mouse oocytes after slow freezing or vitrification. *J Assist Reprod Genet* **22**, 119-27.

Van den Abbeel, E., Schneider, U., Liu, J., Agca, Y., Critser, J. K., and Van Steirteghem, A. (2007). Osmotic responses and tolerance limits to changes in external osmolalities, and oolemma permeability characteristics, of human in vitro matured MII oocytes. *Hum Reprod*, doi: 10.1093/humrep/dem083 *In Press*

Van den Abbeel, E., Van der Elst, J., and Van Steirteghem, A. C. (1994). The effect of temperature at which slow cooling is terminated and of thawing rate on the survival of one-cell mouse embryos frozen in dimethyl sulfoxide or 1,2-propanediol solutions. *Cryobiology* **31**, 423-33.

Vincent, C., and Johnson, M. H. (1992). Cooling, cryoprotectants, and the cytoskeleton of the mammalian oocyte. *Oxford Reviews of Reproductive Biology* **14**, 73-100.

Watson, P. F., and Holt, W. V. (2001). Germplasm cryopreservation and non-human primates. *In* "Cryobanking the genetic resource" (P. F. Watson and W. V. Holt, eds.), pp. 407-426. Taylor and Francis, London.

Whittingham, D. G. (1974). Embryo banks in the future of developmental genetics. *Genetics* **78**, 395-402.

Whittingham, D. G. (1977). Fertilization in vitro and development to term of unfertilized mouse oocytes previously stored at --196 degrees C. *Journal of Reproduction & Fertility* **49**, 89-94.

Whittingham, D. G., Leibo, S. P., and Mazur, P. (1972). Survival of mouse embryos frozen to -196 degrees and -269 degrees C. *Science* **178**, 411-4.

Whittingham, D. G., Wood, M., Farrant, J., Lee, H., and Halsey, J. A. (1979). Survival of frozen mouse embryos after rapid thawing from -196 degrees C. *J Reprod Fertil* **56**, 11-21.

Wildt, D. E. (2000). Genome resource banking for wildlife research, management, and conservation. *Ilar Journal* **41**, 228-34.

Wilmut, I. (1972). The effect of cooling rate, warming rate, cryoprotective agent and stage of development on survival of mouse embryos during freezing and thawing. *Life Sci II* **11**, 1071-9.

Wood, M. J., Barros, C., Candy, C. J., Carroll, J., Melendez, J., and Whittingham, D. G. (1993). High rates of survival and fertilization of mouse and hamster oocytes after vitrification in dimethylsulphoxide. *Biol Reprod* **49**, 489-95.

Wood, M. J., and Farrant, J. (1980). Preservation of mouse embryos by two-step freezing. *Cryobiology* **17**, 178-80.

Wu, B., Tong, J., and Leibo, S. P. (1999). Effects of cooling germinal vesicle-stage bovine oocytes on meiotic spindle formation following in vitro maturation. *Molecular Reproduction & Development* **54**, 388-95.

Yoon, T. K., Chung, H. M., Lim, J. M., Han, S. Y., Ko, J. J., and Cha, K. Y. (2000). Pregnancy and delivery of healthy infants developed from vitrified oocytes in a stimulated in vitro fertilization-embryo transfer program. *Fertility & Sterility* **74**, 180-1.

Yoon, T. K., Kim, T. J., Park, S. E., Hong, S. W., Ko, J. J., Chung, H. M., and Cha, K. Y. (2003). Live births after vitrification of oocytes in a stimulated in vitro fertilization-embryo transfer program. *Fertil Steril* **79**, 1323-6.

Zenzes, M. T., Bielecki, R., Casper, R. F., and Leibo, S. P. (2001). Effects of chilling to 0 degrees C on the morphology of meiotic spindles in human metaphase II oocytes. *Fertil Steril* **75**, 769-77.

Zeron, Y., Sklan, D., and Arav, A. (2002). Effect of polyunsaturated fatty acid supplementation on biophysical parameters and chilling sensitivity of ewe oocytes. *Mol Reprod Dev* **61**, 271-8.

CHAPTER 11. ACKNOWLEDGEMENTS

The work presented in this dissertation could not have been completed without the assistance and dedication of numerous individuals. First and foremost, I would like to thank Dr. Andras Dinnyes for all of his support, kindness, understanding, and patience in relation to both science and life. He gave me the opportunity to study and work in this great country with a group of wonderful colleagues who provided me strength, companionship, encouragement, humility, and humor. My staying in Hungary is one of the most memorable experiences of my life.

I have had the pleasure of working with many most knowledgeable, kindest, and most respectable people I have ever encountered. Among them, Dr. John Critser has taught me many things, encouraged me in my pursuit of ideas, supported me in times of need and worry, and provided me with numerous opportunities; Dr. Yuksel Agca and Dr. Steve Mullen have been great colleagues, mentors, and friends. I am particularly appreciative of all of those with whom I have worked directly and assisted me with the work presented here. I will apologize in advance for those who are not directly named. None of this work could have been completed without the diligence and kindness of these colleagues of the various institutions of which I have been affiliated.

Finally yet importantly, I would like to express my gratitude to my dear wife, my parents and parents in law for their nourishment, guidance, encouragement, sacrifice and believing. Especial thanks to my daughter for being such a wonderful baby in days and nights I spent on this dissertation preparation.